STUDIES

OF

MAGNETIC OPTICAL

ACTIVITY

IN

RAMAN SCATTERING

A Thesis

Submitted for the Degree of

DOCTOR OF PHILOSOPHY

in the Department of Chemistry of

the

University of Glasgow

by

CORNELIUS MEEHAN

April 1986

ProQuest LLC.
789 East Eisenhower Parkway
P.O. Box 1346
Ann Arbor, MI 48106 – 1346

To the memory of my recently deceased father, to my mother and to the rest of my family, in particular to my deceased sister Anne-Marie.

The great thing is to last and to get your work done, and see and hear and understand and write when there is something you know and not before and not too damn much after.

Ernest Hemingway

Ah, but that is a fine hypothesis. It explains so many things.

Lagrange (On hearing Laplace's remark that God was a hypothesis he did not require.)

CONTENTS

LIST OF TABLES

LIST OF FIGURES

ACKNOWLEDGEMENTS

I wish to express my sincere gratitude to Professor Laurence D. Barron, my supervisor, for suggesting the topic, for his interest and for his continual encouragement. I would also like to thank him for his friendly and proficient advice and guidance throughout the course of this work, for his patience and finally for his help in the preparation of this thesis.

My thanks are also extended to my colleagues in the Theoretical Chemistry Department for their company and encouragement. My thanks in particular go to Dr Brian Clark, with whom I had many interesting discussions.

I gratefully acknowledge the award of a research studentship for the duration of my research project by the Science Research Council.

Finally, I would like to thank my employer's at St. Margaret Mary's, Castlemilk, for allowing me the use of their computing facilities during the preparation of this thesis.

DECLARATION

Several parts of this thesis contain material which has already been published.

The experimental results given in Section 6.2.2 have already been published in a paper in Chemical Physics Letters along with L.D. Barron (see Chapter 6, ref. (1).)

The material in Section 6.4.5 concerning the observation of a negative g-factor for iridium hexachloride has also already been published, in a paper in Molecular Physics, along with L.D. Barron and J. Vrbancich.

Much of the material in Section 5.6 has already been published in a paper in the Journal of Raman Spectroscopy, along with L.D. Barron and J. Vrbancich. The spectra published in that paper, and in particular Figures 5.3-7 reproduced here were obtained by J. Vrbancich after the experimental work for the present project had been completed.

SUMMARY

This thesis consists mainly of theoretical and experimental studies in Magnetic Raman Optical Activity (M.R.O.A.), although the main theoretical result also allows general deductions to be made about conventional vibrational Raman scattering.

The main new experimental result presented in the thesis is the discovery of the phenomenon called Raman Electron Paramagnetic Resonance, which is a new category of vibrational M.R.O.A., involving scattering by degenerate ground state molecules.

The main objective of the theoretical research was to apply the general magnetic optical activity expressions to explain the spectral features obtained for molecules exhibiting the effect. The main tool used for doing this was Irreducible Tensor Methods. The theoretical framework developed falls naturally into two parts, one for molecules having a non-degenerate ground state, and one for molecules having a degenerate ground state.

For the former case, general formulae were obtained for the perturbed and unperturbed polarizability tensor patterns. These allow all the scattering parameters of interest to be calculated. They also allow very general deductions to be made about the form of the M.R.O.A. spectra for various classes of normal mode, along with information about the frequency dependence of M.R.O.A. General conclusions concerning the conditions under which non-degenerate molecules should exhibit signifigant M.R.O.A. are also deduced.

For the latter, irreducible tensor methods were used to obtain general expressions for the polarizability tensor patterns. These show that all degenerate ground state molecules satisfying certain conditions should exhibit Raman E.P.R., and facilitate the calculation of detailed tensor patterns for specific molecules.

These results are then applied to explain the form of the spectra of various types of molecule which have exhibited M.R.O.A.

CHAPTER 1

INTRODUCTION TO THE PHENOMENON OF MAGNETIC RAMAN OPTICAL ACTIVITY

1.1 Introduction

Some objects possess the property of handedness , i.e. they are not superimposable on their mirror image. Objects possessing this property are said to be chiral. Many everyday objects possess this property, e.g. gloves,shoes etc. It is also a property possessed by numerous organic compounds, including many biologically active molecules.[1] The first discovery of a chiral molecule was made by Pasteur, who in 1848 discovered that sodium ammonium tartrate crystals actually have two forms which are mirror images of each other. He immediately realised that it must be the molecules making up the crystals which were mirror images of each other.[2] Since then, a large branch of organic chemistry called stereochemistry has been developed. This branch includes the study of chiral molecules, a term first used by Lord Kelvin.[3]

Pairs of objects which are mirror images behave identically when interacting with any achiral external influence or object. However, the pair can be distinguished by their different behaviour when they interact with some chiral influence or object. For example, a chiral object will react differently from it s mirror image when irradiated with circularly polarized light, which is itself chiral. This phenomenon is called optical activity.[4]

Magnetically induced optical activity

Now the above mentioned chiral objects have optical activity as an inherent property. There is another class of objects, which although achiral in their natural state, can have optical activity induced in them by associating them in some way with a chiral object. An example of this might be the adding of a chiral substituent onto an achiral molecule. Another example is when an external magnetic field is applied to a molecule possessing a permanent magnetic moment. In this case a coupling occurs between the magnetic field and the magnetic moment of the molecule. This coupled system, like the one above, also constitutes a chiral system. A slight variation of the above can occur. It may be that a molecule does not have a permanent magnetic moment, so that it can't couple with the applied magnetic field in its ground state. However, it may possess excited state(s) which either have a dipole moment or between which a transition magnetic dipole moment exists. Suppose now we have an incident radiation field which excites the molecule to these excited states. When so excited, the molecule may couple with the magnetic field, again producing an optically active system.

In the two cases above, the coupled system of achiral molecule and chiral magnetic field constitues a chiral object. (It should be noted that we are here using the term chiral loosely. In fact, these objects possess what has been termed "false chirality".[5]) As such it possesses the property of optical activity. This is called magnetic optical activity.[6]

Areas of Optical Activity Study

There are many experimental situations involving the interaction between light and matter in which optical activity effects may be studied. These have evolved into research fields which have yielded much detailed information on molecular structure. In all cases, where a naturally occuring optically active interaction has been observed involving a chiral substance, it has been possible to induce the effect using a magnetic field. Thus to each of the naturally occuring effects there is a magnetic analogue, which is exhibited by all molecules, not just those which are chiral. (Electric fields may also induce optical activity, but generally the magnitude of such effects is smaller than for a magnetic field, and no further mention will be made of these.[7])

Below, a brief account will be given of the major areas of optical activity investigation, together with a historical note on the first observation of the effect. The major reference used was Barron's volume on optical activity.[8]

(a) Optical rotation and magnetic optical rotation.

(i) Historically, the first observation of optical activity was made by Arago (1811), who noticed that coloured light emerged after sunlight was passed successively through a polarizer, a quartz crystal and another polarizer set at 90° to the first one.(see Fig. 1.1)

In the following year, Biot discovered that one of the

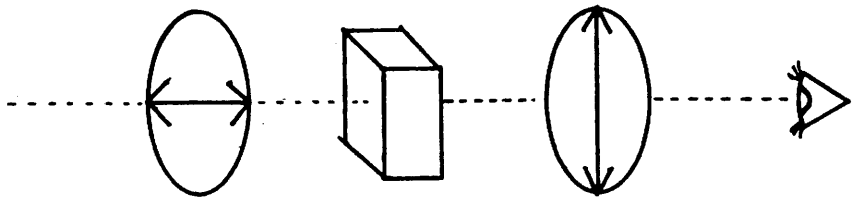

Fig. 1.1 Experimental set up used by Arago in his discovery of optical rotation

contributory mechanisms producing the coloured light was optical rotation, i.e. the rotation of the plane of polarization of a linearly polarized light beam. The following equation, the Drude equation (a modification of a relationship first noticed by Biot) relates the angle of rotation α to the wavelength of the radiation used and the absorption wavelegths λ_j of the rotating medium

$$\alpha = \sum_j \frac{A_j}{\lambda^2 - \lambda_j^2} \qquad (1.1.1)$$

where the A_j are constants relating to the absorption wavelenghths.

Equation (1.1.1) is a purely empirical relationship. The first theoretical explanation of optical rotation was made by Fresnel in 1825. Subsequent to his discovery of circularly polarized light, he realised that linearly polarized light can be regarded as a superposition of left and right circularly polarized light beams of equal magnitude. Using this fact, he explained optical rotation in terms of the different velocities of propagation of the left

and right circularly polarized components. This difference , according to Fresnel, caused the phase difference between the left and right components to change, thus causing a change in the plane of polarizaton of the linearly polarized beam, of which they are components. Using the fact that the velocity of a beam of light is inversely proportional to it's refractive index, it is a simple matter to obtain the following equation for the optical rotation per unit length of a given medium:

$$\alpha = (\pi/\lambda)(n^L - n^R) \qquad (1.1.2)$$

In the above ($n^L - n^R$), the difference of the respective refractive indices for left and right cicularly polarized light, is known as the circular birefringence of the medium. Thus optical rotation is a consequence of circular birefringence.

This classical argument can be further developed using quantum mechanical arguments. The refractive index of a substance is related through Maxwell's equation to the dielectric constant, which is in turn related to the polarization of the substance. From quantum mechanical arguments concerning the polarization of a substance caused by the time derivative of the magnetic field, one can deduce the Rosenfeld equation (1928)[9]:

$$\alpha = N(2\omega^2\mu_o/3\hbar)\sum_n \frac{R_{no}}{(\omega_{no}^2 - \omega^2)} \qquad (1.1.3)$$

where R_{no} is the rotational strength of the $n \longleftarrow 0$ transition. This provides a theoretical explanation for the form of (1.1.1).

Optical rotation measurements are routinely made on all optically active compounds. The device used is called a

polarimeter, which has a configuration very similar to that used by Biot (Fig. 1.1) The experimental quantity which is measured is the specific optical rotatory power, or the optical rotation. This is related to the measured optical rotation angle by the following expression:-

$$[\alpha] = \frac{\alpha V}{ml} \qquad (1.1.4)$$

where V is the volume containing a mass m of the optically active substance, and l is the path length. This is a fundamental property of the molecule, and can be either (+) or (-), depending on which stereochemical form of the species is used. Molecules giving these signs are designated the D or L forms respectively.

The main uses of optical rotation measurements are to identify whether we have the D or L form of a molecule, and to check the optical purity of a sample, i.e. to check that we have only one form of a molecule present in a sample.[10]

A phenomenon closely associated with optical rotation is optical rotary dispersion. This originates in the variation of the optical rotation angle as we vary the frequency of the incident radiation, and was first identified by Biot in 1812.

(ii) The first observation of magnetic optical rotation was made by Faraday in 1846. He first measured the effect (subsequently termed the Faraday effect) using a rod of lead borate glass which was placed between the poles of an electromagnet, with the direction of propagation of the light beam parallel to the applied magnetic field. Further studies by Verdet in 1854 showed that the following law

holds for the optical rotation angle per unit path length:-

$$\alpha = VB\cos\Theta \qquad (1.1.5)$$

where B is the magnitude of the applied magnetic field, Θ is the angle between the magnetic field and the light beam and V is the Verdet constant. V in general depends on both the temperature and the wavelength.

As well as (1.1.4), magnetic optical rotation also obeys (1.1.2). This can be used as the starting point for a quantum mechanical derivation of equation (1.1.4). As in the natural case, we use the relatonship between the refractive index and the polarization of the medium to express the former in terms of the polarizability tensor. We then consider the perturbation of the polarizability tensor caused by the applied magnetic field. This yields the following expression for the optical rotation [18]

$$\Delta\Theta = \frac{-u_0 c l N B_z}{3h}\left[\frac{2w_{jn}w^2}{\hbar}(f^2-g^2)A + w^2 f\left(B + \frac{C}{kT}\right)\right] \qquad (1.1.6)$$

In the above, l is the path length of the beam, N is the total number of molecules per unit volume, B_z is the magnetic field strength, f and g are the lineshape functions (see Section 3.6) and the Faraday A,B, and C terms are

$$A = \frac{3}{d_n}\sum_n (m_{jz} - m_{nz})\,\mathrm{Im}(\langle n|u_x|j\rangle\langle j|u_y|n\rangle) \qquad (1.1.7a)$$

$$B = \frac{3}{d_n}\times \mathrm{Im}\left[\sum_{k\neq j}\frac{\langle k|m_z|n\rangle}{\hbar w_{kn}}\left(\langle n|u_x|j\rangle\langle j|u_y|k\rangle - \langle n|u_y|j\rangle\langle j|u_x|k\rangle\right)\right.$$

$$\left. + \sum_{k\neq j}\frac{\langle j|m_z|k\rangle}{\hbar w_{kj}}\left(\langle n|u_x|j\rangle\langle k|u_y|n\rangle - \langle n|u_y|j\rangle\langle k|u_x|n\rangle\right)\right] \qquad (1.1.7b)$$

$$C = \frac{3}{d_n}\sum_n m_{nz}\,\mathrm{Im}(\langle n|u_x|j\rangle\langle j|u_y|n\rangle) \qquad (1.1.7c)$$

(d_n is the degeneracy of the ground molecular state. For an explanation of the rest of the notation used in (1.1.6), see Section 2.2.)

From the Faraday terms, we see that there are three separate mechanisms for generating magnetic optical rotation. These are when there is a ground state magnetic moment, an excited state magnetic moment, or when there exists a transition magnetic dipole moment between two different states. The mechanisms originating from the A and C terms have very distinctive spectral lineshapes.[11](see Fig. 1.2)

Fig. 1.2 Lineshape functions for optical rotation generated by the Faraday A and C terms.

Because of this, ground state and excited state degeneracy can be readily identified by studying the magnetic optical rotation spectra of a molecule. By performing specific calculations, one can also deduce information about the nature of these degenerate states. Thus such spectra are a valuable tool in the elucidation of the configuration of the electronic states of a molecule.[12] (See also magnetic circular dichroism below.)

(b) C.D. and M.C.D.

(i) As we have seen, the difference in the transmission properties of right and left cicularly polarized light through an optically active medium gives rise to the optical rotation of a plane polarized beam of light. One might expect to see analagous effects caused by the difference in the absorption properties of right and left circularly polarized light. Such an effect was first observed by Haidinger in amethyst quartz crystals in 1848, and by Cotton in solutions of copper chromium tartrate in 1895.

The effect they actually observed was that a beam of light which was initially linearly polarized, became elliptically polarized after it had been passed through an optically active absorbing medium. To explain this, we again consider linearly polarized light as a superposition of two equal amplitude circularly polarized beams. If the right and left components are absorbed differently by the optically active medium, then their superposition would indeed produce an elliptically polarized beam.(see Fig. 1.3)

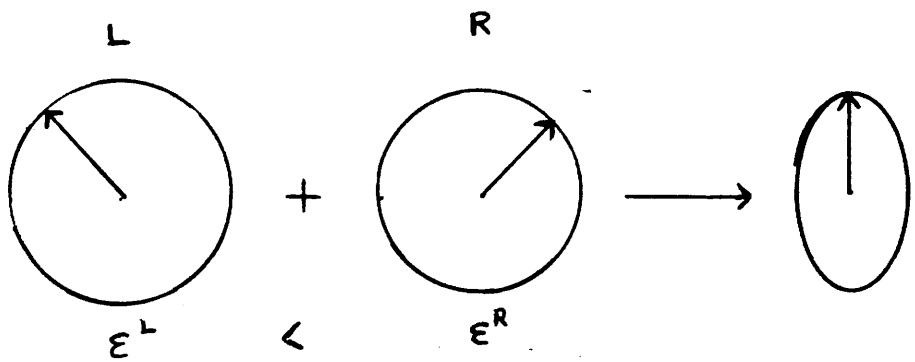

Fig. 1.3 Production of elliptically polarized light from circularly polarized light by circular dichroism.

From this figure, we can see that the ellipticity ψ of the emergent beam is given by

$$\tan\psi = (E_R - E_L)/(E_R + E_L) \qquad (1.1.8)$$

From a simple consideration of the absorption indices n'^R and n'^L for the right and left circularly polarized beams, and assuming that the ellipticity is small, we can write

$$\psi = (\pi/\lambda)x(n'^L - n'^R) \qquad (1.1.9)$$

From this, we see that the ellipticity depends on the quantity $(n'^L - n'^R)$, the circular dichroism of the medium. Hence the name given to the phenomenon is Circular Dichroism (C.D.).

There are two experimental quantities which are usually measured in C.D. experiments on an optically active substance. The first of these is the specific ellipticity, which is given by

$$[\psi] = \frac{V\psi}{ml} \qquad (1.1.10)$$

where m is the mass of substance, V is it's volume, l is the path length and ψ is the measured ellipticity. The second quantity, which is nowadays more common, is the decadic molar extinction coefficient for right and left cicularly polarized light respectively.

This is given by

$$\varepsilon = \frac{1}{cl}\log\frac{I_i}{I_f} \qquad (1.1.11)$$

where c is the molarity of the substance and l is the path length. These two measurements are connected through the following relationship:

$$[\theta] = 3300(\varepsilon^L - \varepsilon^R) = 3300\Delta\varepsilon \qquad (1.1.12)$$

Another quantity which is often quoted is the dissymmetry

factor g first defined by Kuhn in 1930. g is defined as

$$g = \frac{\varepsilon^L - \varepsilon^R}{1/2(\varepsilon^L + \varepsilon^R)} \qquad (1.1.13)$$

Circular dichroism spectra are usually measured using either visible or ultraviolet incident radiation. Since these frequencies correspond to the energy differences between the electronic states of a molecule, it is information about the electronic structure of a molecule which is usually obtained from C.D. studies. Since the stereochemical structure of the molecule determines the nature of the electronic states, one can thus deduce very valuable information on the former. This is especially true when there is a chromophore in the molecule, for then the C.D. spectra can give information on the stereochemical environment of this chromophore. For the special case when the chromophore is a carbonyl group, deductions can be made using the famous "octant rule".[13]

(ii) The magnetic analogue of C.D. is called Magnetic Circular Dichroism (M.C.D.). The molecular mechanism which generates this effect is the Zeeman splitting of degenerate electronic states.[14] Now transitions between different components of degenerate states are mediated by either right or left circularly polarized light. Thus the Zeeman splitting causes slight differences between the absorption of left and right circularly polarized light. A detailed quantum mechanical treatment produces an expression for the ellipticity of the transmitted beam which is very similar to that obtained for the optical rotation angle, namely[15]

$$\eta = \frac{-\mu_o c l N B_z}{3h}\left[\frac{4w_{jn}w^2(fg)A}{h} + w^2 g\left(B + \frac{C}{kT}\right)\right] \qquad (1.1.14)$$

The terms A,B and C are the Faraday terms defined earlier. The presence of different combinations of the lineshape functions in (1.1.14) compared to those in (1.1.6) should be noted.[16] Because of this, the experimentally observed lineshapes for M.C.D. signals corresponding to the A and C terms are different from those for optical rotation. The appropriate lineshapes are shown below. (Fig. 1.4)

Fig. 1.4 Lineshape functions for circular dichroism generated by the Faraday A and C terms.

M.C.D. is one of the main tools for obtaining detailed information about the ground and excited electronic states of a molecule. It not only extends the measurement of Zeeman splittings to many molecules for which conventional measurements are impossible because of band-width problems, but allows detailed assignments of symmetry species to the ground and excited electronic states, often utilizing information available from vibronic transitions. It has been most fruitfully used in the study of inorganic complexes.[17,18] However, important information has been obtained about certain classes of organic compounds, including porphyrins.[19]

(Note: Circular dichroism is also involved in a phenomenon

called the Cotton effect. This involves circular dichroism accompanied by anomalous optical rotary dispersion, and occurs when the incident light frequency falls within an absorption band.)

(c) V.C.D. and M.V.C.D.

As we have seen, conventional C.D and M.C.D. measurements involve the use of visible or uv incident radiation. Thus they mainly yield information concerning the electronic structure of the molecule. Until fairly recently, it was difficult to measure circular dichroism using infrared incident radiation, although infrared optical rotation had been observed by Biot and Mellini in 1836. The main problem was that because the magnitude of optical activity effects depend on the incident radiation frequency, using infrared meant that the effects were too small to be observed. However, such experiments are now being performed, many of the technical problems having been overcome. The first observation of Vibrational C.D. (V.C.D.) was made by Dudley, Mason and Peacock[20] in 1972. Since then, V.C.D. has become a routine experimental technique.[21,22]

Important information concerning the vibrational structure and molecular conformation of a molecule can be obtained from V.C.D. experiments. Thus this field are likely to be of increasing importance in the future. It's one serious limitation seems to be the difficulty in obtaining spectra when the frequency goes below about 900 cm^{-1}.

In the analagous field of magnetic V.C.D., the first observation was made by Keiderling[23] in 1981.

(d) R.O.A. and M.R.O.A.

Comparatively recently, optical activity has been detected in the field of Raman scattering. As in the case of absorption spectra, both natural and magnetic optical activity have been observed. These phenomena are called respectively Raman Optical Activity (R.O.A.) and Magnetic Raman Optical Activity (M.R.O.A.).

To measure R.O.A., one performs a Raman scattering experiment on a chiral molecule using both right and left circularly polarized light. The scattered intensity is measured separately for the two circularities (involving the measurement of both the polarized and depolarized components.) We then subtract the Raman spectrum obtained from the left circularly polarized light from that obtained from the right, giving a difference spectra $I^R - I^L$ for species which exhibit the effect. For the bands in the difference spectra we calculate the following dimensionless quantities.

$$\Delta x = \frac{I_x^R - I_x^L}{I_x^R + I_x^L} \qquad \Delta z = \frac{I_z^R - I_z^L}{I_z^R + I_z^L} \qquad (1.1.14)$$

These are respectively the polarized and depolarized Circular Intensity Differentials (C.I.D.s). When we are measuring the magnetic analogue, these are called the Magnetic C.I.D.s, or M.C.I.D.s.

Before they had been observed, both of these effects had been predicted in the seminal papers of Barron and Buckingham.[24,25]

The first observation of Raman Optical Activity was made by Barron, Buckingham and Bogaard in the Raman spectra of 1-

phenylethylamine in 1973[26]. Since then, R.O.A. spectra have been obtained for many molecules.[27] As mentioned above, much information about vibrational structure and molecular conformation can be obtained from V.C.D. However, as also already mentioned, it cannot penetrate beyond 900cm^{-1}. R.O.A. on the hand can be measured down to 50^{-1}, and is thus a complimentary technique to V.C.D.

However, in order to elicit all the information potentially available, a detailed theory is required. Such a theory, the bond polarizability theory, has begun to be developed for R.O.A. It was originated by the work of Barron[28], and has been refined and applied by Barron, Clark et al.[29,30]

One of the limitations of early R.O.A. experiments was the difficulty in measuring polarized C.I.D.s, due to the presence of artifacts. Recently however, these experimental difficulties have been overcome, and polarized C.I.D.s can now be obtained.[31] Their measurement has allowed a further application of R.O.A. to be developed. From a theoretical treatment, it emerges that the polarized C.I.D. for certain bands should be exactly double the depolarized C.I.D. However, this depends upon the bonds being axially symmetric. Thus the presence of this feature in a molecule's R.O.A. spectra provides evidence for axially symmetric bonds in that molecule.

Magnetic Raman Optical was first observed by Barron[32], in the resonance Raman spectrum of ferrocytochrome c. At the start of the present project, no detailed theory had emerged for calculating specific spectral features.

1.2 Summary of Thesis

When this Ph.D. project was started, it's aim was to account for the M.R.O.A. spectrum of ferrocytochrome c, and to try and discover other molecules which displayed magnetic optical activity. As will be seen in the following pages, both of these aims have been realised with at least some success.

After the introductory chapter, the second chapter contains all the established background theory.
First of all the basic expressions for the molecular scattering tensors are developed (a slightly modified approach is used when vibronic coupling expressions are considered.) Included are expressions for the magnetically perturbed polarizability tensor. A brief discussion of the conditions necessary for this to have an observable magnitude constitutes, along with the modification mentioned above, the only original work in this chapter. This is followed by the derivation of the basic expressions for the scattering observables which are of interest to us. Finally, a summary of irreducible tensor methods that are used later on in the thesis is presented.

The remainder of the thesis contains the main original work done during the research project.

Chapter 3 contains the main new theory in the thesis. First of all, we build upon the different approach taken in dealing with the vibronic polarizability expressions in Chapter 2. This leads to the derivation of simple formulae which greatly facilitate the calculation of polarizability and perturbed polarizability tensor patterns. From this

development, we also obtain the relationship between the 0-0 and 0-1 vibronic scattering pathways for both the unperturbed and perturbed polarizability tensors. Secondly, irreducible tensor methods are used to deduce some properties of the polarizability tensor for the case of molecules with degenerate ground states. These properties are useful when calculating the Raman E.P.R. spectra. Then a slightly more detailed development of the M.R.O.A. is presented, showing the two different contributory mechanisms. This is followed by some simplification of these expressions. The chapter is rounded off by a consideration of the frequency dependance of the various scattering observables.

Chapter 4 starts with a description of the experimental set-up. Following this, a brief description of the preparation of samples is given. Finally, some of the problems involved in measuring M.R.O.A. are discussed.

The remainder of the thesis contains work on specific systems.

Chapter 5 contains calculations on the Raman spectra of ferrocytochrome c, followed by comparison with experiment.

Chapter 6 contains the main new experimental results of the thesis. These consist of the discovery of the phenomenon of Raman E.P.R for three complex metal ions. These results are followed by calculations on the Raman spectra of iridium hexachloride, followed by comparison with experiment.

Chapter 7 contains two parts. The first involves general considerations concerning atomic Rayleigh scattering. The second contains calculations involving the resonance Rayleigh scattering of atomic sodium.

Chapter 8 is concerned with using the formulae developed earlier to deduce information on the Raman scattering which is independent of the molecule and dependent only on the molecular point group. This is done for all the simply reducible point groups, apart from O.

Chapter 9 consists of two parts. The first part summarises the new developments made during the course of the thesis. The second part contains predictions for possible future work in the field of M.R.O.A., and gives an account of M.R.O.A. studies performed between the end of the present project and the present.

Chapter 1 : References

(Because of their frequent occurence, the following references are designated the following abbreviations.
[A] - L.D. Barron, Molecular Light Scattering and Optical Activity, Cambridge University Press, Cambridge, 1982.
[B] - L.D. Landau and E.M. Lifshitz, The Classical Theory of Fields, 4th edition, Pergamon Press, Oxford.
[C] - J.S. Griffith, The Irreducible Tensor Method for Molecular Point Groups, Prentice-Hall, New Jersey.
[D] - B.L. Silver, Irreducible Tensor Methods, Academic Press, New York.)

1) E.L. Eliel, Stereochemistry of Carbon Compounds, Magraw-Hill, New York, 1966
2) Morrison and Boyd, Organic Chemistry, Allyn and Bacon, Boston, 1973, p.120.
3) See ref. 2, p.124.
4) [A], preface
5) L.D. Barron, Chem. Phys. Letts. 123,423(1986).
6) [A], p.14
7) [A], p.17, 147-148
8) [A]
9) P.W. Atkins, Molecular Quantum Mechanics, Vol.II, Clarendon Press, Oxford, p.466(277)
10) See ref. 1
11) [A],p.292-293
12) [A], p.8
13) W. Moffit, R. Woodward, R.B. Moscowitz, W. Klyne and C. Djerassi, J. Amer. Chem Soc. 83,4013(1961)

14) [A] - p.12-14

15) [A] - p.293(6.2.2a)

16) [A] - p.296-297

17) [A] - p.14

18) A.D. Buckingham and P.J. Stephens, A. Rev. Phys. Chem. 17,399(1966)

19) [A] - p.298-301

20) E.C. Hsu and G. Holzworth, J. Chem. Phys. 59,4678(1973)

21) L.A. Nafie, T.A. Keiderling and P.J. Stephens, J. Amer. Chem. Soc. 98,2715(1976)

22) L.A. Nafie, P.L. Polavarapu, J. Chem. Phys. 75,2935 & 2945(1981)

23) T.A. Kiederling, J. Chem. Phys. 75,3639(1981)

24) L.D. Barron and A.D. Buckingham, Mol. Phys. 20,1111(1971)

25) L.D. Barron and A.D. Buckingham, Mol. Phys. 23,145(1972)

26) L.D. Barron, M.P. Bogaard and A.D. Buckingham, J. Amer. Chem. Soc. 95,603(1973)

27) L.D. Barron and J. Vrbancich, Topics in Current Chemistry. 12,151(1984)

28) L.D. Barron and A.D. Buckingham, J. Amer. Chem. Soc. 96,4769(1974)

29) L.D. Barron and A.D. Buckingham, J. Amer. Chem. Soc.96,4769(1974)

30) L.D. Barron and B.P. Clark, Mol. Phys. Soc.46,539(1982)

31) L.D. Barron, J.R. Escribano and J.F. Torrance, Polarized Raman Optical Activity and the Bond Polarizability Theory, Mol. Phys.-- in the press.

32) L.D. Barron Nature. 257,372(1975)

CHAPTER 2

GENERAL THEORETICAL BACKGROUND TO MOLECULAR SCATTERING

2.1 Introduction

In this chapter, the general theoretical framework upon which the calculations in the subsequent chapters are based will be presented. First of all, quantum mechanical expressions for the molecular scattering tensors are calculated. This is done initially for a general system, and then for the specific case of vibronic coupling (based on the work of Albrecht[1]). Following this, the expressions for the Rayleigh and Raman scattering intensities in terms of the scattering tensors are calculated. Using these, the general equations governing magnetic optical activity (both Rayleigh and Raman) are calculated.

After this, various general properties of the scattering tensors are developed. These include magnetically perturbed tensors, line shape functions etc.

The remainder of the chapter is devoted to a short summary of the irreducible tensor methods which will be used throughout the thesis. This will include equations for the full rotation group and both simply and non-simply reducible point groups.

The approach taken in this chapter follows closely that of Barron's review article[2], which in turn is based on the papers of Barron and Buckingham, which inaugurated the subject of magnetic Raman optical activity.

2.2 Calculation of the Basic Quantum Mechanical Expressions for the Molecular Scattering Tensors

2.2.1 Introduction

This section is devoted to the calculation of quantum mechanical expressions for the molecular scattering tensors in terms of molecular wave functions. Before starting to derive the expressions, some general points on the approach to be taken should be noted.

The process with which we are concerned is the scattering of an incident light beam by a liquid sample. This scattering originates in the induction of oscillating multipole moments in the sample by the incident electromagnetic wave. These oscillating moments then produce electromagnetic radiation, which constitutes the scattered light which we observe. There are various contributions to this radiation e.g. electric dipole, electric quadrupole, magnetic dipole etc.[3] In the particular case which we are considering, the dominant contribution to the scattered intensity is that arising from the induced electric dipole moment. Therefore in what follows we shall confine ourselves solely to this contribution.

The first step in calculating the scattered intensity is to obtain an expression, in terms of molecular wave functions, for the induced electric dipole moment. We do this within a semi-classical framework, i.e. we treat the the electromagnetic field classically and the molecular scattering system quantum mechanically.

At this stage, it is necessary to introduce some notation

and definitions. These follow in the next section.

2.2.2 Notation and definitions

Notation Throughout what follows, S.I. units are used. Cartesian tensor notation is also used throughout, where appropriate. Under this system, any Greek symbol takes on the values x,y and z, and vectors are written as first rank tensors, i.e. a vector $\underline{A}$ is written as A_α. The appearance of a repeated Greek symbol in an expression means that a summation over x, y and z is to be performed, e.g.

$$A_\alpha B_\alpha = AxBx + AyBy + AzBz \qquad (2.2.1)$$

A quantity which is made use of later is the first rank antisymmetric pseudotensor $\varepsilon_{\alpha\beta\gamma}$. This takes the values +1 and -1, depending on whether $\alpha\beta\gamma$ is an even or an odd permutation of xyz respectively. From this definition it is easily deduced that interchanging any pair of symbols changes it's sign. It is most commonly met in the definition of the vector product i.e.

$$[\underline{A} \times \underline{B}]_\alpha = \varepsilon_{\alpha\beta\gamma} A_\beta B_\gamma \qquad (2.2.2)$$

N or n denotes initial state, M or m denotes final state. J or j denotes the excited state involved in the virtual transition from the ground state. Finally, K or k denotes the excited state involved in vibronic mixing with J or j. Extra notation will be introduced as it is needed.

Definitions For any collection of charges, we define the magnetic and electric dipole moments operators respectively to be[4,5]

$$m_\alpha = \sum_i e_i/2m_i (l_{i\alpha} + g_i s_{i\alpha}) \qquad (2.2.3)$$

$$u_\alpha = \sum_i e_i r_{i\alpha} \qquad (2.2.4)$$

where

i = the i^{th} particle

$r_{i\alpha}$ = the position vector w.r.t. some chosen axis system

e_i = the charge

$l_{i\alpha}$ = the orbital angular momentum vector

$s_{i\alpha}$ = the spin angular momentum vector

g_i = the electronic g-factor

(2.2.5)

Other definitions will be introduced in the course of the development.

2.2.3 Derivation of the general polarizability expressions

In the absence of external electric and magnetic fields, the quantum states Ψ_n of a molecular system satisfy the time dependent Schrodinger equation[6]

$$\mathcal{H}_o \Psi_n = -h/i \frac{\partial \Psi_n}{\partial t} \qquad (2.2.6)$$

where

$\mathcal{H}_o$ = the Hamiltonian of the system.

We assume that the Hamiltonian is independent of time. We further assume that we have a complete orthonormal set of solutions of (2.3.1), of the form $\psi_n(q)\, e^{i w_n t}$ which satisfy

$$\mathcal{H}_o \psi_n = E_n \psi_n \qquad (2.2.7a)$$

where

E_n = the energy of the n^{th} state ψ_n

q = the spatial coordinates of the system (2.2.7b)

$w_n = E_n/\hbar$

We now apply to this system a plane electromagnetic wave

propagating along the z-direction, where the origin of our reference frame is taken to be some point within the molecular system (note that the direction of propagation of the incident light wave defines the +ve z-direction). The electric and magnetic field components of the incident beam are respectively[7,8]

$$\tilde{E}_\alpha = \tilde{E}_\alpha \exp[-i\omega(t-z/c)] \qquad (2.2.8a)$$

$$\tilde{B}_\alpha = 1/c\, \epsilon_{\alpha\beta\gamma} k_\beta E_\gamma \qquad (2.2.8b)$$

where ω is the angular frequency of the light beam and $\underline{k}$ is the direction of propagation.

Classically, the interaction energy of the electric field component of the incident light beam with the electric dipole moment of the molecule is[9]

$$W = -(\tilde{E}_\alpha)_{(0)} u_\alpha \qquad (2.2.9)$$

where

$$(\tilde{E}_\alpha)_{(0)} = [(\tilde{E}_\alpha)^0 e^{i\omega t} + (\tilde{E}_\alpha)^{*0} e^{-i\omega t}] \qquad (2.2.10)$$

Thus the perturbation term $\mathcal{H}'$ in the Hamiltonian for the field and the molecule together is given by

$$\mathcal{H}' = -(\tilde{E}_\alpha)_0 u_\alpha \qquad (2.2.11)$$

where u is the electric dipole moment operator defined earlier.

The Schrodinger equation for the perturbed system is now

$$(\mathcal{H}_0 - ih\frac{\partial}{\partial t})|n'\rangle = -\mathcal{H}'|n'\rangle \qquad (2.2.12)$$

We next derive the general expressions for the polarizability tensors in terms of molecular wavefunctions. The development given here is based on the approaches used by Placzek[10] (1934) and by Born and Huang[11] (1954).

We assume that the wave function $|n'\rangle$ for the perturbed system can be written in the form

$$|n'\rangle = |n\rangle + \sum_{j\neq n} [\, a_{jn\alpha}(\tilde{E}_\alpha) + b_{jn\alpha}(\tilde{E}^*_\alpha) \,]|j\rangle\, e^{-i\omega_n t} \qquad (2.2.13)$$

where the coefficients $a_{jn\alpha}$ and $b_{jn\alpha}$ are constants. To determine their values, we substitute (2.3.8) into (2.3.7). This gives

$$(W_n - ih\cdot - iW_n)|n\rangle - ih\sum_{j\neq n}\{[a_{jn\alpha}(\tilde{E}_\alpha) + b_{jn\alpha}(\tilde{E}_\alpha^*)]|j\rangle + -iW_n[a_{jn\alpha}(\tilde{E}_\alpha) + b_{jn\alpha}(\tilde{E}_\alpha^*)]|j\rangle\ e^{-iW_n t}\}$$

$$= -(\tilde{E}_\alpha)\,u_\alpha\,|n\rangle + \sum_{j\neq n}[a_{jn\alpha}(\tilde{E}_\alpha) + b_{jn\alpha}(\tilde{E}_\alpha^*)]|j\rangle\ e^{-iW_n t} \quad (2.2.14)$$

If in (2.2.14) we ignore the terms above first order in the field, then after multiplying from the left by $\langle m|$, integrating and equating the coefficients of e^{iWt} and e^{-iWt}, we obtain

$$a_{jn\alpha} = \langle j|u_\alpha|n\rangle/2h(W_{jn}-W) \quad (2.2.15a)$$

$$b_{jn\alpha} = \langle j|u_\alpha|n\rangle/2h(W_{jn}+W) \quad (2.2.15b)$$

Thus the wavefunctions for the perturbed system have the form

$$|n'\rangle = |n\rangle + \sum_{j\neq n}\frac{\langle j|u_\alpha|n\rangle E_\alpha}{2h}\left(\frac{e^{-iWt}}{(W_{jn}-W)} + \frac{e^{iWt}}{(W_{jn}+W)}\right)|j\rangle\ e^{-iW_n t} \quad (2.2.16)$$

In the case of Rayleigh scattering, we now simply calculate the expectation value of the electric dipole moment operator for the state given by (2.3.11), and from this we obtain the desired expression for the electric polarizability tensor. For Raman scattering, we have to calculate the corresponding transition dipole moment between the initial state m and the final state n. Since this is in general complex, the appropriate expression for the real transition dipole moment is[12]

$$(u_\alpha)_{mn} = \langle m|u_\alpha|n\rangle + \langle m|u_\alpha|n\rangle^*$$

$$= 2\mathrm{Re}(\langle m|u_\alpha|n\rangle) \quad (2.2.17)$$

Using our perturbed wave functions, we therefore have

$$(u_\alpha)_{m'n'} = 2\mathrm{Re}\left[\left[\langle m| + \sum_{j\neq m}\left(\frac{\tilde{E}_\beta\langle j|u_\beta|m\rangle^*}{2h}\left\{\frac{e^{iwt}}{(w_{jm}-w)} + \frac{e^{-iwt}}{(w_{jm}+w)}\right\}\langle j|\right)\right]\right.$$

$$\left.\times\left[e^{iw_mt}u_\alpha\left(|n\rangle + \sum_{j\neq n}\frac{\tilde{E}_\gamma\langle j|u_\gamma|n\rangle^*}{2h}\left\{\frac{e^{-iwt}}{(w_{jn}-w)} + \frac{e^{iwt}}{(w_{jn}+w)}\right\}\langle j|\right)e^{-iw_nt}\right)\right]\right]$$

$$= 2\mathrm{Re}\left(e^{iw_{mn}t}\langle m|u_\alpha|n\rangle\right.$$

$$+ \sum_{\substack{j\neq\\ m}}\left[\frac{\langle m|u_\beta|j\rangle\langle j|u_\gamma|n\rangle\tilde{E}_\beta e^{i(w+w_{mn})t}}{2h(w_{jm}-w)}\right.$$

$$\left.+ \frac{\langle m|u_\beta|j\rangle\langle j|u_\gamma|n\rangle E\, e^{-i(w-w_{mn})t}}{2h(w_{jm}+w)}\right]$$

$$+ \sum_{\substack{j\neq\\ n}}\left[\frac{\langle m|u_\beta|j\rangle\langle j|u_\gamma|n\rangle\tilde{E}_\gamma e^{-i(w-w_{mn})t}}{2h(w_{jn}-w)}\right.$$

$$\left.\left.+ \frac{\langle m|u_\beta|j\rangle\langle j|u_\gamma|n\rangle E\, e^{-i(w+w_{mn})t}}{2h(w_{jn}+w)}\right]\right) \qquad (2.2.18)$$

+ terms of higher order in the field

We are concerned with the anti-Stokes and Stokes contributions to the scattered radiation. Because of this, we need only consider terms linear in the field which have the frequency factor $e^{-i(w-w_{mn})t}$.[13] Thus we have

$$(u_\alpha)_{mn} = \qquad (2.2.19)$$

$$2\mathrm{Re}\left(\sum_{\substack{j\neq\\ m,n}}\left[\frac{\langle m|u_\alpha|j\rangle\langle j|u_\beta|n\rangle}{2h(w_{jn}-w)} + \frac{\langle m|u_\alpha|j\rangle\langle j|u_\beta|n\rangle}{2h(w_{jn}+w)}\right]\tilde{E}_\beta e^{-i(w-w_{mn})t} + \ldots\right)$$

In the above we have included j=m,n for both terms. This is permissible because we are dealing mainly with vibrational Raman, for which case the terms omitted are usually zero.

Thus we can write the complex dipole moment as

$$(u_\alpha)_{m'n'} = \tilde{a}_{\alpha\beta}\tilde{E}_\beta \qquad (2.2.20)$$

Taking the real part of expression (2.2.20) yields (2.2.19). $\tilde{a}_{\alpha\beta}$ is the complex electric polarizability tensor, and as can be seen from (2.2.20), it determines, to first order, the response of a molecule to an applied electric field. This can be modified by making use of the following expression[14]

$$w_{jm}\langle m|u_\alpha|j\rangle\langle j|u_\beta|n\rangle + w_{jn}\langle m|u_\beta|j\rangle\langle j|u_\alpha|n\rangle$$
$$= 1/2(w_{jm}+w_{jn})(\langle m|u_\alpha|j\rangle\langle j|u_\beta|n\rangle + \langle m|u_\beta|j\rangle\langle j|u_\alpha|n\rangle)$$
$$+1/2w_{nm}(\langle m|u_\alpha|j\rangle\langle j|u_\beta|n\rangle-\langle m|u_\beta|j\rangle\langle j|u_\alpha|n\rangle) \qquad (2.2.21)$$

When used in (2.2.19) this gives us

$$(a_{\alpha\beta})_{mn} = 1/2h \sum_{j\neq m,n} 1/(w_{jn}-w)(w_{jm}+w)$$
$$\times [(w_{jn}+w_{jm})\mathrm{Re}(\langle m|u_\alpha|j\rangle\langle j|u_\beta|n\rangle+\langle m|u_\beta|j\rangle\langle j|u_\alpha|n\rangle)$$
$$+ (2w+w_{nm})\mathrm{Re}(\langle m|u_\alpha|j\rangle\langle j|u_\beta|n\rangle-\langle m|u_\beta|j\rangle\langle j|u_\alpha|n\rangle)] \qquad (2.2.22a)$$

$$(a'_{\alpha\beta})_{mn} = -1/2h \sum_{j\neq m,n} 1/(w_{jn}-w)(w_{jm}+w)$$
$$\times [(w_{jn}+w_{jm})\mathrm{Im}(\langle m|u_\alpha|j\rangle\langle j|u_\beta|n\rangle+\langle m|u_\beta|j\rangle\langle j|u_\alpha|n\rangle)$$
$$+ (2w+w_{nm})\mathrm{Im}(\langle m|u_\alpha|j\rangle\langle j|u_\beta|n\rangle-\langle m|u_\beta|j\rangle\langle j|u_\alpha|n\rangle)] \qquad (2.2.22b)$$

where $a_{\alpha\beta}$ and $a'_{\alpha\beta}$ are the real and imaginary parts of the polarizability tensor. The complex polarizability is expressed in terms of these as

$$(\tilde{a}_{\alpha\beta})_{mn} = (a_{\alpha\beta})_{mn} - i(a'_{\alpha\beta})_{mn} \qquad (2.2.23)$$

Inspection of the above expressions show that both the real and imaginary parts of the polarizability contain a symmetric and an antisymmetric part. Thus it is possible for antisymmetric scattering to occur with the imaginary part of the polarizability zero.

In the next section, the above expressions are developed to include vibronic coupling.

2.3 Vibronic Coupling Expressions for the Polarizability Tensors

2.3.1 Introduction

In the expressions developed in the last section, we were dealing with general molecular states $|n\rangle$ without going into any detail about the states. In this section we are going to consider these states in more detail. We shall see that if we use the adiabatic approximation, the expressions as they stand are inadequate for the generation of vibrational Raman intensities. For this reason, it is necessary to include vibronic coupling. This is done later in this section using the crudest of the adiabatic approximations, the Herzberg-Teller approximation.

2.3.2 Specification of quantum states for a molecular system

The molecular states $|n\rangle$ dealt with in the last section were assumed to be exact wave functions of the molecule,depending on both the electronic and nuclear positions, i.e.

$$|n\rangle = |n(\underline{r},\underline{R})\rangle \qquad (2.3.1)$$

with $\underline{r}$ and $\underline{R}$ representing the electronic and nuclear coordinates respectively.

They therefore satisfy the following equation[15]

$$[\, T(\underline{r}) + T(\underline{R}) + V(\underline{r},\underline{R}) + V(\underline{R}) \,]|n\rangle = W(\underline{r},\underline{R})|n\rangle \qquad (2.3.2)$$

where $T(\underline{r})$ and $T(\underline{R})$ are respectively the kinetic energy operators for the electrons and nuclei in the molecule, $V(\underline{r},\underline{R})$ includes the potential energy terms for the electron

-electron and electron-nuclei interactions and $V(\underline{R})$ is the potential energy for the nuclear-nuclear interactions. In general this is impossible to solve, so we must resort to some approximation.

The first approximation normally applied is the adiabatic approximation. Under this approximation, we write $|n\rangle$ as

$$|n(\underline{r},\underline{R})\rangle = |n_e(\underline{r},\underline{R})\rangle|n_v(\underline{R})\rangle \qquad (2.3.3)$$

The electronic part of the wavefunction, $|n_e(\underline{r},\underline{R})\rangle$, satisfies the following equation[16]

$$H(\underline{r},\underline{R})|n_e\rangle = w_e(\underline{R})|n_e\rangle \qquad (2.3.4)$$

where $$H(\underline{r},\underline{R}) = T(\underline{r}) + V(\underline{r},\underline{R}) \qquad (2.3.5)$$

In the above, we treat the nuclear coordinates as if they were fixed, so that they appear as parameters in the solution. As the nuclei move, they cause a change in the form of the electronic wavefunction. The vibrational part $|n_v(\underline{R})\rangle$ satisfies a corresponding equation involving only nuclear coordinates.

We next use a much cruder approximation, in order to totally separate the electronic and nuclear coordinates in the zeroth order. (Although coupling of the two is involved from first order upwards).

The approximation we use is the Herzberg-Teller approximation. In this approximation, we expand the Hamiltonian (2.3.5) as a power series in the normal coordinates[17,18] i.e.

$$H(\underline{r},\underline{R}) \qquad (2.3.6)$$
$$= H(\underline{r},\underline{R}) + \sum_{p} (\partial H/\partial Q_p)_o Q_p + \sum_{p,q} (\partial^2 H/\partial Q_p \partial Q_q)_o Q_p Q_q) + \ldots.$$

We treat the first term as the unperturbed Hamiltonian of the system. This corresponds to treating the equilibrium nuclear coordinates as fixed and solving the electronic

Schrodinger equation using these. The crudeness of the approximation lies in the use only of the first order term as the perturbation. In this section we follow the standard procedure and use only this first term. In the next chapter, we will see that it is not necessary to make this gross approximation.

Using the above approximations, we write the wavefunction $|j\rangle = |j_e j_v\rangle$ in the form

$$|j_e j_v\rangle = |j_e^{(o)} j_v\rangle + (1/h)\sum_{k \neq j} \frac{\langle k_e^{(o)} k_v | H_Q Q_p | j_e^{(o)} j_v\rangle}{w_j^{(o)} - w_k^{(o)}} |k_e^{(o)} k_v\rangle \qquad (2.3.7)$$

(in the above the $^{(o)}$ signifies that we are using the equilibrium nuclear coordinates. We also use the abbreviation H_Q for the term $(\partial H/\partial Q_p)_o$.)

It will be noted that this is a slightly different approach from that taken in ref. [A]. There, only the perturbation to the electronic state j_e is considered. However, it will be seen later that this leads to considerable simplifications.

With the same approximations, the energy of the state $|j\rangle$ becomes

$$hw_j = hw_{j_e j_v} + \sum_{j \neq n} \langle j_e^{(o)} j_v | H_Q Q | j_e^{(o)} j_v\rangle + \ldots . \qquad (2.3.8)$$

Using these perturbed wavefunctions and energies, we now go on to develop further the polarizability expressions.

2.3.3 Vibronic coupling expressions for the electronic polarizability tensors

To obtain the required vibronic expressions, we insert the perturbed wavefunctions and energies into (2.2.22).

Doing this, we obtain the following expressions

$$(\tilde{a}_{\alpha\beta})_{mn} = (\tilde{a}^{s}_{\alpha\beta})_{mn} + (\tilde{a}^{a}_{\alpha\beta})_{mn} \qquad (2.3.9)$$

$$(\tilde{a}^{s}_{\alpha\beta})_{mn} = \sum_{j\neq n} w_{jn}/h(w^{2}_{je}{}_{jv}{}_{ne}{}_{nv} - w^{2})(X^{s}_{\alpha\beta} + Z^{s}_{\alpha\beta}) \qquad (2.3.10a)$$

$$(\tilde{a}^{a}_{\alpha\beta})_{mn} = \sum_{j\neq n} (w/h)(w^{2}_{je}{}_{jv}{}_{ne}{}_{nv} - w^{2})(X^{a}_{\alpha\beta} + Z^{a}_{\alpha\beta}) \qquad (2.3.10b)$$

where

$$X_{\alpha\beta} = \langle me|u_{\alpha}|je\rangle\langle je|u_{\beta}|ne\rangle\langle mv|jv\rangle\langle jv|nv\rangle \qquad (2.3.11)$$

$$Z_{\alpha\beta} = \sum_{k\neq j} \left[\frac{\langle ke|H_{0}|ne\rangle}{hw_{ne}k_{e}} \left(\langle me|u_{\alpha}|je\rangle\langle je|u_{\beta}|ke\rangle \times \langle mv|jv\rangle\langle jv|kv\rangle\langle kv|Q_{p}|nv\rangle \right) \right. \qquad (2.3.12)$$

$$\frac{\langle ke|H_{0}|me\rangle}{hw_{me}k_{e}} \left(\langle ke|u_{\alpha}|je\rangle\langle je|u_{\beta}|ne\rangle \times \langle kv|jv\rangle\langle jv|nv\rangle\langle kv|Q_{p}|mv\rangle \right)$$

$$\frac{\langle ke|H_{0}|je\rangle}{hw_{je}k_{e}} \left(\langle me|u_{\alpha}|je\rangle\langle ke|u_{\beta}|ne\rangle \times \langle mv|jv\rangle\langle kv|nv\rangle\langle kv|Q_{p}|jv\rangle \right)$$

$$\left. \frac{\langle ke|H_{0}|je\rangle}{hw_{je}k_{e}} \left(\langle me|u_{\alpha}|ke\rangle\langle je|u_{\beta}|ne\rangle \times \langle mv|kv\rangle\langle jv|nv\rangle\langle kv|Q_{p}|jv\rangle \right) \right]$$

$$X^{s}_{\alpha\beta} = 1/2(X_{\alpha\beta} + X_{\beta\alpha}) \qquad X^{a}_{\alpha\beta} = 1/2(X_{\alpha\beta} - X_{\beta\alpha}) \qquad (2.3.13a)$$

$$Z^{s}_{\alpha\beta} = 1/2(Z_{\alpha\beta} + Z_{\beta\alpha}) \qquad Z^{a}_{\alpha\beta} = 1/2(Z_{\alpha\beta} - Z_{\beta\alpha}) \qquad (2.3.13b)$$

In the above development we have omitted the contribution to the perturbation originating from the vibronic perturbation of the electronic energies. This gives rise to Albrecht's B term.[19] It has been omitted because it is only non-zero for A_1 modes, and in that case the major contribution to the polarizability is made by the X tensor.

(In obtaining the above expressions, we see that the X tensor is the zero-order term, and that the Z tensor originates from the vibronic perturbation of the adiabatic wavefunctions. Thus the X and Z terms are clearly equivalent to Albrecht's A and C terms.[20])

Expressions (2.3.11-12) are similar to, but not identical with, the corresponding expressions in Barron's book.[21]

This is due to the different treatment of the Herzberg-Teller approximation, which we commented on earlier. However, we can invoke closure, since in the above we have an infinite sum involving $|k_v\rangle\langle kv|$. When we do this, the above expressions revert back to those normally quoted. In the remainder of the thesis, we shall use either these expressions or else the expressions which are obtained from these by invoking closure.

Various properties of the X and Z tensors for the case of transparent scattering can be deduced[22]. Since we are mainly interested in resonance Raman, we do not pursue the matter further here.

The above expressions apply not only to Raman scattering but also to Rayleigh scattering. In the latter case, as with the case of totally symmetric modes of vibration, the main contribution comes from the X tensor. However, the X tensor vanishes when we are dealing with non-totally symmetric modes.[23] Thus we see that non-totally symmetric scattering derives its intensity from the Z tensors, which have their origins in vibronic coupling. It is for this reason that it was necessary to introduce vibronic coupling earlier.

2.4 The Magnetically Perturbed Polarizability Tensor

2.4.1 Introduction

In the previous section, expressions for the electronic polarizability tensor were derived. These arose from vibronic coupling, which we treated as a perturbation. Another perturbation, which we consider in this section, is that arising from the presence of an applied static magnetic field. This gives rise to the magnetically perturbed polarizability tensors. These are responsible for producing Raman optical activity in molecules which do not possess a ground state magnetic moment, as we shall see in a later chapter.

2.4.2 Derivation of the expressions for the magnetically Perturbed Polarizability Tensor.

In the presence of a magnetic field, the magnetic dipole moment interacts to give the following contribution to the Hamiltonian[24,25] :

$$H' = -m_\alpha B_\alpha \qquad (2.4.1)$$

With this as the perturbation, we can apply first order perturbation theory as before. There are three different mechanisms by which the perturbation can couple with the molecule. These are via a ground state magnetic moment, an excited state magnetic moment, and a transition dipole moment between two electronic states. These give rise respectively to the Faraday C, A and B terms (1.1.7-9) mentioned in Chapter 1. We shall see later that there is a

separate mechanism for the generation of magnetic optical activity when the molecule has a ground state magnetic moment. Thus we assume here that the ground state magnetic moment is zero. We consider only the effect of the perturbation on the energies of the molecular states, assuming that an excited electronic state of the system possesses a non-zero magnetic dipole moment. We are therefore including only the equivalent of the Faraday A term contribution. We omit the modifications to the wavefunction, which correspond to the Faraday B term contribution. This is because the A term is the dominant contribution. (However, the B term generates a residual contibution even when all the magnetic dipole moments of the system are zero. Hence all molecules in principle exhibit M.R.O.A.)

The effect of the perturbed energies are incorporated in general by using the expression

$$w_{j'n'} = w_{jn} - 1/\hbar \tilde{B}_\alpha (m^j_\alpha - m^n_\alpha) \qquad (2.4.2)$$

However, as we mentioned earlier, we assume that m^n_α is zero. We now insert the modified value for $w_{j'n'}$ into the frequency factor $1/(w^2_{j'n'}-w^2)$. Having done this, we expand the denominator as a power series in the field, and retain only the first term in the field. We then obtain the following expression for the polarizability

$$\tilde{a}_{\alpha\beta}(\tilde{B}_\sigma) = \tilde{a}_{\alpha\beta} + \tilde{a}_{\alpha\beta\sigma}\tilde{B}_\sigma \qquad (2.4.3)$$

where $\tilde{a}_{\alpha\beta}$ is as in 2.3.3 and the symmetric and antisymmetric parts of $\tilde{a}_{\alpha\beta\sigma}$, the magnetically perturbed polarizability tensor, are given by

$$\tilde{a}^s_{\alpha\beta\sigma} = 1/\hbar \sum_{j\neq n} \frac{(w^2_{jn} + w^2)}{\hbar(w^2_{jn}-w^2)^2} \left(X^s_{\alpha\beta} + Z^s_{\alpha\beta} \right) m^j_\sigma \qquad (2.4.4a)$$

$$\tilde{a}^{a}_{\alpha\beta\delta} = 1/\hbar \sum_{j\neq n} \frac{2w_{jn}w}{\hbar(w^2_{jn}-w^2)^2} \left(X^{a}_{\alpha\beta} + Z^{a}_{\alpha\beta} \right) m^{j}_{\delta} \qquad (2.4.4b)$$

These expressions will be used later for the case of molecules with a non-degenerate ground state.

2.4.3 Discussion of the magnetically perturbed polarizability tensor

There are several important general points which can be made from the form of the expressions for $\tilde{a}_{\alpha\beta\delta}$ developed above. The first of these concerns the magnitude of $\tilde{a}_{\alpha\beta}$ relative to $\tilde{a}_{\alpha\beta\delta}$ To investigate this, we consider first of all the contribution to each from a single excited electronic state j_e. From the above, we see that the ratio of the contributions to $\tilde{a}_{\alpha\beta}$ and $\tilde{a}_{\alpha\beta\delta}$ is of the same order of magnitude for both the symmetric and antisymmetric parts. Assuming that w_{jn} is of the same order of magnitude as w, this ratio is approximately

$$\frac{2wm_{\delta}B_{\delta}}{\hbar(w^2_{jn}-w^2)} \qquad (2.4.5)$$

Now $m_{\delta}B_{\delta}$ represents the splitting of the excited electronic state j_e caused by the magnetic field. In order to study the rest of the ratio, we assume that we are not at resonance and that w_{jn} is roughly twice w. Then the frequency term reduces to $4/\hbar w_{jn}$. Now this is the frequency of the electronic transition from the n_e to j_e. This is always much greater than the splitting caused by an applied magnetic field (for a large applied magnetic field, the ratio would be of the order of 10^{-4}). From this comparison, we see that even for a strong magnetic field, it would be

expected that the magnetic polarizability would be roughly a ten-thousandth of the ordinary polarizability. These relative values are reflected in the magnitude of the M.C.I.D.'s, as we shall see later on. The above argument provides an explanation for the fact that M.C.I.D.s have not been observed at transparent frequencies.

For the case of resonance, however, the above ratio is at least an order of magnitude higher, since the denominator becomes very small. From these considerations, we would expect it to be much easier to observe M.C.I.D. for the case of resonance scattering. In fact, the only case where M.C.I.D.s arising from the magnetically perturbed polarizability tensor have been observed has been in the case of resonance Raman scattering.

A further point to note is that it is not sufficient to be in resonance with any excited electronic state for $\tilde{a}_{\alpha\beta\delta}$ to have a reasonable magnitude. The state with which we are in resonance must be a degenerate electronic state. This is because it is essential that we be in resonance with a state with a non-zero magnetic moment. Hence, for most cases, we must be in resonance with an E state. However, this is exactly the condition for good resonance enhancement of non-totally symmetric scattering (see later). Thus the theory predicts that good candidates for exhibiting an M.C.I.D. spectrum are molecules which show strong resonance enhancement of non-totally symmetric modes.

2.5 General Formulae for the Scattered Intensities

2.5.1 Introduction

This section is concerned with deriving the general expressions for the scattered intensities in terms of molecular transition tensors. The approach followed is essentially that covered by Barron[26]. First of all, the Stokes parameters of the incident beam are defined. Following this, the Stokes parameters of the scattered beam are expressed in terms of the Stokes parameters of the incident beam and the molecular transition tensors. These are then used to obtain the formulae for the depolarization ratio and the M.C.I.D.s which will be used in the rest of the thesis.

2.5.2 Stokes parameters for the incident beam

In order to measure the polarization of a light beam, one needs to let it interact with some object and then study the intensities of the transmitted light. Thus the experimental quantities which give information on the polarization of a light beam are quadratics in the field. From a simple analysis, one sees that the appropriate quantities have the form $\tilde{E}_\alpha \tilde{E}^*_\beta$. Using these one can contruct various sets of parameters to describe the polarization state of a monochromatic plane wave light beam.[27] The three main sets of quantities used are the polarization tensor, the Jones vector and the Stokes parameters of the beam. We will make use of the latter set of quantities.

The Stokes parameters of a light beam are defined in terms of the above products of electric field components as follows[28]:

$$S_0 = \tilde{E}_x\tilde{E}_x^* + \tilde{E}_y\tilde{E}_y^* \qquad (2.5.1a)$$

$$S_1 = \tilde{E}_x\tilde{E}_x^* - \tilde{E}_y\tilde{E}_y^* \qquad (2.5.1b)$$

$$S_2 = -(\tilde{E}_x\tilde{E}_y^* + \tilde{E}_y\tilde{E}_x^*) \qquad (2.5.1c)$$

$$S_3 = -i(\tilde{E}_x\tilde{E}_y^* - \tilde{E}_y\tilde{E}_x^*) \qquad (2.5.1d)$$

In terms of the intensity I, the azimuth Θ, the ellipticity η and the degree of polarization P these can be rewritten as[29] (see Fig. 2.1)

$$S_0 = E^{(0)2} \qquad (2.5.2a)$$

$$S_1 = PE^{(0)2}\cos 2\eta \cos 2\Theta \qquad (2.5.2b)$$

$$S_2 = PE^{(0)2}\cos 2\eta \sin 2\theta \qquad (2.5.2c)$$

$$S_3 = PE^{(0)2}\sin 2\eta \qquad (2.5.2d)$$

The Stokes parameters can also be expressed in terms of another set of parameters, namely the degree of circular polarization, the degree of maximum linear polarization and the angle between the principal axis of the polarization ellipse and the y-axis. However, we do not pursue this approach here.[30]

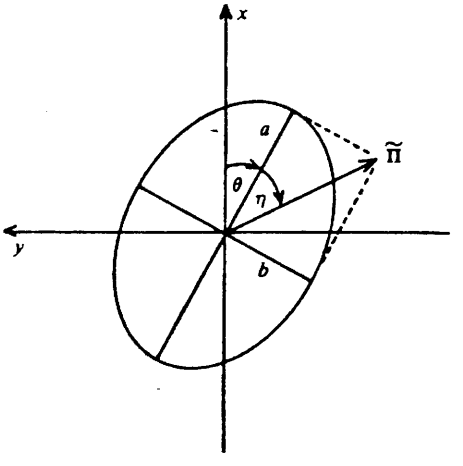

Fig. 2.1 Polarization ellipse with respect to the ($\underline{i}$,$\underline{j}$,$\underline{k}$) coordinate system, and also showing the azimuth and the ellipticity.

2.5.3 Stokes parameters for the scattered beam in terms of the incident beam

The Stokes parameters have been defined for the incident light beam with respect to the coordinate system defined by the unit vectors ($\underline{i},\underline{j},\underline{k}$). (See Fig. 2.1)

We can similarly define the Stokes parameters for the scattered beam w.r.t. the coordinate system defined by the unit vectors ($\underline{i}^d,\underline{j}^d,\underline{k}^d$) (where d stands for light scattered in the direction $\underline{d}$.)[31]

$$S_0 = |\tilde{E}_x|^2 + |\tilde{E}_Y|^2 \qquad (2.5.3a)$$

$$S_1 = |\tilde{E}_x|^2 - |\tilde{E}_Y|^2 \qquad (2.5.3b)$$

$$S_2 = -2\mathrm{Re}(\tilde{E}_x \tilde{E}_Y^*) \qquad (2.5.3c)$$

$$S_3 = 2\mathrm{Im}(\tilde{E}_x \tilde{E}_Y^*) \qquad (2.5.3d)$$

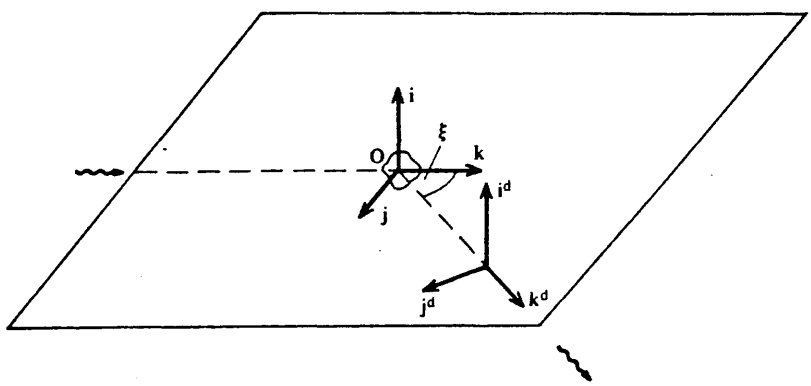

Fig. 2.2 Diagram showing the relationship between the incident wave coordinate system ($\underline{i},\underline{j},\underline{k}$) and the scattered wave coordinate system ($\underline{i}^d,\underline{j}^d,\underline{k}^d$).

We need to be able to express the electric field vectors of the scattered beam with respect to the (i^d, j^d, k^d) coordinate system in terms of the (i,j,k) coordinate system. From Fig. 2.2 we see that the following relations hold[32] (ξ is the scattering angle)

$$i^d = i \tag{2.5.4a}$$

$$j^d = j\cos\xi - k\sin\xi \tag{2.5.4b}$$

$$k^d = j\sin\xi + k\cos\xi \tag{2.5.4c}$$

Using the above relations, we obtain the following expressions[33]

$$S_0^d = |\tilde{E}_x|^2+|\tilde{E}_y|^2\cos^2\xi +|\tilde{E}_z|^2\sin^2\xi -2\mathrm{Re}(\tilde{E}_y \tilde{E}_z^*)\cos\xi\sin\xi \tag{2.5.5a}$$

$$S_1^d = |\tilde{E}_x|^2-|\tilde{E}_y|^2\cos^2\xi -|\tilde{E}_z|^2\sin^2\xi +2\mathrm{Re}(\tilde{E}_y \tilde{E}_z^*)\cos\xi\sin\xi \tag{2.5.5b}$$

$$S_2^d = -2\mathrm{Re}(\tilde{E}_x \tilde{E}_y^*)\cos\xi + 2\mathrm{Re}(\tilde{E}_x \tilde{E}_z^*)\sin\xi \tag{2.5.5c}$$

$$S_3^d = 2\mathrm{Im}(\tilde{E}_x \tilde{E}_y^*)\cos\xi + 2\mathrm{Im}(\tilde{E}_x \tilde{E}_z^*)\sin\xi \tag{2.5.5d}$$

In ref. [A] these are used to obtain general expressions for scattering for any angle. Such expressions allow calculations involving forward scattering, backscattering etc. to be performed.[34] In this thesis, however, we are concerned solely with 90° scattering ($\xi = 90^\circ$). We therefore use the modified version of the above i.e.

$$S_0^d = |\tilde{E}_x|^2 + |\tilde{E}_z|^2 \tag{2.5.6a}$$

$$S_1^d = |\tilde{E}_x|^2 - |\tilde{E}_z|^2 \tag{2.5.6b}$$

$$S_2^d = 2\mathrm{Re}(\tilde{E}_x\tilde{E}_z^*) \tag{2.5.6c}$$

$$S_3^d = 2\mathrm{Im}(\tilde{E}_x\tilde{E}_z^*) \tag{2.5.6d}$$

Now the electric field intensities for the scattered beam can be expressed in terms of those for the incident beam and the scattering tensor using the relation[35,36]

$$E^dE^d = (w^2\mu_0/4\pi R)^2\tilde{a}_{\alpha\beta}\tilde{a}^*_{\gamma\delta}\tilde{E}^{(0)}_\beta \tilde{E}^{(0)*}_\delta$$

$$= 2K\tilde{a}_{\alpha\beta}\tilde{a}^*_{\gamma\delta}\tilde{E}^{(0)}_\beta\tilde{E}^{(0)*}_\delta \tag{2.5.7}$$

Using this, we obtain the following expressions.

$$S_0^d = K[(|\tilde{a}_{xx}|^2 + |\tilde{a}_{xy}|^2 + |\tilde{a}_{zx}|^2 + |\tilde{a}_{zy}|^2)S_0 + (|\tilde{a}_{xx}|^2 + |\tilde{a}_{zx}|^2 - |\tilde{a}_{xy}|^2 - |\tilde{a}_{zy}|^2)S_1$$
$$-2\mathrm{Re}(\tilde{a}_{xx}\tilde{a}_{xy}^* + \tilde{a}_{zx}\tilde{a}_{zy}^*)S_2 - 2\mathrm{Im}(\tilde{a}_{xx}\tilde{a}_{xy}^* + \tilde{a}_{zx}\tilde{a}_{zy}^*)S_3]$$

$$S_1^d = K[(|\tilde{a}_{xx}|^2 + |\tilde{a}_{xy}|^2 - |\tilde{a}_{zx}|^2 - |\tilde{a}_{zy}|^2)S_0 + (|\tilde{a}_{xx}|^2 + |\tilde{a}_{zy}|^2 - |\tilde{a}_{xy}|^2 - |\tilde{a}_{zx}|^2)S_1$$
$$-2\mathrm{Re}(\tilde{a}_{xx}\tilde{a}_{xy}^* - \tilde{a}_{zx}\tilde{a}_{zy}^*)S_2 - 2\mathrm{Im}(\tilde{a}_{xx}\tilde{a}_{xy}^* - \tilde{a}_{zx}\tilde{a}_{zy}^*)S_3]$$

$$S_2^d = 2K[\mathrm{Re}(\tilde{a}_{xx}\tilde{a}_{zx}^* + \tilde{a}_{xy}\tilde{a}_{zy}^*)S_0 + \mathrm{Re}(\tilde{a}_{xy}\tilde{a}_{zy}^* - \tilde{a}_{xx}\tilde{a}_{zx}^*)S_1$$
$$-\mathrm{Re}(\tilde{a}_{xx}\tilde{a}_{zy}^* + \tilde{a}_{zx}\tilde{a}_{xy}^*)S_2 - \mathrm{Im}(\tilde{a}_{xx}\tilde{a}_{zy}^* + \tilde{a}_{zx}\tilde{a}_{xy}^*)S_3]$$

$$S_3^d = -2K[\mathrm{Im}(\tilde{a}_{xx}\tilde{a}_{zx}^* + \tilde{a}_{xy}\tilde{a}_{zy}^*)S_0 + \mathrm{Im}(\tilde{a}_{xx}\tilde{a}_{zx}^* - \tilde{a}_{xy}\tilde{a}_{zy}^*)S_1$$
$$-\mathrm{Im}(\tilde{a}_{xx}\tilde{a}_{zy}^* - \tilde{a}_{zx}\tilde{a}_{xy}^*)S_2 + \mathrm{Re}(\tilde{a}_{xx}\tilde{a}_{zy}^* - \tilde{a}_{zx}\tilde{a}_{xy}^*)S_3]$$

(2.5.8a-d)

The above results enable us to obtain expressions for all the scattering intensities which might be of interest. In this thesis we are interested in two specific areas. The first of these is the case of the scattering of light which is linearly polarized perpendicular to the plane. The second is the case of the scattering of right and left circularly polarized light. The first of these cases involves the measurement of the depolarization ratio for linearly polarized incident radiation. The second case corresponds to the measurement of optical activity. We deal with these two cases in the next section.

2.5.4 Molecular expressions for the depolarization ratio and the M.C.I.D. components.

(a) The Depolarization Ratio.

The depolarization ratio for linearly polarized incident radiation is given by[37]

$\rho(x)=I_z/I_x$ To measure it, incident light which is linearly polarized perpendicular to the scattering plane is used. For such a beam, $P=1$, $\Theta=0$ and $\eta=0$. Thus it has Stokes parameters $S_0=1$ and $S_1=1$.

From the above expressions we have

$$I_z = S_0^d(90^0) - S_1^d(90^0) = 2K(|\tilde{a}_{zx}|^2) \quad (2.5.10a)$$

$$I_x = S_0^d(90^0) + S_1^d(90^0) = 2K(|\tilde{a}_{xx}|^2) \quad (2.5.10b)$$

Now for a liquid sample, these expressions must be averaged over all orintations. We use the following averages[38]

$$\begin{aligned}\langle i_\alpha i_\beta i_\gamma i_\delta\rangle &= \langle j_\alpha j_\beta j_\gamma j_\delta\rangle \\ &= \langle k_\alpha k_\beta k_\gamma k_\delta\rangle \\ &= 1/15(\delta_{\alpha\beta}\delta_{\gamma\delta}+\delta_{\alpha\gamma}\delta_{\beta\delta}+\delta_{\alpha\delta}\delta_{\beta\gamma}) \quad (2.5.11)\end{aligned}$$

$$\begin{aligned}\langle i_\alpha i_\beta j_\gamma j_\delta\rangle &= \langle j_\alpha j_\beta k_\gamma k_\delta\rangle \\ &= \langle i_\alpha i_\beta k_\gamma k_\delta\rangle \\ &= 1/30(4\delta_{\alpha\beta}\delta_{\gamma\delta}-\delta_{\alpha\gamma}\delta_{\beta\delta}-\delta_{\alpha\delta}\delta_{\beta\gamma}) \quad (2.5.12)\end{aligned}$$

Thus $$\begin{aligned}\langle\tilde{a}_{xx}\tilde{a}^*_{xx}\rangle &= \tilde{a}_{\alpha\beta}\tilde{a}^*_{\gamma\delta}\langle i_\alpha i_\beta i_\gamma i_\delta\rangle \\ &= 1/15(\tilde{a}_{\alpha\alpha}\tilde{a}^*_{\beta\beta}+\tilde{a}_{\alpha\beta}\tilde{a}^*_{\alpha\beta}+\tilde{a}_{\alpha\beta}\tilde{a}^*_{\beta\alpha}) \quad (2.5.13)\end{aligned}$$

Similarly

$$\langle\tilde{a}_{zx}\tilde{a}^*_{zx}\rangle = 1/30(4\tilde{a}_{\alpha\beta}\tilde{a}^*_{\alpha\beta}-\tilde{a}_{\alpha\alpha}\tilde{a}^*_{\beta\beta}-\tilde{a}_{\alpha\beta}\tilde{a}^*_{\beta\alpha}) \quad (2.5.14)$$

We define the following invariants in terms of the symmetric and antisymmetric parts of the polarizability.

$$\alpha^2 = 1/9 \times \tilde{a}_{\alpha\alpha}\tilde{a}^*_{\beta\beta} \quad (2.5.15)$$

$$\beta(\alpha)^2 = 1/2(3\tilde{a}_{\alpha\beta}\tilde{a}^*_{\alpha\beta}-\tilde{a}_{\alpha\alpha}\tilde{a}^*_{\beta\beta}) \quad (2.5.16)$$

$$\beta(\alpha')^2 = 3/2 \times \tilde{a}_{\alpha\beta}\tilde{a}^{*}_{\alpha\beta} \qquad (2.5.17)$$

These invariants correspond to isotropic,anisotropic and antisymmetric scattering respectively. We now obtain our final expression for $\rho(x)$ in terms of these invariants.[39]

$$\rho(x) = \frac{3\beta(\alpha)^2 + 5\beta(\alpha')^2}{45\alpha^2 + 4\beta(\alpha)^2} \qquad (2.5.18)$$

(b) The M.C.I.D. components

When we are measuring the M.C.I.D. components for the Raman scattering of a particular molecule, we use right and left circularly polarized incident radiation (see Chapter 4 for experimental details). We denote the scattering intensity obtained for these two polarization by I^R and I^L. In terms of these, the M.CI.D. components are given by

$$\Delta_x = \frac{(I^R_x - I^L_x)}{(I^R_x + I^L_x)} \qquad \Delta_z = \frac{(I^R_z - I^L_z)}{(I^R_z + I^L_z)} \qquad (2.5.19)$$

For right and left circularly polarized incident light, $P=1;\eta = \pi/4$. This gives the Stokes parameters $S_0=1, S_3= 1$. From the expressions (2.5.8) we can write[40]

$$I^R_x - I^L_x = 4K\mathrm{Im}(\tilde{a}_{xy}\tilde{a}^{*}_{xx}) \qquad (2.5.20)$$

$$I^R_z - I^L_z = 4K\mathrm{Im}(\tilde{a}_{zy}\tilde{a}^{*}_{zx}) \qquad (2.5.21)$$

$$I^R_x + I^L_x = 2K\mathrm{Im}(|\tilde{a}_{xx}|^2 + |\tilde{a}_{xy}|^2) \qquad (2.5.22)$$

$$I^R_z + I^L_z = 2K\mathrm{Im}(|\tilde{a}_{zy}|^2 + |\tilde{a}_{zx}|^2) \qquad (2.5.23)$$

As they stand, the first two expressions average to zero. However, as we saw in the last section, in the presence of a magnetic field, we can write $\tilde{a}_{\alpha\beta}(Bz)$ as $\tilde{a}_{\alpha\beta} + \tilde{a}_{\alpha\beta z}Bz$. Thus we can write

$$\tilde{a}_{xy}(Bz)\tilde{a}^{*}_{xx}(Bz) = \tilde{a}_{xy}\tilde{a}^{*}_{xx} + (\tilde{a}_{xyz}\tilde{a}^{*}_{xx} + \tilde{a}_{xy}\tilde{a}^{*}_{xxz})Bz + \ldots (2.5.24)$$

If we now take an orientational average, only the first term will give zero. The second term in Bz can be averaged using

the following expression[41]

$$\begin{aligned}
&\langle i_\alpha j_\beta k_\gamma k_\delta k_\varepsilon \rangle \\
&= \langle j_\alpha k_\beta i_\gamma i_\delta i_\varepsilon \rangle \\
&= \langle k_\alpha i_\beta j_\gamma j_\delta j_\varepsilon \rangle \\
&= 1/30(\varepsilon_{\alpha\beta\gamma}\delta_{\delta\varepsilon} + \varepsilon_{\alpha\beta\delta}\delta_{\gamma\varepsilon} + \varepsilon_{\alpha\beta\varepsilon}\delta_{\gamma\delta}) \qquad (2.5.25)
\end{aligned}$$

After using these to average (2.5.24) above, we obtain the following expressions

$$\begin{aligned}
I_x^R - I_x^L = \; & 2/15KBzIm(2\tilde{a}_{\alpha\beta}\varepsilon_{\beta\gamma\delta}\tilde{a}^*_{\alpha\delta\gamma} + \tilde{a}_{\alpha\beta}\varepsilon_{\alpha\gamma\delta}\tilde{a}^*_{\beta\delta\gamma} + \\
& \tilde{a}_{\alpha\alpha}\varepsilon_{\gamma\beta\delta}\tilde{a}^*_{\gamma\delta\beta} - \tilde{a}_{\alpha\beta}\varepsilon_{\alpha\gamma\beta}\tilde{a}^*_{\delta\delta\gamma} - \tilde{a}_{\alpha\beta}\varepsilon_{\gamma\delta\beta}\tilde{a}^*_{\gamma\alpha\delta}) \qquad (2.5.26)
\end{aligned}$$

$$\begin{aligned}
I_z^R - I_z^L = \; & 2/15KBzIm(\tilde{a}_{\alpha\beta}\varepsilon_{\beta\alpha\delta}\tilde{a}^*_{\gamma\delta\gamma} + \tilde{a}_{\alpha\beta}\varepsilon_{\beta\gamma\delta}\tilde{a}^*_{\gamma\delta\alpha} + \\
& \tilde{a}_{\alpha\beta}\varepsilon_{\delta\beta\gamma}\tilde{a}^*_{\alpha\delta\gamma}) \qquad 2.5.27)
\end{aligned}$$

We also have to average the expressions for the sum spectra. These are done using (2.5.11-12). When we do this we obtain the following

$$I_x^R + I_x^L = 2/15 \times KIm(6\tilde{a}_{\alpha\beta}\tilde{a}^*_{\alpha\beta} + \tilde{a}_{\alpha\alpha}\tilde{a}^*_{\beta\beta} + \tilde{a}_{\alpha\beta}\tilde{a}^*_{\beta\alpha}) \qquad (2.5.28)$$

$$I_z^R + I_z^L = 4/15 \times KIm(4\tilde{a}_{\alpha\beta}\tilde{a}^*_{\alpha\beta} - \tilde{a}_{\alpha\alpha}\tilde{a}^*_{\beta\beta} - \tilde{a}_{\alpha\beta}\tilde{a}^*_{\beta\alpha}) \qquad (2.5.29)$$

It will be found that in almost all the cases for which we use the above formulae, we will be able to greatly simplify the above expressions.

(It should be noted that in Chapter 3, we consider under what circumstances we should perform an orientational average. We will then see that the above averaged expressions apply only for molecules with non-degenerate ground states.)

2.6 Summary of Irreducible Tensor Methods

2.6.1 Introduction

This section contains a brief outline of the Irreducible Tensor Methods (I.T.M.s) which will be used in the remainder of the book. It consists mainly of a statement of the irreducible tensor equations which will be used. There are three distinct areas in which I.T.M.s are used, namely for the full rotation group, simply reducible and non-simply reducible molecular point groups. However, the basic ideas behind each of them are identical.

The theory for each is built upon two fundamental ideas. These are the concepts of high symmetry coupling coefficients and the Wigner-Eckart theorem. Before stating the theorems which we shall use in the various different situations, we say a brief word about these two concepts.

2.6.2 The basic concepts

Suppose that in a general symmetry group G, A and B are two irreducible representations. If we take the direct product of these two representations, AxB, then in general these can be reduced to a sum of irreducible representations, for which we use the symbol C (in general there is more than one C.) Let Aa and Bb be basis functions for the irreducible representations A and B respectively. Then we can choose appropriate combinations of these basis functions to act as basis functions for the C representations. This is done in terms of the coupling

coefficients $\langle ABCc|AaBb\rangle$[42].

Using these we have

$$|Cc\rangle = \sum_{a,b} \langle ABCc|AaBb\rangle |Aa\rangle |Bb\rangle \qquad (2.6.1)$$

Now these coupling coefficients have very limited symmetry with respect to a change in the roles of A, B and C. However, we can define high symmetry coefficients in terms of these. [These are called 3-j symbols or V coefficients depending on the context. This was first done for the full rotation group by Fano and Racah[43], who extended the pioneering work of Wigner[44], and for simply reducible molecular point groups by Tanabe[45] and Griffith [46]. The latter pair's work has been extended by various authors[47,48] to include non-simply reducible point groups.]

Although the definition of these high symmetry coefficients varies depending on the type of group involved, they all have the following form

$$V\begin{pmatrix} A & B & C \\ a & b & c \end{pmatrix} = d(C)^{-1/2}(-1)^u \langle ABCc|AaBb\rangle \qquad (2.6.2)$$

where d(C) is the dimension of the representation C and u is an integer which depends on the representations and components involved.

Having defined V coefficients for the group in question, one then constructs invariant sums of products of V coefficients. The most interesting of these involve products of four and six V coefficients, with a summation performed over all the relevant pairs of components. These are called respectively 6-j and 9-j symbols in the context of the full roation group, and W and X coefficients respectively in the context of molecular point groups. As we shall see later, the evaluation of complicated matrix elements is greatly

simplified by using these invariant sums.

Associated with the idea of V coefficients or their equivalent is the Wigner-Eckart theorem. This theorem allows us to express the matrix element $\langle Aa|O^c|Bb\rangle$ involving particular components of the irreducible representations in the form

$$\langle Aa|O^c|Bb\rangle = (-1)^u V \begin{pmatrix} A & B & C \\ a^* & b^* & c^* \end{pmatrix} \langle A||O^c||B\rangle \qquad (2.6.3)$$

In the above equation, a*, b* and c* either have the same value as the corresponding component in the matrix element or the negative of this. u is either an odd or an even integer, depending on the representations and the components involved. $\langle A||O^c||B\rangle$ is called a reduced matrix element, and is independent of the particular components involved, being dependent only on the irreducible representations A, B and C. In general, these states A,B and C will have been built up from products of other states ,e.g.

$$|A\rangle = |(a_1 a_2)A\rangle \qquad (2.6.4)$$

Depending on the form of the operator O^c, one can often simplify the reduced matrix element, using formulae involving either 6-j or W coefficients, expressing it in terms of simpler reduced matrix elements.

Using the ideas outlined above, irreducible tensor methods allow any matrix element, no matter how complicated, to have all the symmetry information contained within it utilised.

There is one prerequisite for using irreducible tensor methods. This is that all quantum states and operators must be expressed as combinations of basis functions of irreducible representations of the appropriate symmetry

group.

We now go on to state all the theorems which will be used in the remainder of the thesis.

2.6.3 Irreducible tensor expressions for the various types of group.

(a) The full rotation group R_3.

Let $|ajm\rangle$ be the general classification of a quantum state in the full rotation group, where j denotes the angular momemtum quantum number and m denotes the particular component of the representation j. Also, let T^K be an operator which spans the irreducible representation K of the full rotation group. Then the Wigner-Eckart theorem for the full rotation group states that[49]

$$\langle a'j'm'|T^K_q|ajm\rangle = (-1)^{j'-m'}\langle a'j'||T^K||aj\rangle \begin{pmatrix} j' & K & j \\ -m' & q & m \end{pmatrix} \qquad (2.6.5)$$

where the symbol in round brackets is called a 3-j symbol. (These have been tabulated by Rotenburg et al[50]. The symmetry properties are also contained in this reference.)

As was noted in Section 2.6.2, all operators must be expressed in terms of irreducible tensors. The appropriate combinations will be given when needed. One further result is used. This involves the reduction of a reduced matrix element when the quantum system is the direct product of two independent systems, and the operator acts on only the first of these. The appropriate expressions are[51]

$$\langle L'S'J'||\underline{T}^k(1)||LSJ\rangle \qquad (2.6.6)$$

$$= \begin{bmatrix} L' & J' & S' \\ J & L & k \end{bmatrix} \times (-1)^{L'+S'+J+k}[(2J+1)(2J'+1)]^{1/2} \times \langle L'||\underline{T}^k(1)||L\rangle$$

(the coefficient in squared brackets is a 6-j symbol.)

A similar result, which we don't require, exists when the operator acts only on the second system.

(b) Simply reducible molecular point groups.

The main work in the development of irreducible tensor methods as applied to simply reducible molecular point groups was done by Tanabe in Japan and Griffiths in Britain.

Let $|Aa\rangle$ be a general quantum state which spans the irreducible representation A of the point group in question (we are assuming that we are using real component systems.) Then if the operator O^c spans the irreducible representation C, the appropriate form of the Wigner-Eckart theorem is[52]

$$\langle A'a'|O^c_c|Aa\rangle = V\begin{pmatrix} A' & A & C \\ a' & a & c \end{pmatrix}\langle A'\|O^c\|A\rangle \qquad (2.6.7)$$

[For tabulated values[53] of the V coefficients for molecular point groups, we refer to the monograph by Griffiths, in which he summarises his development of the method, which was originally published in the form of papers. This also contains the symmetry properties of the V coefficients.]

The following expressions for simplifying reduced matrix elements are also used.[54]

$$\langle ABCc|D^dE^d|A'B'Cc\rangle=(-1)^{A+B+C+D}\langle A\|D^d\|A'\rangle\langle B\|E^d\|B'\rangle W\begin{pmatrix} A & B & C \\ B' & A' & D \end{pmatrix} \qquad (2.6.8)$$

$$\langle ABC|D^d|\acute{A}\acute{B}\acute{C}\rangle=(-1)^{A'+B+C'+D}\delta_{BB'}d(C,C)\ \langle A\|D^d\|A'\rangle W\begin{pmatrix} A & B & C \\ B' & A' & D \end{pmatrix} \qquad (2.6.9)$$

$$\langle ABC\|D^d\|ABC\rangle=(-1)^{A+B'+C+E}\delta_{AA'}d(C,C)\ \langle B\|D^d\|B'\rangle W\begin{pmatrix}B' & B & E\\ C & C' & A\end{pmatrix}$$

(2.6.10)

In the last three expressions, the operator D acts within the A and A' system. This is independent of the B and B', within which the operater E acts. The W coefficient which is contained in these expressions is an invariant composed of sums of products of V coefficients. If it contains an A_1 representation, then it reduces according to the following formula.[55]

$$W\begin{pmatrix}A_1 & B & C\\ D & E & F\end{pmatrix} = (-1)^{B+D+E}d(B,C)^{-1/2}\delta_{BC}\delta_{EF} \qquad (2.6.11)$$

If we are dealing with situations where we need to use complex components for the irreducible representations, then we use the following modified form of the Wigner-Eckart theorem. This applies to all the proper subgroups of the octahedral group, but not the octahedral group itself.[56]

$$\langle Ar|O^c|Bs\rangle = V\begin{pmatrix}A & B & C\\ -r & s & t\end{pmatrix}\langle A\|O^c\|B\rangle \qquad (2.6.12)$$

For the real and the complex cases, the following results hold for V coefficients containing the totally symmetric representation[57] A_1.

$$V\begin{pmatrix}B & C & A_1\\ b & c & i\end{pmatrix}= d(B)^{-1/2}\delta_{Bc}\delta_{bc} \qquad V\begin{pmatrix}B & C & A_1\\ r & s & i\end{pmatrix}= d(B)^{-1/2}\delta_{Bc}\delta_{r,-s} \qquad (2.6.13)$$

The appropriate combinations to be used for the various operators will be given as they are required.

(c) Non-simply reducible groups.

(We use Harnung's formulation in what follows, except that we use the terms V and W coefficients.)

For these groups the following form of the Wigner-Eckart theorem is used.[58]

$$\langle aGg|D^K|a'G'g'\rangle = \sum_{\epsilon} (-1)^{u(G-g)} \langle aG\|eD^K\|a'G'\rangle \begin{pmatrix} G & K & G' \\ -g & k & g' \end{pmatrix}_{\epsilon} \tag{2.6.14}$$

Here, e takes the values p or s. These stand for principal and secondary. Thus this form of the Wigner-Eckart theorem can in general involve two different V coefficients for the same matrix element, along with two different reduced matrix elements. Both s and p are needed only when repeated representations occur. Otherwise, we need only the p contributions.

The symmetry properties of these V coefficients, as well as tables for the V and W coefficient, can be obtained from Harnung.[59]

The following results[60] are also used later . If Aa and Bb are the components of two representations A and B, then the combinations spanning C where C = AxB are given by

$$|(a_1A)(a_2B)Cc\rangle \tag{2.6.15}$$
$$= \sum_{a,b} (-1)^{u(2B+C-c)} (-1)^{p(A+B+C)} [C]^{1/2} V \begin{pmatrix} A & B & C \\ a & b & c \end{pmatrix} |a_1Aa\rangle |a_2Bb\rangle$$

We also use the following result, which is the inverse of the previous result.

$$|a_1Aa\rangle |a_2Bb\rangle$$
$$= \sum_{C,c} (-1)^{p(A+B+C)} (-1)^{u(2B+C-c)} [C]^{1/2} V \begin{pmatrix} A & B & C \\ a & b & c \end{pmatrix} |(a_1A)(a_2B)Cc\rangle \tag{2.6.16}$$

Chapter 2 : References

1) A.C. Albrecht, J. Chem. Phys. 34,1476(1961)

2) L.D. Barron, Adv. Infrared Raman Spectrosc. 4,271(1978)

3) [A], p.74-76

4) [B], p.96

5) A.S. Davydov, Quantum Mechanics, 2nd Edition, Pergamon Press, Oxford, 1976, p. 283

6) L.D. Landau and E.M. Lifshitz, Quantum Mechanics, 3rd edition,Pergamon Press, Oxford.

7) [B], p.115

8) [B], p.111

9) [B], p.100

10) G. Placzek, Handbuch der Radiologie(1934)

11) M. Born and K. Huang, Dynamical Theory of Crystal Lattices, Clarendon Press, Oxford, 1954.

12) [A], p.92

13) [A], p.93

14) See ref. 13

15) [A], p.97-99

16) See ref. 15

17) [A], p. 104-106

18) G. Herzberg and E. Teller, Z. Phys. Chem.B21,410(1933)

19) A.C. Albrecht, J. Chem. Phys. 34,1476(1961)

20) See ref. 19

21) [A], p.362

22) [A], p.362-363

23) See ref. 22

24) See ref. 5

25) [B], p. 105

26) [A], p.129-148

27) [B], p.119

28) [A], p.47

29) [A], p.48

30) [B], p.122

31) [A], p.129-130

32) See ref. 31

33) See ref. 31

34) [A], p.133-146

35) [A], p.130

36) [B], p.170-176

37) [A], p.133

38) [A], p.163,164

39) [A], p.137

40) L.D. Barron, C. Meehan, Chem. Phys. Lett. 66,444(1979)

41) [A], p.164

42) [C], p.7

43) U. Fano and G. Racah, Irreducible Tensorial Sets, Academic Press, New York, (1959).

44) E.P. Wigner, Z. Phys. 43,624(1927)

45) [D], preface

46) [C]

47) P.A. Dobosh, Phys. Rev. A5,2376(1972)

48) S.E. Harnung, Molec. Phys. 26,473(1976)

49) [D], p.69

50) M. Rotenberg, R. Bivens, N. Metropolis, J.K. Wooten, The 3-j and 6-j Symbols, Technology Press,Cambridge, Massachussetts, 1959

51) [C], p.92

52) [C], p.15

53) [C], p.109-125

54) [C], p.46-47(5.24, 5.25 and 5.26)

55) [C], p.34(4.2)

56) [C], p.31(3.11)

57) [C], p.17(2.20)

58) S.E. Harnung, Molec. Phys. 26,473(1976). p.494

59) S.E. Harnung, Molec. Phys. 26,473(1976) :-

(a) Properties of V coefficients - p. 479(22), 484(25),485(29), 489(39), 489(41), 489(footnote)

(b) Tables for V coefficients - p.491 and W coefficients - p.493.

60) S.E. Harnung, Molec. Phys. 26,473(1976). p.484(26), p.488(38a and 38b)

CHAPTER 3

FURTHER DEVELOPMENT OF THE MOLECULAR SCATTERING TENSORS

3.1 Introduction

In this chapter, the main new theoretical ideas of the thesis are presented.

In Section 3.2, a new development of the vibronic coupling expressions for non-totally symmetric modes is presented, which makes use of irreducible tensor methods. It will be seen that for the case of a molecule with a totally symmetric ground electronic state, an important general expression for the polarizability tensor can be deduced. This expression allows depolarization ratios to be predicted, using only the point group to which the molecule belongs. The development of the polarizability tensor continues with a discussion of the relationship between the 0-0 and the 0-1 scattering contributions for various types of scattering.

In Section 3.3, the development of the previous section is extended to include the perturbed polarizability tensor. Again a general expression is obtained, and the 0-0 and 0-1 contributions are again considered.

For molecules with non-totally symmetric ground electronic states (i.e. a molecule with an odd number of electrons), it has not been possible so far to obtain an analagous general formula. However, irreducible tensor methods are used in Section 3.4 to obtain some general properties of the polarizability tensor.

In section 3.5, the two main mechanisms for Raman optical activity are outlined in detail. It will be seen that a modification of the earlier magnetically perturbed polarizability tensors is necessary when we are considering the second mechanism.

The final section in the chapter, Section 3.6, contains a discussion of the frequency dependence of the various scattering observables which are of interest to us. This is of considerable importance when we come to compare theory with experiment.

3.2 Vibronic Coupling for Molecules with a Totally Symmetric Ground Electronic State

3.2.1 Introduction

What follows is restricted to molecules which have a totally symmetric ground state. Because of this restriction, the following facts are true about the molecule :-

(i) all its wave functions can be expressed in real form.

(ii)it's point group is simply reducible.

Because of point (ii), we may use the irreducible tensor results given in Section 2.6.3(b).

3.2.2 Extended use of the Herzberg-Teller approximation

In the previous chapter, vibronic coupling was developed using the Herzberg-Teller approximation, with the Hamiltonian expanded as follows

$$H(\underline{r},Q) = H(\underline{r},Q_0) + \sum_p (\partial H(\underline{r},Q)/\partial Q_p)Q_p + \tfrac{1}{2}\sum_{p,q} (\partial^2 H(\underline{r},Q)/\partial Q_p \partial Q_q)Q_p Q_q + \ldots \quad (3.2.1)$$

Previously, only the first term of the expansion was used as a perturbation. In the development which follows, we use the above to write our Hamiltonian as

$$H(\underline{r},Q) = H(\underline{r},Q_0) + H'(\underline{r},Q) \quad (3.2.2)$$

where $H(\underline{r},Q)$ contains all the expansion terms. Since this is the Hamiltonian for the system, all the terms in it must be totally symmetric. In particular we can say that $H'(\underline{r},Q)$ transforms as A_1.

3.2.3 Derivation of the general polarizability expressions

Following first order perturbation theory, we can write the perturbed wavefunction for the vibronic state $|jejv\rangle$ as

$$|jejv\rangle = |je^{(0)}jv\rangle + \sum_{k\neq j} \frac{\langle kekv\ H(\underline{r},Q)\ jejv\rangle\ kekv\rangle}{\hbar\omega_{jejvkekv}} \quad (3.2.3)$$

Now electronic energies are very much greater than vibrational energies. Also, the differences in energy between vibrational states are small[1]. Thus it is a very good approximation to ignore the vibrational terms in the frequency denominator. In what follows, we make this approximation, and incorporate the frequency denominator into the operator $H(\underline{r},Q)_{jeke}$. We shall omit the subscripts in what follows.

Inserting this in (2.2.22), we obtain the following expression for the Z tensor contribution to the polarizability tensor

$$\begin{aligned} Z_{\alpha\beta} = \sum_{k\neq j} \Big[& \langle nemv|u_\alpha|jejv\rangle\langle kekv|u_\beta|nenv\rangle\langle kekv|H(\underline{r},Q)|jejv\rangle \\ & + \langle nemv|u_\alpha|kekv\rangle\langle jejv|u_\beta|nenv\rangle\langle kekv|H(\underline{r},Q)|jejv\rangle^* \\ & + \langle nemv|u_\alpha|jejv\rangle\langle jejv|u_\beta|kekv\rangle\langle kekv|H(\underline{r},Q)|nenv\rangle \\ & + \langle kekv|u_\alpha|jejv\rangle\langle jejv|u_\beta|nenv\rangle\langle kekv|H(\underline{r},Q)|nemv\rangle^* \Big] \end{aligned} \quad (3.2.4)$$

for systems of interest later,

(We shall see later that the excited electronic states are usually degenerate. Hence for non-degenerate normal modes of vibration, the last two terms in the above expression are zero.)

Now we consider the symmetry of the vibronic state $|jejv\rangle$. In general, the direct product $\Gamma(je) \times \Gamma(jv)$ of the irreducible representations of je and jv will contain a sum of irreducible products J. For any degenerate J, we denote

it s components by Jj. This applies to all the vibronic states in (3.2.4) above. Hence we can rewrite this as

$$Z_{\alpha\beta} = \sum_{k \neq j} \Big[\langle (nemv)Mm|u_\alpha|(jejv)Jj\rangle\langle (kekv)Kk|u_\beta|(nenv)Nn\rangle \times \langle (kekv)Kk|H(\underline{r},Q)|(jejv)Jj\rangle + \langle (nemv)Mm|u_\alpha|(kekv)Kk\rangle\langle (jejv)Jj|u_\beta|(nenv)Nn\rangle \times \langle (kekv)Kk|H(\underline{r},Q)|(jejv)Jj\rangle^* \Big] \quad (3.2.5)$$

Take the first line of (3.2.5) and apply the Wigner-Eckart theorem to each of the three matrix elements. This gives us

$$\langle (nemv)Mm|u_\alpha|(jejv)Jj\rangle\langle (kekv)Kk|u_\beta|(nenv)Nn\rangle \times \langle (kekv)Kk|H(\underline{r},Q)|(jejv)Jj\rangle \quad (3.2.6)$$

$$= V\begin{pmatrix} M & J & \Gamma_\mu \\ m & j & \alpha \end{pmatrix} V\begin{pmatrix} K & N & \Gamma_\mu \\ k & n & \beta \end{pmatrix} V\begin{pmatrix} K & J & A_1 \\ k & j & i \end{pmatrix} \times \langle nemvM||u(\Gamma_\mu)||jejvJ\rangle\langle kekvK||u(\Gamma_\mu)||nenvN\rangle\langle kekvK||H||jejvJ\rangle$$

This can be simplified considerably. We have stipulated a totally symmetric ground state. Therefore N is A_1. This gives us two V coefficients containing A_1. Using formula (2.6.13), we can therefore simplify the above to

$$\langle nemvMm||u||jejvJj\rangle\langle kekvKk||u||nenvNn\rangle \times \langle kkvKk|H(\underline{r},Q)|jejvJj\rangle$$

$$= V\begin{pmatrix} M & J & \Gamma_\mu \\ m & j & \alpha \end{pmatrix} d(\Gamma_\mu)^{-1/2}\delta_{KG}\,\delta_{k\beta}\,d(J)^{-1/2}\delta_{KJ}\delta_{kj} \times$$

$$\langle nemvM||u(\Gamma_\mu)||jejvJ\rangle\langle kekvK||u(\Gamma_\mu)||nenvN\rangle\langle kekvK||H||jejvJ\rangle$$

$$= V\begin{pmatrix} M & \Gamma_\mu & \Gamma_\mu \\ m & \beta & \alpha \end{pmatrix} d(\Gamma_\mu)^{-1} \times$$

$$\langle nemvM||u(\Gamma_\mu)||jejv\Gamma_\mu\rangle\langle kekvG||u(\Gamma_\mu)||nenvN\rangle\langle kekv\Gamma_\mu||H||jejv\Gamma_\mu\rangle$$

$$= \frac{1}{d(\Gamma_\mu)} \times V\begin{pmatrix} M & \Gamma_\mu & \Gamma_\mu \\ m & \beta & \alpha \end{pmatrix} \times a_1(Q,\Gamma_\mu,\Gamma_\mu,je,jv,ke,kv) \quad (3.2.7)$$

Similar arguments apply for the second term in (3.2.5). The only difference is that the reduced matrix elements contained in a_2 are different.

Putting these results into (2.3.9) we obtain

$$Z_{\alpha\beta} = \frac{1}{d(\Gamma_\mu)} \times V\begin{pmatrix} M & \Gamma_\mu & \Gamma_\mu \\ m & \beta & \alpha \end{pmatrix} \sum_i [\, a_1(Q,\Gamma_\mu,\Gamma_\mu,je,jv,ke,kv)] \qquad (3.2.8)$$

(In the above, we were free to take the V coefficient outside the summation because it was independent of the summation parameters.)

The order of Γ_{μ_1} and Γ_{μ_2} would seem to be important in the constants a_1. However, inspection of the various simply reducible point groups shows that V-coefficients involving different dipole moment representations Γ_{μ_1} and Γ_{μ_2} are always zero for non-degenerate modes. Usually, only one representation is involved in the non-zero polarizability tensor components (see below for details). We can thus consider the a_1 to be constants. (Their exact form is of importance however, and is discussed later on in the section.)

This gives us the result

$$a_{\alpha\beta} = \frac{a}{d(\Gamma_\mu)} \times V\begin{pmatrix} M & \Gamma_\mu & \Gamma_\mu \\ m & \beta & \alpha \end{pmatrix} \qquad (3.2.9)$$

where $a = [\, a_1 + a_2 \,]$ is a polarizability constant whose magnitude depends on the molecular system in question.

It must be emphasised that this result is exact. (Although we have used the Herzberg-Teller approach, we have included all the expansion terms.) (3.2.9) allows us to state a necessary and sufficient condition for a molecule in a non-degenerate ground state to support antisymmetric scattering: namely the direct product $\Gamma_\mu \times \Gamma_\mu$ of the dipole moment representations must contain the representation A_2. Molecules having higher than a two-fold axis of symmetry satisfy this condition.

3.2.4 Discussion of equation (3.2.9)

At first sight, it might appear, as mentioned above, that (3.2.9) is of restricted use. It does allow us to compare directly some of the components of the polarizability tensor. But to do this, the components being considered must involve the same irreducible representations. However, a glance through the point groups will show that one of two cases always holds for any non-commutative group.

(x,y) transforms as E ; z transforms as A_1 or A_2

(x,y,z) transforms as T_1

This means that a_{xx}, a_{xy}, a_{yx} and a_{yy} may always be compared directly for non-commutative groups. (The commutative groups are those containing no representation of degree higher than one.) Also for such groups, it will be seen in Chapter 8 that the polarizability tensor contains either diagonal terms or non-diagonal terms - but never both. Also, whenever a polarizability component involving z and either x or y is non-zero, these are the only non-zero components. The only case in practice where the relative values of all the polarizability tensors cannot be measured is when we have diagonal scattering (usually involving the totally symmetric mode.) For this case, the general rules governing the polarizability hold.

In view of the previous discussion, it is clear that (3.2.9) can be used, apart from one case, to calculate the relative values of the polarizability tensor, and thus the depolarization ratios. It further follows from (3.2.9) that for non-diagonal scattering, the depolarization ratios depend only on the point group to which the molecule

belongs. In Chapter 8, the polarizability tensor patterns and the depolarization ratios will be calculated for each of the point groups. (Apart from D_{4h}, which is dealt with in Chapter 5.) These tensor patterns have been reported previously, e.g. for example, by Koningstein.[3] He obtained his results by applying irreducible tensor methods to individual normal mode representations for each point group. Using (3.2.9) not only allows us to calculate the patterns automatically, however. Further developments in forthcoming sections allow extra information to deduced which is not accesible by the method used by Koningstein.

Another result which follows directly from (3.2) is that the tensor patterns are independent of the nature of the excited states of the molecule. In particular, as we reach resonance, the tensor patterns should remain unchanged, although the absolute magnitude of the tensors will in general be greatly affected. We shall come back to this point when the frequency dependence of the molecular scattering tensors and observables is discussed.

A final general point emerging from (3.2.9), and mentioned above, is the necessary condition for antisymmetric scattering to exist. As will be seen later, real antisymmetric tensor components can exist. Because of this, a slight modification to the depolarization ratio expressions must be made.

Further consequences arise from (3.2.9), once detailed calculations are made using it. A discussion of these is contained in Chapter 8.

In the next section, we investigate the physical significance of the two constants a_1 and a_2.

3.2.5 Identification of the constants a_1 and a_2 with the 0-1 and 0-0 scattering pathways

In the previous section, we obtained a general result which involved two polarizability constants a_1 and a_2. These consisted of products of reduced matrix elements. However, we can use (2.9.5a) to simplify the reduced matrix elements. When we do this, it emerges that the constants correspond to physically different scattering pathways.

First of all, we consider the constant a_1. From the previous section, we have

$$a_1 = \langle (nemv)M||u(\Gamma_\mu)||(jejv)\Gamma_\mu\rangle\langle (kekv)\Gamma_\mu||u(\Gamma_\mu)||(nenv)N\rangle$$
$$\times \langle (jejv)\Gamma_\mu||H||(kekv)\Gamma_\mu\rangle \qquad (3.2.10)$$

Before using irreducible tensor methods, we note that the two electric dipole moment operators involve only electronic coordinates. Therefore mv and jv must be identical, and kv and nv must also be identical. Thus jv, the virtual intermediate vibrational state, must be identical to the

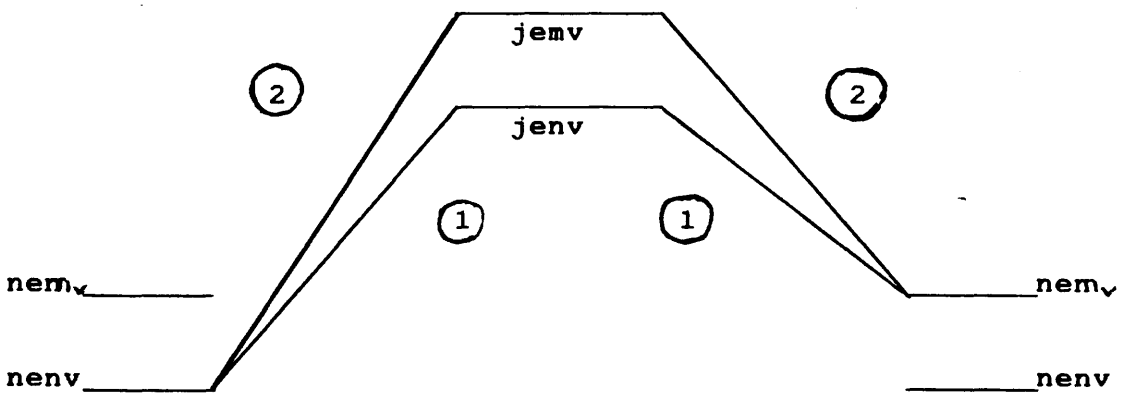

1 = 0-0 vibronic transition pathway 2 = 0-1 vibronic transition pathway

Fig. 3.1 Diagram illustrating the 0-0 and 0-1 scattering pathways

final excited vibrational state mv. For this reason, this scattering pathway is called the 0-1 pathway.[4] Hence the constant a_1 may be written as $a_{0\text{-}1}$, since it describes the 0-1 scattering contribution. (see Fig. 3.1)

Using irreducible tensor methods, since the operator u acts only on the electronic part of the vibronic wave function, we have $\langle (n_e m_v) M \| u(\Gamma_\mu) \| (j_e j_v) \Gamma_\mu \rangle$

$$= (-1)^{n_\alpha + m_v + \Gamma + \Gamma} d(m_v)^{1/2} d(\Gamma_\mu)^{1/2} \times W \begin{pmatrix} j_e & n_e & \Gamma_\mu \\ m_v & \Gamma_\mu & m_v \end{pmatrix} \times \langle n_e \| u(\Gamma_\mu) \| j_e \rangle$$

$$= (-1)^{A_1 + m_v + \Gamma + \Gamma} d(m_v)^{1/2} d(\Gamma_\mu)^{1/2} \times W \begin{pmatrix} j_e & A_1 & \Gamma_\mu \\ m_v & \Gamma_\mu & m_v \end{pmatrix} \times \langle n_e \| u(\Gamma_\mu) \| j_e \rangle$$

(since n_e is totally symmetric)

$$= (-1)^{A_1 + m + \Gamma + \Gamma} d(m_v)^{1/2} d(\Gamma_\mu)^{1/2} (-1)^{j_e + \Gamma + m_v} \times d(m_v)^{-1/2} d(j_e)^{-1/2} \times \langle n_e \| u(\Gamma_\mu) \| j_e \rangle$$

$$= d(\Gamma_\mu)^{1/2} d(\Gamma_\mu)^{-1/2} \langle n_e \| u(\Gamma_\mu) \| j_e \rangle \qquad (3.2.11)$$

(because j_e must equal Γ_μ and all the exponents come in pairs, apart from A_1, which is equal to zero.)

Similarly, we have

$$\langle (k_e k_v) \Gamma_\mu \| u(\Gamma_\mu) \| (n_e n_v) N \rangle = \langle k_e \| u(\Gamma_\mu) \| n_e \rangle \qquad (3.2.12)$$

In order to simplify the third reduced matrix element, we now use for the first time the approximation that

$$H(\underline{r}, \underline{Q}) = (H_e Q)^A \qquad (3.2.13)$$

We then have

$$\langle (j_e j_v) \Gamma_\mu \| H \| (k_e k_v) \Gamma_\mu \rangle$$

$$= \langle (j_e j_v) \Gamma_\mu \| (H_e Q)^A \| (k_e k_v) \Gamma_\mu \rangle$$

$$= (-1)^{k + j + \Gamma + m_v} d(\Gamma_\mu)^{1/2} d(m_v)^{-1/2} W \begin{pmatrix} j_e & j_v & \Gamma_\mu \\ k_v & k_e & m_v \end{pmatrix} \times \langle j_e \| H_e \| k_e \rangle \langle j_v \| Q \| k_v \rangle$$

$$= (-1)^{k + j + \Gamma + m_v} d(\Gamma_\mu)^{1/2} d(m_v)^{-1/2} (-1)^{j + k + m_v} \times d(j_e)^{-1/2} d(m_v)^{-1/2} \langle j_e \| H_e \| k_e \rangle \langle j_v \| Q \| k_v \rangle$$

$$= d(m_v)^{-1} \times \langle j_e \| H_e \| k_e \rangle \langle j_v \| Q \| k_v \rangle$$

$$= d(mv)^{-1} \times \langle je||H_a||ke\rangle\langle mv||Q||nv\rangle \qquad (3.2.14)$$

since we have already identified kv and jv with nv and mv.

Putting all these together, we obtain

$$a_{o-1} = d(\Gamma_\mu)^{1/2} d(\Gamma_\mu)^{-1/2} d(mv)^{-1} \langle mv\ Q\ nv\rangle \qquad (3.2.15)$$
$$\times \langle ne||u(\Gamma_\mu)||je\rangle\langle ke||u(\Gamma_\mu)||ne\rangle\langle je||H_a||ke\rangle$$

We next simplify a_2. From the previous section we see that

$$a_2 = \langle (nemv)M||u(\Gamma_\mu)||(kekv)\Gamma_\mu\rangle\langle (jejv)\Gamma_\mu||u(\Gamma_\mu)||(nenv)N\rangle$$
$$\times \langle (kekv)\Gamma_\mu||H||(jejv)\Gamma_\mu\rangle \qquad (3.2.16)$$

Again because the dipole moment operator involves only the electronic coordinates, we see that for this particular pathway mv and kv are identical, and jv and nv are also identical. Because the intermediate vibrational state is equal to the initial vibrational state, we call this pathway the O-O pathway. Hence the constant a_2 may be written as a_{o-o}, since it describes the O-O scattering contribution.

Proceeding as before, we obtain the following

$$\langle (nemv)M||u(\Gamma_\mu)||(kekv)\Gamma_\mu\rangle = d(\Gamma_\mu)^{1/2} d(\Gamma_\mu)^{-1/2} \langle ne||u(\Gamma_\mu)||ke\rangle \qquad (3.2.17)$$

$$\langle (jejv)\Gamma_\mu||u(\Gamma_\mu)||(nenv)n\rangle = \langle je||u(\Gamma_\mu)||ne\rangle \qquad (3.2.18)$$

$$\langle (kekv)\Gamma_\mu||H||(jejv)\Gamma_\mu\rangle = d(mv)^{-1} \langle ke||H_a||je\rangle\langle mv||Q||nv\rangle \qquad (3.2.19)$$

Putting these three results together, we obtain

$$a_{o-o} = d(\Gamma_\mu)^{1/2} d(\Gamma_\mu)^{-1/2} d(mv)^{-1} \langle mv||Q||nv\rangle \qquad (3.2.20)$$
$$\times \langle ne||u(\Gamma_\mu)||ke\rangle\langle je||u(\Gamma_\mu)||ne\rangle\langle ke||H_a||je\rangle$$

It will be immediatly noted that the simplified expressions for a_{o-1} and a_{o-o} are very similar but not identical. In the next section, we investigate the relative values of these two contributions.

3.2.6 Comparison of the 0-0 and 0-1 scattering contributions to symmetric and antisymmetric scattering

In Section 3.2.4, expressions were obtained for the constants a_{0-1} and a_{0-0} which describe the two different scattering pathways. The only differences between these two expressions involve the reduced matrix elements containing electronic states. In this section, we show that a_{0-1} and a_{0-0} are simply related to one another.

From the previous section, we can write the ratio of a_{0-1} to a_{0-0} as

$$a_{0-1}/a_{0-0} = \langle ne\|u(\Gamma_\mu)\|je\rangle\langle ke\|u(\Gamma_\mu)\|ne\rangle\langle je\|H_{op}\|ke\rangle \quad (3.2.21)$$
$$\langle ne\|u(\Gamma_\mu)\|ke\rangle\langle je\|u(\Gamma_\mu)\|ne\rangle\langle ke\|H_{op}\|je\rangle$$

Now the operators involved in these reduced matrix elements are hermitian. We use this fact to simplify this ratio. Consider first of all operator H_{op} connecting the states $|ej\rangle$ and $|ek\rangle$. Then by hermiticity we have

$$\langle ek|H_{op}|ej\rangle = \langle ej|H_{op}|ek\rangle^* \quad (3.2.22)$$

As has previously been mentioned, all the states we are considering are real. We can therefore ignore the complex conjugate which appears above. If we now apply the Wigner-Eckart theorem to both sides we obtain

$$V\begin{pmatrix} ke & je & Q \\ k & j & p \end{pmatrix}\langle ke\|H_{op}\|je\rangle = V\begin{pmatrix} je & ke & Q \\ j & k & p \end{pmatrix}\langle je\|H_{op}\|ke\rangle \quad (3.2.23)$$

Using the permutation properties of V-coefficients, we therefore deduce that

$$\langle ke\|H_{op}\|je\rangle = (-1)^{ke+je+\Gamma} \times \langle je\|H_{op}\|ke\rangle \quad (3.2.24)$$

As has been previously noted, the states ke and je involved in the scattering expressions normally have the same symmetry . Thus we can write

$$\langle k\|H_\alpha\|j\rangle = (-1)^a \times \langle j\|H_\alpha\|k\rangle \qquad (3.2.25)$$

In a similar way, it can be shown that

$$\langle n\|u(\Gamma_\mu)\|j\rangle = \langle j\|u(\Gamma_\mu)\|n\rangle \qquad (3.2.26)$$

$$\langle j\|u(\Gamma_\mu)\|n\rangle = \langle n\|u(\Gamma_\mu)\|j\rangle \qquad (3.2.27)$$

Again using the fact that in practise non-zero contributions occur only when k_e is equal to j_e, we deduce that

$$a_{o-1}/a_{o-o} = (-1)^a \qquad (3.2.28)$$

To obtain our final expressions for the polarizability tensor for non-totally symmetric modes of vibration, it is convenient to consider separately the cases of symmetric and antisymmetric scattering. This is because of the different frequency factors involved.

(a) Symmetric scattering

From expression (3.2.9), we deduce that symmetric scattering will occur when the V-coefficient which gives the tensor patterns is invariant to permutations of its columns. Inspection of the various simply-reducible point groups shows that this is the case whenever the normal mode does not have symmetry A_2. In this case, the factor $(-1)^a$ is equal to +1. Hence we can use the development given in this section so far to write

$$\tilde{a}_{\alpha\beta} = V\begin{pmatrix} Q & \Gamma_\mu & \Gamma_\mu \\ q & \beta & \alpha \end{pmatrix} \sum_j a(j) \left[\frac{w_{o-1}}{(w_{o-1}^2 - w^2)} + \frac{w_{o-o}}{(w_{o-o}^2 - w^2)} \right] \qquad (3.2.29)$$

Later in this chapter, we will see that the frequency factors are modified when we are close to resonance. If we are far away from resonance, the frequency factors for the O-1 and O-O scattering pathways are roughly equal, and as can be seen from (3.2.29), they reinforce each other.

(b) Antisymmetric scattering

As mentioned in (a) above, antisymmetric scattering occurs when the V-coefficient contained in (3.2.29) is odd with respect to permutation of it's columns. As also mentioned above, this occurs only when the normal mode is A_2. For this case, the factor $(-1)^q$ is equal to -1. Thus we obtain for antisymmetric scattering the expression

$$\tilde{a}_{\alpha\beta} = V\begin{pmatrix} Q & \Gamma_\mu & \Gamma_\mu \\ q & \beta & \alpha \end{pmatrix} \sum_j a(j) \left[\frac{w}{(w_{o-1}^2 - w^2)} - \frac{w}{(w_{o-o}^2 - w^2)} \right] \quad (3.2.30)$$

(In both expressions above, a(j) is a constant which depends on the excited electronic state je, and whose magnitude is determined by the molecular structure of the particular system involved.)

The resonance situation will be discussed later. If we are far from resonance, the above equation shows that the O-O and O-1 contributions are approximately equal in magnitude but opposite in sign, resulting in very low magnitude for antisymmetric scattering away from resonance. Thus the non-appearance of antisymmetric scattering in transparent scattering is due to the cancellation of the O-1 and O-O scattering contributions. This explanation was first obtained by Barron[5], without using irreducible tensor methods.

3.3 The Magnetically Perturbed Polarizability Tensor in Molecules With a Totally Symmetric Ground Electronic State

3.3.1 Introduction.

For non-totally symmetric modes, it was shown in (2.4.) that the magnetically perturbed polarizability tensor is given by

$$a_{\alpha\beta z} = \sum_{j \neq n} \langle j e j v | m_z | j e j v \rangle Z_{\alpha\beta} \qquad (3.3.1)$$

This was because, for molecules with non-degenerate ground states, $\langle n_e n_v \; m \; n_e n_v \rangle$ is zero. Also, only the z-component of the magnetic dipole moment operator has a non-zero expectation value expectation. With these points in mind, we now develop the above expression in a similar way to the treatment of $Z_{\alpha\beta}$ in the previous section.

3.3.2 Symmetry considerations.

Because we are dealing with the magnetic dipole moment operator, it is necessary to use complex representations for all the molecular states considered. A glance through the simply reducible molecular point groups shows an important point. This is that, except for O, the z component of the magnetic dipole moment operator always transforms as A_2. A further point is that only states having the irreducible representation E can have a non-zero expectation value involving an operator with symmetry A_2. Thus, only excited states with symmetry E can contribute to the magnetically perturbed polarizability. It also means that, again apart from the octahedral group, no perturbed polarizability with

z as a component can have a non-zero value.

The first restriction effectively reduces the magnitude of the perturbed polarizability considerably. This is because many fewer excited states can contribute to it than to the unperturbed polarizability, which in theory can have contributions from every excited state.

We use the following complex components for the representations E and A_2.[6]

$$g_X = i2^{-1/2}(g_1 - g_{-1}) \qquad g_Y = 2^{-1/2}(g_1 + g_{-1})$$

$$g_Z = -ig_0 \qquad (3.3.2)$$

Using complex components, we now express the Z tensors in terms of the quantities $Z_{r,s,z}$, where these are obtained from (3.3.1) by using complex components for the operators and states. The appropriate expressions are

$$Z_{XX} = -1/2(Z_{1,1} - Z_{1,-1} - Z_{-1,1} + Z_{-1,-1}) \qquad (3.3.3a)$$

$$Z_{XY} = 1/2i(Z_{1,1} + Z_{1,-1} - Z_{-1,1} - Z_{-1,-1}) \qquad (3.3.3b)$$

$$Z_{YX} = 1/2i(Z_{1,1} - Z_{1,-1} + Z_{-1,1} - Z_{-1,-1}) \qquad (3.3.3c)$$

$$Z_{YY} = 1/2(Z_{1,1} + Z_{1,-1} + Z_{-1,1} + Z_{-1,-1}) \qquad (3.3.3d)$$

(All terms involving z are zero.)

Having completed the general symmetry preliminaries, we go on in the next section to simplify the quantity $Z_{r,s,z}$ using irreducible tensor methods.

3.3.3 Derivation of general expression in complex form.

In this section, irreducible tensor methods are used to develop an expression for Z_{rsz} similar to that obtained earlier for $Z_{\alpha\beta}$. As before, we combine the electronic and vibrational states into a vibronic state, and take a sum over all the vibronic state symmetries possible. This gives

$$Z_{rs,z} = \sum_{j \neq k} \qquad (3.3.4)$$

$$\Big[\langle (nemv)Mm|u_r|(jejv)Jj\rangle\langle (kekv)Kk|u_s|(nenv)Nn\rangle$$

$$\times \langle (jejv)Jj|m_z|(jejv)Jj\rangle\langle (kekv)Kk|H(\underline{r},Q)|(jejv)Jj\rangle$$

$$+ \langle (nemv)Mm|u_r|(kekv)Kk\rangle\langle (jejv)Jj|u_s|(nenv)Nn\rangle$$

$$\times \langle (jejv)Jj|m_z|(jejv)Jj\rangle\langle (kekv)Kk|H(\underline{r},Q)|(jejv)Jj\rangle^* \Big]$$

Using the complex form of the Wigner-Eckart theorem, the first term becomes

$$[-1]^{M+r}[-1]^{J+m}[-1]^{J+m}V\begin{pmatrix} M & K & \Gamma_\mu \\ -r & k & i \end{pmatrix} V\begin{pmatrix} J & N & \Gamma_\mu \\ -m & s & j \end{pmatrix} V\begin{pmatrix} K & J & A \\ -k & m & i \end{pmatrix}$$

$$\times \langle (nemv)M\|u\|(jejv)J\rangle\langle (kekv)K\|u\|(nenv)N\rangle$$

$$\times \langle (kekv)K\|H(\underline{r},Q)\|(jejv)J\rangle\langle (jejv)Jj\|m_z\|(jejv)Jj\rangle \qquad (3.3.5)$$

The factors involving [-1] combine to give 1, and the product of V coefficients simplifies in a similar way to the previous section. This leaves us with the matrix element involving m_z. However,

$$\langle (jejv)Jj\|m\|(jejv)Jj\rangle = [-1]^{J+j}V\begin{pmatrix} J & J & A \\ j & j & i \end{pmatrix}\langle jejvJ\|m\|jejv\rangle$$

$$= i2^{-1/2}j\langle jejvJ\|m\|jejvJ\rangle \qquad (3.3.6)$$

where the last line follows by inspection of the V coefficients for groups other than O. Thus we have,

$$\langle (nemv)Mm|u_r|(jejv)Jj\rangle\langle (kekv)Kk|u_s|(nenv)Nn\rangle \times$$

$$\langle (jejv)Jj|m_z|(jejv)Jj\rangle\langle (kekv)Kk|H(\underline{r},Q)|(jejv)Jj\rangle$$

$$= \frac{i2^{-1/2}sV}{d(\Gamma_\mu)}\begin{pmatrix} M & \Gamma_\mu & \Gamma_\mu \\ m & s & r \end{pmatrix} \times \langle nemvM\|u\|jejvJ\rangle\langle kekvK\|u\|nenvN\rangle$$

$$\times \langle jejvJ\|m_z\|jejvJ\rangle\langle kekvK\|H(\underline{r},Q)\|jejvJ\rangle$$

$$= \frac{i2^{-1/2}sV}{d(\Gamma_\mu)}\begin{pmatrix} M & \Gamma_\mu & \Gamma_\mu \\ m & s & r \end{pmatrix} \times b_1(Q,\Gamma_\mu,\Gamma_\mu,je,jv,ke,kv) \qquad (3.3.7)$$

A similar result holds for the second term above. Combining these results we obtain

$$Z_{r,s,z} = \frac{i2^{-1/2}sV}{d(\Gamma_\mu)}\begin{pmatrix} M & \Gamma_\mu & \Gamma_\mu \\ m & s & r \end{pmatrix} \sum_i \; [\, b_1(Q,\Gamma_\mu,\Gamma_\mu,je,jv,ke,kv)] \qquad (3.3.8)$$

(we again take the V coefficient outside the summation since it is independent of the summation parameters)

This gives us finally

$$Z_{r,s,z} = \frac{i2^{-1/2}s}{d(\Gamma_\mu)} \times V\begin{pmatrix} M & \Gamma_\mu & \Gamma_\mu \\ m & s & r \end{pmatrix} \times b(Q,\Gamma_\mu,\Gamma_\mu) \qquad (3.3.9)$$

where

$$b(Q,\Gamma_\mu,\Gamma_\mu) = b_1(Q,\Gamma_\mu,\Gamma_\mu,je,jv,ke,kv) + b_2(Q,\Gamma_\mu,\Gamma_\mu,je,jv,ke,kv). \qquad (3.3.10)$$

(As before, we can consider $b(Q,\Gamma_\mu,\Gamma_\mu)$ to be a constant. Also as before, the two contributions b_1 and b_2 correspond to the 0-1 and 0-0 scattering pathways. The sign of the perturbed polarizability tensor patterns relative to the unperturbed polarizability tensor patterns is dependent in general on the scattering pathway involved. This important matter, which has consequences for the form of the M.C.I.D. spectra, is investigated in Section 3.3.5.)

The above expression involves the complex components of the perturbed polarizability, and contains a complex V coefficient. In the next section, we convert this complex form of the general expression back to a more easily used real form.

3.3.4 Conversion to the real form of the general expression.

We use expressions (3.3.) to convert the complex equation to it's real version. For clarity, we write the above in the following abbreviated form.

$$Z_{rs,z} = isC_{rs,z} \qquad (3.3.11)$$

We write this to illustrate the fact that the R.H.S. is equal to a tensor written in complex components multiplied

by the factor s. Each real component must now be considered separately. We present the explicit calculation for the xy component.

$$\begin{aligned} Z_{xy,z} &= i/2\,[\,Z_{1,1,z} + Z_{1,-1,z} - Z_{-1,1,z} - Z_{-1,-1,z}] \\ &= i.i/2[\,C_{1,1,z} - C_{1,-1,z} - C_{-1,1,z} + C_{-1,-1,z}] \\ &= C_{x x,z} \\ &= \frac{2^{-1/2}}{d(\Gamma_\mu)} \times V\begin{pmatrix} M & \Gamma_\mu & \Gamma_\mu \\ m & x & x \end{pmatrix} \times b(Q,\Gamma_\mu,\Gamma_\mu) \end{aligned} \qquad (3.3.12)$$

In the above, we have converted back to real V coefficients Using the above method, we obtain the following result for the components of the magnetically perturbed polarizability tensor.

$$\begin{bmatrix} Z_{x,x,z} & Z_{x,y,z} \\ Z_{y,x,z} & Z_{y,y,z} \end{bmatrix} = K \begin{bmatrix} -V\begin{pmatrix} Q & E & E \\ q & y & x \end{pmatrix} & V\begin{pmatrix} Q & E & E \\ q & x & x \end{pmatrix} \\ -V\begin{pmatrix} Q & E & E \\ q & y & y \end{pmatrix} & V\begin{pmatrix} Q & E & E \\ q & x & y \end{pmatrix} \end{bmatrix} \qquad (3.3.13)$$

where K contains the frequency dependance.

[We have already noted that only components involving x and y are non-zero, and these both belong to the representation E. Thus we can cosider b in the above as a constant.]

These results can be summarised by writing

$$Z_{\alpha\beta,z} = KxV\begin{pmatrix} \Gamma_Q x A_2 & E & E \\ q & \beta & \alpha \end{pmatrix} \qquad (3.3.14)$$

i.e. the perturbed polarizability tensor pattern for the normal mode Q is equal to the unperturbed polarizability tensor pattern for the normal mode $\Gamma_{Q}xA_2$. Following Konigstein's approach, mentioned in Section 3.2.4, this

means that we can consider that the magnetic perturbation has the effect of changing the symmetry of the states which are connected by the operator $A_{\alpha\beta,z}$, whilst having no effect on the effective symmetry of this operator.

3.3.5 Calculation of the relative signs of the perturbed tensor patterns for the 0-1 and 0-0 scattering pathways.

As we saw earlier, there are two contributions b_1 and b_2 to the magnetically perturbed polarizability constant b. Now it is clear from Section 3.3.3 that

$$b_1 = \langle (jejv)J \| m_z \| (jejv)J \rangle \times a_1 \qquad (3.3.15)$$

Thus we can identify b_1 and b_2 with the 0-1 and 0-0 scattering pathways respectively. We have already calculated the form of the tensor patterns for the perturbed polarizability tensor. As we have seen in Section 2.5, the M.R.O.A. spectrum is determined by terms involoving the products of the perturbed and unperturbed polarizability tensor. Thus we need to know the relative signs of the constants a and b. This is determined by the sign of the reduced matrix elements $\langle (jejv)J \| m_z \| (jejv)J \rangle$.

Thus we need to further reduce this reduced matrix element. To do this we use equation (2.6.9). For simply reducible groups (except O), this gives us

$$\begin{aligned} &\langle (jejv)J \| m^{A} \| (jejv)J \rangle \\ &= (-1)^{je+jv+J+A} d(J) \langle je \| m_z \| je \rangle W \begin{pmatrix} je & je & A_2 \\ J & J & jv \end{pmatrix} \\ &= -2(-1)^{J+v} W \begin{pmatrix} A_2 & E & E \\ jv & E & E \end{pmatrix} \langle je \| m^{A} \| je \rangle \end{aligned} \qquad (3.3.16)$$

We now consider the separate cases of 0-0 and 0-1 scattering.

0-0 scattering.

For 0-0 scattering, jv is equal to A_1. Hence for all normal modes,

$$\langle (jejv)J\|m^{A}\|(jejv)J\rangle = -2(-1)^{A} W\begin{pmatrix} A_2 & E & E \\ A_1 & E & E \end{pmatrix} \langle je\|m^{A}\|je\rangle$$

$$= \langle je\|m^{A}\|je\rangle \qquad (3.3.17)$$

(above we use (2.6.11) to simplify the W coefficient.)

This reduced electronic matrix element is positive if the molecular system has a positive g-factor.[6] Hence we expect b_{o-o} to have the same sign as a_{o-o}. (We can interpret this as meaning that the g-factor for the ground electronic state and the intermediate vibronic state have the same sign.)

0-1 scattering.

In this case, jv is equal to the normal mode which we are considering. Now from inspection of the various S.R. groups[7] other than O, it is clear that the following result holds:-

$$W\begin{pmatrix} A_2 & E & E \\ jv & E & E \end{pmatrix} = 1/2 \qquad (3.3.18)$$

(this result can be also deduced from a consideration of the definition of the W coefficient.)

Hence we obtain the following result:-

$$\langle (jejv)J\|m^{A_2}\|(jejv)J\rangle = -(-1)^{jv}\langle je\|m^{A_2}\|je\rangle$$

Now the term $(-1)^{jv}$ is +1 except when jv = A_2, in which case it equals -1. Therefore we deduce that for A_2 modes,

$$\langle (jejv)J\|m\|(jejv)J\rangle = \langle je\|m\|je\rangle \qquad (3.3.19)$$

and for all other non-totally symmetric modes

$$\langle (jejv)J\|m\|(jejv)J\rangle = -\langle je\|m\|je\rangle \qquad (3.3.20)$$

Result (3.3.20) is a generalization of the result already reported for the B modes of cytochrome c.[8] This change of sign for modes other than A_1 and A_2 can be interpreted as a change in the sign of the electronic g-factor for the excited vibronic state $(jejv)Jj\rangle$. This change is important

when we compare our calculated results with experiment.

3.3.6 Final expressions for the perturbed polarizability tensor

As we did for the unperturbed polarizability tensor, we can now give explicit expressions for the perturbed tensors. There are two different situations, which we consider separately below. These are scattering involving A modes, and scattering involving non-degenerate modes other than A modes. (Below, and in the remainder of the thesis, we use the abbreviation ⟨m⟩ for ⟨je|m|je⟩.)

A1 and A2 modes

$$a_{\alpha\beta} = V \begin{pmatrix} QxA_2 & \Gamma_\mu & \Gamma_\mu \\ q & \beta & \alpha \end{pmatrix} \sum_j \langle m\rangle a(j) 2w^2 \left[\frac{w}{(w_0^2 - o - w^2)^2} + \frac{w}{(w_0^2 - o - w^2)^2} \right] \qquad (3.3.21)$$

Other non-degenerate modes

$$a_{\alpha\beta} = V \begin{pmatrix} QxA_2 & \Gamma_\mu & \Gamma_\mu \\ q & \beta & \alpha \end{pmatrix} \sum_j \langle m\rangle a(j) 2w^2 \left[\frac{w_{0-o}}{(w_0^2 - o - w^2)^2} - \frac{w_{0-1}}{(w_0^2 - o - w^2)^2} \right] \qquad (3.3.22)$$

From the above results, we can see that when we are far from resonance, the 0-0 and 0-1 contributions for non-degenerate modes other than A modes tend to cancel each other out. As we have already seen, the polarizability tensor for A2 scattering tends to zero for this case also. Hence when far from resonance, the only modes for which we would expect observable magnitudes for the perturbed tensors are the A1 modes. This is another reason why M.C.I.D.'s have not been observed in transparent scattering.

3.4 The Polarizability Tensor for Molecules With Degenerate Electronic Ground States

3.4.1 Introduction

In Section 3.2, a general formula was obtained for the polarizability for molecules with an A_1 ground state. Unfortunately no such simple formula seems possible for molecules with a degenerate ground state. However, two useful results can be obtained using irreducible tensor methods. The simplest case is for A_1 vibrational modes, which we consider first.(Note: some results in this section are similar to those obtained by Barron using time-reversal arguments.[10] However, such arguments have not yet been successfully applied for non-totally symmetric modes.)

3.4.2 Symmetry preliminaries

For a molecule with a degenerate ground state, it is appropriate to use complex components for all operators and states. There are two situations of interest to be considered. Either the dipole moment operator transforms as T_1, or else (u_x,u_Y) transforms as E and u_z as A_2. For both of these cases, we can express (u_x, u_Y,u_z) as follows[9]

$$u_x = i2^{-1/2}(u_{+1} - u_{-1}) \qquad u_z = -iu_o$$
$$u_Y = 2^{-1/2}(u_{+1} + u_{-1}) \qquad (3.4.1)$$

where for the two cases we need to consider the appropriate irreducible representations. The reverse expressions are

$$u_{+1} = -i2^{-1/2}(u_x + iu_Y) \qquad u_o = iu_z$$
$$u_{-1} = i2^{-1/2}(u_x + u_Y) \qquad (3.4.2)$$

Using the above, we can express the cartesion components of a second rank Cartesian tensor in terms of the complex components as follows

$$A_{xx} = -1/2(A_{1,1} - A_{1,-1} - A_{-1,1} + A_{-1,-1})$$

$$A_{xy} = 1/2i(A_{1,1} + A_{1,-1} - A_{-1,1} - A_{-1,-1})$$

$$A_{yx} = 1/2i(A_{1,1} - A_{1,-1} + A_{-1,1} - A_{-1,-1})$$

$$A_{yy} = 1/2(A_{1,1} + A_{1,-1} + A_{-1,1} + A_{-1,-1})$$

$$A_{xz} = 2^{-1/2}(A_{1,0} - A_{-1,0}) \quad A_{yz} = -i2^{-1/2}(A_{1,0} + A_{-1,0})$$

$$A_{zx} = 2^{-1/2}(A_{0,1} - A_{0,-1}) \quad A_{zy} = -i2^{-1/2}(A_{0,1} + A_{0,-1})$$

$$A_{zz} = -A_{0,0} \qquad (3.4.3)$$

These expressions will be used explicitly in the development below, and implicitly in later calculations.

3.4.3 Totally symmetric modes

We assume that we are dealing with resonance Raman scattering, so that the main contribution to the polarizability comes from the X tensor. Now in this case the initial and final electronic states n_e and m_e are both components of the degenerate ground state. Assume that it is a doubly degenerate ground state (which is normally the case). We then have 4 different combinations of the initial and final electronic states. We label the complex components of the X tensor for each of these contributions as $(X_{ij})_{rs}$. We now develop expressions for these $(X_{ij})_{rs}$.

$$(X_{ij})_{rs} = \langle n_e r|u_i|j e m\rangle\langle j e m|u_j|n_e s\rangle \qquad (3.4.4)$$

$$= \langle n_e r|u_i|j e m\rangle\langle n_e s|u_j|j e m\rangle^* \qquad (3.4.5)$$

(by the hermiticity of the dipole moment operator)

$$= (-1)^{u(n_e - r)}(-1)^{u(n-s)} \sum_{\mu} \begin{pmatrix} n_e & \Gamma_\mu & j_e \\ -r & i & m \end{pmatrix} \sum_{\mu} \begin{pmatrix} n_e & \Gamma_\mu & j_e \\ -s & j & m \end{pmatrix} \qquad (3.4.6)$$

$$\times \langle n\|u\|j\rangle\langle n\|u\|j\rangle^*$$

(using version (2.6.14) of the Wigner-Eckart theorem)

$$= (-1)^{u(n-r)} x (-1)^{u(n-s)} V\begin{pmatrix} n_e & \Gamma_\mu & j_e \\ r & -i & -m \end{pmatrix} V\begin{pmatrix} n_e & \Gamma_\mu & j_e \\ s & -j & -m \end{pmatrix}$$
$$x \langle n \| u \| j \rangle x \langle n \| u \| j \rangle^* \quad (3.4.7)$$
$$x (-1)^{u(n+\Gamma+j+n+\Gamma+j)}$$

(using the tranformation properties of V coeeficients)

$$= (-1)^{u(n-r)} x (-1)^{u(n-s)} V\begin{pmatrix} n_e & \Gamma_\mu & j_e \\ r & -i & m \end{pmatrix} V\begin{pmatrix} n_e & \Gamma_\mu & j_e \\ s & -j & m \end{pmatrix}$$
$$x \langle n \| u \| j \rangle x \langle n \| u \| j \rangle^* \quad (3.4.8)$$
$$x (-1)^{u(n+\Gamma+j+n+Gj+j)}$$

(because the summation variable m is a dummy variable)

$$= (-1)^{u(n+r)} x (-1)^{u(n+s)} V\begin{pmatrix} n_e & \Gamma_\mu & j_e \\ r & -i & m \end{pmatrix} V\begin{pmatrix} n_e & \Gamma_\mu & j_e \\ s & -j & m \end{pmatrix}$$
$$x \langle n \| u \| j \rangle x \langle n \| u \| j \rangle^* \quad (3.4.9)$$
$$x (-1)^{u(n+\Gamma+j+n+\Gamma+j)}$$

(because u(2r+2s) is even for a doubly degenerate state)

$$= (X_{-i,-j})_{-r,-s} \times (-1)^{u(n+\Gamma+j+n+\Gamma+j)} \quad (3.4.10)$$

Now both electronic states j_e and n_e are degenerate. So whether we are in O* or one of the simply reducible double groups, we can write $(-1)^{u(n+n+j+j)} = 1$. This leaves us with the factor $(-1)^{u(\Gamma+\Gamma)}$. Now if we are in O*, both Γ_{μ_1} and Γ_{μ_2} are T_1 and therefore this factor is 1. If we are not in O*, this factor is 1 anyway.

Hence we can write

$$(X_{ij})_{rs} = (X_{-i,-j})_{-r,-s} \quad (3.4.11)$$

Deductions about X Using (3.4.11)

(a) Off-Diagonal Scattering Pathways

The following are an immediate consequence of (3.4.11).

$$(X_{ij})_{-1/2,1/2} = (X_{-i,-j})_{1/2,-1/2} \quad (3.4.12)$$

$$(X_{ij})_{-1/2,-1/2} = (X_{-i,-j})_{1/2,1/2} \quad (3.4.13)$$

Using expressions (3.3.) along with (3.3.) allows us to

deduce the following type of result

$$(X_{xy})_{-1/2,1/2} = 1/2i[(X_{1,1} + X_{1,-1} - X_{-1,1} - X_{-1,-1}]_{-1/2,1/2}$$
$$= 1/2i[(X_{-1,-1} + X_{-1,1} - X_{1,-1} - X_{1,1}]_{1/2,-1/2}$$
$$= -1/2i[(X_{1,1} + X_{1,-1} - X_{-1,1} - X_{-1,-1}]_{1/2,-1/2}$$
$$= -(X_{xy})_{1/2,-1/2} \qquad (3.4.14)$$

Proceeding thus, we obtain the following results. (For convenience, the results are given as a matrix, with the initial and final electronic states given at the bottom right.)

$$\begin{bmatrix} X_{xx} & X_{xy} & X_{xz} \\ X_{yx} & X_{yy} & X_{yz} \\ X_{zx} & X_{zy} & X_{zz} \end{bmatrix}_{-1/2,1/2} = \begin{bmatrix} +X_{xx} & -X_{xy} & -X_{xz} \\ -X_{yx} & +X_{yy} & +X_{yz} \\ -X_{zx} & +X_{zy} & +X_{zz} \end{bmatrix}_{1/2,-1/2} \qquad (3.4.15)$$

In order to proceed further, we make use of the hermiticity of the dipole moment operator to deduce that

$$(X_{\alpha\beta})_{r,s} = (X_{\beta\alpha})_{s,r} \qquad (3.4.16)$$

We can write this in matrix form as

$$\begin{bmatrix} X_{xx} & X_{xy} & X_{xz} \\ X_{yx} & X_{yy} & X_{yz} \\ X_{zx} & X_{zy} & X_{zz} \end{bmatrix}_{-1/2,1/2} = \begin{bmatrix} X_{xx} & X_{yx} & X_{zx} \\ X_{xy} & X_{yy} & X_{zy} \\ X_{xz} & X_{yz} & X_{zz} \end{bmatrix}_{1/2,-1/2} \qquad (3.4.17)$$

We make use of one further result. Because all the V coefficients we use are real, we can deduce that all the complex components (X_{ij}) are real. (see (3.4.8), where a reduced matrix element times it's complex conjugate appears.) From (3.3.)we obtain the following table.

Table 4.1 : classifying tensor components as real or imaginary

REAL		IMAGINARY	
X_{xx}	X_{yy}	X_{xy}	X_{yx}
X_{xz}	X_{zx}	X_{yz}	X_{zy}
X_{zz}			

We now combine (3.4.15) and (3.3.17) to give us

$$2(X\ )_{-1/2,1/2} = \begin{bmatrix} X_{xx} + X_{xx} & X_{yx} - X_{xy} & X_{zx} - X_{xz} \\ X_{xy} - X_{yx} & X_{yy} + X_{yy} & X_{zy} + X_{yz} \\ X_{xz} - X_{zx} & X_{yz} + X_{zy} & X_{zz} + X_{zz} \end{bmatrix}$$

$$= \begin{bmatrix} 2X_{xx} & -(X_{yx} + X_{xy}) & -(X_{xz} - X_{zx}) \\ -(X_{xy} + X_{yx}) & 2X_{yy} & -(X_{zy} - X_{yz}) \\ (X_{xz} - X_{zx}) & (X_{zy} - X_{yz}) & 2X_{zz} \end{bmatrix} \qquad (3.4.18)$$

Thus we can write

$$(X\ )_{-1/2,1/2} = \begin{bmatrix} A & iD & -E \\ iD & B & -iF \\ E & iF & C \end{bmatrix} \qquad (3.4.19)$$

where A,B,C,D,E,F are all real.

Similarly, using (3.3.), we have

$$(X\ )_{1/2,-1/2} = \begin{bmatrix} A & -iD & E \\ -iD & B & -iF \\ -E & iF & C \end{bmatrix} \qquad (3.4.20)$$

These expressions have been derived without any assumptions about the molecular system in question, and without any specification of whether the scattering is Rayleigh or Raman. Thus (3.4.18) and (3.4.19) are true for either Rayleigh or totally symmetric Raman scattering involving an off-diagonal scattering pathway between a doubly degenerate electronic ground state. They show that for such systems, both real and imaginary antisymmetric scattering exists. They also demonstrate, as will become clear later, that such systems yield an M.C.I.D. couplet.

The above expressions also provide a useful check when detailed calculations are being performed on a specific system.

(a) Diagonal Scattering Pathways

From (3.4.11) we see immediatly that

$$(X\ )_{-1/2,-1/2} = (X\ )_{1/2,1/2} \qquad (3.4.21)$$

Proceeding as before, we obtain the following results, which correspond to (3.4.16):

$$\begin{bmatrix} Xxx & Xxy & Xxz \\ Xyx & Xyy & Xyz \\ Xzx & Xzy & Xzz \end{bmatrix}_{-1/2,-1/2} = \begin{bmatrix} +Xxx & -Xxy & -Xxz \\ -Xyx & +Xyy & +Xyz \\ -Xzx & +Xzy & +Xzz \end{bmatrix}_{1/2,1/2} \qquad (3.4.22)$$

In an identical manner to the method detailed above, we obtain the following general expressions for the diagonal scattering pathway.

$$(X\ )_{1/2,1/2} = \begin{bmatrix} A & -iD & E \\ iD & B & -iF \\ E & iF & C \end{bmatrix} \qquad (3.4.23)$$

$$(X\ )_{-1/2,-1/2} = \begin{bmatrix} A & iD & -E \\ -iD & B & -iF \\ -E & iF & C \end{bmatrix} \qquad (3.4.24)$$

(the above A,B,C,D,E,F are all real, and are unrelated to those quantities appearing in the previous subsection.)

From (3.4.23) we deduce that for diagonal scattering, there are only real symmetric and imaginary antisymmetric contributions. It can also be deduced, as will be seen later, that the two contributions to the M.C.I.D.'S from -1/2,-1/2 and 1/2,1/2 cancel each other out.

As before, these expressions are a good guideline when performing detailed calculations.

Having obtained the above expressions for the X tensor, we next consider the properties of the Z tensor, which is responsible for scattering in non-totally symmetric modes.

3.4.4 Non-totally symmetric modes

For non-totally symmetric modes, the only non-zero contribution to the polarizability tensor comes from the Z tensor. We now carry out a similar development to the one for the X tensor in the previous section. As before, we go into details for only one of the four contributions to the Z tensor, since the details for the others are very similar.

We assume initially that the normal mode is degenerate. Then we write

$$(Zdf)_{s,t} = \langle me\,mv\,q|ud|ke\,kv\,p\rangle \qquad (3.4.25)$$

$$\times \langle je\,cjv\,f|uf|ne\,tnv\rangle\langle ke\,kv\,p|(HqQ)|je\,cjv\,f\rangle$$

$$= (-1)^{p(me+mv+M)}(-1)^{u(2mv+M-r)}[M]^{1/2}V\begin{pmatrix} me & mv & M \\ s & q & r \end{pmatrix}$$

$$\times \langle(nemv)Mr|ud|(kekv)Kk\rangle$$

$$\times \langle(jejv)Jj|uf|(nenv)net\rangle\langle(kekv)Kk|HqQ|(jejv)Jj\rangle$$

(where me and mv have been coupled using (2.6.16))

$$= TxP(-1)^{u(M-r)+u(M-r)u+(J-j)+u(J-j)}$$

$$V\begin{pmatrix} ne & mv & M \\ s & q & r \end{pmatrix}V\begin{pmatrix} M & \Gamma_\mu & J \\ -r & d & j \end{pmatrix}V\begin{pmatrix} J & A & J \\ -j & i & j \end{pmatrix}V\begin{pmatrix} J & \Gamma_\mu & ne \\ j & f & t \end{pmatrix}$$

where

$$T = (-1)^{p(me+mv+M)+u(2m_v)}d(M)^{1/2} \qquad (3.4.26a)$$

$$P = \langle(nemv)M||u||(kekv)K\rangle\langle(jejv)J||u||(nenv)ne\rangle \qquad (3.4.26b)$$

$$\times \langle(kekv)K||(HqQ)||(jejv)J\rangle$$

Thus $(Zdf)_{s,t}$ (3.4.27)

$$= TP \times V\begin{pmatrix} ne & mv & M \\ s & q & r \end{pmatrix}V\begin{pmatrix} M & \Gamma_\mu & J \\ -r & d & j \end{pmatrix}V\begin{pmatrix} J & A & J \\ -j & i & j \end{pmatrix}V\begin{pmatrix} J & \Gamma_\mu & ne \\ -j & f & t \end{pmatrix}$$

(since the sum of the factors involving u is even)

$$= TxP(-1)^{u(me+mv+M)+u(M+Gx+J)+u(J+A+J)+u(J+Gy+ne)}$$

$$V\begin{pmatrix} ne & mv & M \\ -s & -q & -r \end{pmatrix}V\begin{pmatrix} M & \Gamma_\mu & J \\ r & -d & -j \end{pmatrix}V\begin{pmatrix} J & A & J \\ j & i & -j \end{pmatrix}V\begin{pmatrix} J & \Gamma_\mu & ne \\ j & -f & -t \end{pmatrix}$$

$$= \quad TxP(-1)^{u(me+mv+M)+u(M+\Gamma+J)+u(J+A+J)+u(J+\Gamma+ne)}$$

$$V\begin{pmatrix} ne & mv & M \\ -s & q & r \end{pmatrix} V\begin{pmatrix} M & \Gamma_\mu & J \\ -r & -d & j \end{pmatrix} V\begin{pmatrix} J & A & J \\ -j & i & j \end{pmatrix} V\begin{pmatrix} J & \Gamma_\mu & ne \\ -j & -f & -t \end{pmatrix}$$

(because all the summation variables are dummy variables)

$$= (-1)^F (Z-d,-f)-s,-t \qquad (3.4.28)$$

Now $(-1)^F$

$$= (-1)^{u(me+mv+M)+u(M+\Gamma+J)+u(J+A+J)+u(J+\Gamma+ne)}$$

$$=(-1)^{u(2me)+u(2M)+u(4J)+u(\Gamma+\Gamma)+u(A+mv)} \qquad (3.4.29)$$

Assuming the degenerate ground electronic state has symmetry E'(which is normally the case), u(2me) is 1. u(2M) is always odd, u(4J) is always even, $u(\Gamma+\Gamma)$ is always even and u(A) is 0. Therefore $(-1)^F$ is equal to $(-1)^{u(mv)}$.

Hence we have

$$(Zdf)_{s,t} = (-1)^{u(mv)}(Z-d,-f)-s,-t \qquad (3.4.30)$$

3.4.5 Deductions about Z using (3.4.29)

(a) Molecules having point groups other than O*

For these molecules, $(-1)^{u(mv)}$ is zero for all normal modes. Thus

$$(Zdf)_{s,t} = (Z-d,-f)-s,-t \qquad (3.4.31)$$

We shall see that this case is identical to the E vibrational mode for the octahedral double group O*, which is dealt with below.

(b) Molecules having point group O*

There are two non-totally symmetric normal modes of interest for this case, namely E and T_{2g}. We deal with these separately.

Normal mode E

For this mode, $(-1)^{u(E)} = 0$. Hence the development for the E mode is similar to that for the totally symmetric mode. We again consider the cases of diagonal and off-diagonal scattering pathways separately.

Off-Diagonal Scattering Pathways

Proceeding exactly as for the totally symmetric mode, we obtain the following two results.

$$\begin{bmatrix} X_{xx} & X_{xy} & X_{xz} \\ X_{yx} & X_{yy} & X_{yz} \\ X_{zx} & X_{zy} & X_{zz} \end{bmatrix}_{-1/2,1/2} = \begin{bmatrix} +X_{xx} & -X_{xy} & -X_{xz} \\ -X_{yx} & +X_{yy} & +X_{yz} \\ -X_{zx} & +X_{zy} & +X_{zz} \end{bmatrix}_{1/2,-1/2} \qquad (3.4.32)$$

and

$$\begin{bmatrix} X_{xx} & X_{xy} & X_{xz} \\ X_{yx} & X_{yy} & X_{yz} \\ X_{zx} & X_{zy} & X_{zz} \end{bmatrix}_{-1/2,1/2} = \begin{bmatrix} X_{xx} & X_{yx} & X_{zx} \\ X_{xy} & X_{yy} & X_{zy} \\ X_{xz} & X_{yz} & X_{zz} \end{bmatrix}_{1/2,-1/2} \qquad (3.4.33)$$

Now for the totally symmetric mode, we were able to predict that certain components were real and some were imaginary. Because the product of reduced matrix elements is more complicated this time, we cannot do this. However, as before we can write

$$2(X_{\alpha\beta})_{-1/2,1/2} = \begin{bmatrix} X_{xx}+X_{xx} & X_{yx}-X_{xy} & X_{zx}-X_{xz} \\ X_{xy}-X_{yx} & X_{yy}+X_{yy} & X_{zy}+X_{yz} \\ X_{xz}-X_{zx} & X_{yz}+X_{zy} & X_{zz}+X_{zz} \end{bmatrix} \qquad (3.4.34)$$

From this, we deduce the following form for the tensor pattern

$$(X_{\alpha\beta})_{-1/2,1/2} = \begin{bmatrix} A & \tilde{D} & \tilde{E} \\ -\tilde{D} & B & \tilde{F} \\ -\tilde{E} & \tilde{F} & C \end{bmatrix} \qquad (3.4.35)$$

where A,B,C, are real and D,E,F are in general complex.

Similarly, using (3.3.), we have

$$(X_{\alpha\beta})_{1/2,-1/2} = \begin{bmatrix} A & -\tilde{D} & -\tilde{E} \\ \tilde{D} & B & \tilde{F} \\ \tilde{E} & \tilde{F} & C \end{bmatrix} \qquad (3.4.36)$$

They show that for such systems, both real and imaginary antisymmetric scattering exists. They also demonstrate, as will become clear later, that such systems yield an M.C.I.D. couplet.

The above expressions also provide a useful check when detailed calculations are being performed on a specific system.

(a) Diagonal Scattering Pathways

Proceeding as before, we obtain the following results

$$(X_{\alpha\beta})_{-1/2,-1/2} = (X_{\alpha\beta})_{1/2,1/2} \qquad (3.4.37)$$

$$\begin{bmatrix} X_{xx} & X_{xy} & X_{xz} \\ X_{yx} & X_{yy} & X_{yz} \\ X_{zx} & X_{zy} & X_{zz} \end{bmatrix}_{-1/2,-1/2} = \begin{bmatrix} +X_{xx} & -X_{xy} & -X_{xz} \\ -X_{yx} & +X_{yy} & +X_{yz} \\ -X_{zx} & +X_{zy} & +X_{zz} \end{bmatrix}_{1/2,1/2} \qquad (3.4.38)$$

In a calculation very similar to the previous one, we obtain the following expressions for the forms for the tensor patterns of the diagonal scattering pathways.

$$(X_{\alpha\beta})_{1/2,1/2} = \begin{bmatrix} A & \tilde{D} & \tilde{E} \\ -\tilde{D} & B & \tilde{F} \\ -\tilde{E} & \tilde{F} & C \end{bmatrix} \qquad (3.4.39)$$

$$(X_{\alpha\beta})_{-1/2,-1/2} = \begin{bmatrix} A & \tilde{D} & \tilde{E} \\ -\tilde{D} & B & \tilde{F} \\ -\tilde{E} & \tilde{F} & C \end{bmatrix} \qquad (3.4.40)$$

where A,B,C are real and D,E,F are complex, and are unrelated to those quantities appearing in the off-diagonal

scattering case.

From (3.4.39-40) we deduce that for diagonal scattering, all 4 different types of the polarizability tensor (real symmetric etc.) can in general exist. It can also be deduced, as will be seen later, that the two contributions to the M.C.I.D.s from -1/2,-1/2 and 1/2,1/2 cancel each other out.

We now move on to study the patterns for the T_{2g} modes.

Normal mode T_{2g}

(i) Off-Diagonal Scattering Pathways

The following expressions are an immediate consequence of (3.4.30).

$$(Z_{ij})_{-1/2,1/2} = -(Z_{-i,-j})_{1/2,-1/2} \quad (3.4.41)$$

$$(Z_{ij})_{-1/2,-1/2} = -(Z_{-i,-j})_{1/2,1/2} \quad (3.4.42)$$

Using expressions (3.3.41) along with (3.3.42) allows us to deduce the following type of result

$$\begin{aligned}(Z_{XY})_{-1/2,1/2} &= +1/2i[(Z_{1,1} + Z_{1,-1} - Z_{-1,1} - Z_{-1,-1}]_{-1/2,1/2} \\ &= -1/2i[(Z_{-1,-1} + Z_{-1,1} - Z_{1,-1} - Z_{1,1}]_{1/2,-1/2} \\ &= +1/2i[(Z_{1,1} + Z_{1,-1} - Z_{-1,1} - Z_{-1,-1}]_{1/2,-1/2} \\ &= +(Z_{XY})_{-1/2,1/2} \end{aligned} \quad (3.4.43)$$

Proceeding thus, we obtain the following set of results, again written in matrix form

$$\begin{bmatrix} Z_{XX} & Z_{XY} & Z_{XZ} \\ Z_{YX} & Z_{YY} & Z_{YZ} \\ Z_{ZX} & Z_{ZY} & Z_{ZZ} \end{bmatrix}_{-1/2,1/2} = \begin{bmatrix} -Z_{XX} & +Z_{XY} & +Z_{XZ} \\ +Z_{YX} & -Z_{YY} & -Z_{YZ} \\ +Z_{ZX} & -Z_{ZY} & -Z_{ZZ} \end{bmatrix}_{1/2,-1/2} \quad (3.4.44)$$

As before, we make use of the hermiticty of the dipole moment operator to deduce that

$$(Z_{\alpha\beta})_{r,s} = (Z_{\beta\alpha})^*_{s,r} \quad (3.4.45)$$

We can write this in matrix form as

$$\begin{bmatrix} Z_{xx} & Z_{xy} & Z_{xz} \\ Z_{yx} & Z_{yy} & Z_{yz} \\ Z_{zx} & Z_{zy} & Z_{zz} \end{bmatrix}_{-1/2,1/2} = \begin{bmatrix} Z_{xx} & Z_{yx} & Z_{zx} \\ Z_{xy} & Z_{yy} & Z_{zy} \\ Z_{xz} & Z_{yz} & Z_{zz} \end{bmatrix}_{1/2,-1/2} \qquad (3.4.46)$$

As for the previous case of the E mode, we can no longer predict that some tensor components are real and some imaginary. We now combine (3.4.44) and (3.4.46) to give us

$$2(Z_{\alpha\beta})_{-1/2,1/2} \qquad (3.4.47)$$

$$= \begin{bmatrix} Z_{xx} - Z_{xx} & Z_{yx} + Z_{xy} & Z_{zx} + Z_{xz} \\ Z_{xy} + Z_{yx} & Z_{yy} - Z_{yy} & Z_{zy} - Z_{yz} \\ Z_{xz} + Z_{zx} & Z_{yz} - Z_{zy} & Z_{zz} - Z_{zz} \end{bmatrix}$$

From this it is easily deduced that

$$(Z_{\alpha\beta})_{-1/2,1/2} = \begin{bmatrix} iA & \tilde{D} & \tilde{E} \\ \tilde{D} & iB & \tilde{F} \\ \tilde{E} & -\tilde{F} & iC \end{bmatrix} \qquad (3.4.48)$$

where A,B,C are all real, and D,E and F are all complex.

Similarly, using (3.3.), we have

$$(Z_{\alpha\beta})_{1/2,-1/2} = \begin{bmatrix} -iA & \tilde{D} & \tilde{E} \\ \tilde{D} & -iB & -\tilde{F} \\ \tilde{E} & \tilde{F} & -iC \end{bmatrix} \qquad (3.4.49)$$

Various conclusions can be drawn from these results. We note first of all that when we sum the isotropic contributions for off-diagonal scattering pathways we get zero. Thus we deduce that there is no isotropic contribution to the scattering for the T_g mode. A second deduction we can make is that for off-diagonal scattering, all types of scattering can be non-zero, unlike the case for totally symmetric scattering. Finally, we can deduce from the form of the tensor patterns that a non-zero M.C.I.D. couplet will be obtained.

(ii) Diagonal Scattering Pathways

Using the same approach as for the E mode, we obtain the following results

$$\begin{bmatrix} Z_{xx} & Z_{xy} & Z_{xz} \\ Z_{yx} & Z_{yy} & Z_{yz} \\ Z_{zx} & Z_{zy} & Z_{zz} \end{bmatrix}_{-1/2,-1/2} = \begin{bmatrix} -Z_{xx} & +Z_{xy} & +Z_{xz} \\ +Z_{yx} & -Z_{yy} & -Z_{yz} \\ +Z_{zx} & -Z_{zy} & -Z_{zz} \end{bmatrix}_{1/2,1/2} \qquad (3.4.50)$$

$$(Z_{\alpha\beta})_{-1/2,-1/2} = \begin{bmatrix} A & \tilde{D} & \tilde{E} \\ \tilde{D} & B & \tilde{F} \\ \tilde{E} & \tilde{F} & C \end{bmatrix} \qquad (3.4.51)$$

where A,B,C are all real.

Similarly, using (3.3.), we have

$$(Z_{\alpha\beta})_{1/2,1/2} = \begin{bmatrix} -A & \tilde{D} & \tilde{E} \\ \tilde{D} & -B & -\tilde{F} \\ \tilde{E} & -\tilde{F} & -C \end{bmatrix} \qquad (3.4.52)$$

Again we note that when we add together the two diagonal contributions, the isotropic part sums to zero. We also note that, as before, the two diagonal M.C.I.D. contributions cancel each other out.

In the next section, we look at the different mechanisms which can give rise to M.R.O.A.

3.5 Mechanisms for Generating Magnetic Optical Activity

3.5.1 Introduction

In this section, we are concerned with the two mechanisms which can generate magnetic optical activity. These two mechanisms were outlined in the opening chapter. The first involves molecules which have a degenerate ground state. The second involves resonance scattering, where the resonance state is degenerate. These two scattering processes have different characteristics, which we now discuss.

3.5.2 M.R.O.A. originating from ground state electronic degeneracy.

In Section 2.3, expressions (2.5.20-23) were developed. These gave the magnitude of $I^R - I^L$ in terms of the molecular scattering tensors. These expressions were then averaged over all orientations, yielding (2.5.26-29). However, it is not always correct to perform this orientational average.

For the case of a molecule which has a degenerate electronic ground state, an orientational average is not required.[11] This is because the magnetic field, assuming it is sufficiently strong, completely orients the molecular magnetic dipole moments[12] , i.e. the dipole moment of one component of the degenerate state aligns with the magnetic field, and the other aligns against the magnetic field. We therefore treat the scattering originating in the +1/2 state independently from that originating in the -1/2 state.

From the above, it is clear that we should use the unaveraged expressions (2.5.20-21) when the electronic ground state is degenerate. Now we have already seen that for the case of totally symmetric scattering, if there is no magnetic field present, all the contributions cancel. (See (3.4.18-19) and (3.4.22-23).)If there is a magnetic field, then in principle the single Raman band is split into three peaks. From (3.4.22-23), we again see that the two diagonal scattering contributions still cancel, and from (3.4.18-19) we see that the two off-diagonal contributions give equal and opposite M.C.I.D.s. This is also true for non-totally symmetric modes. Thus, for magnetic optical activity generated by this first mechanism, we obtain an M.R.O.A. spectrum composed of positive-negative couplets.

3.5.3 M.R.O.A. originating from excited state electronic degeneracy.

For the case of a molecule without a degenerate ground state, it is correct to take an orientatioal average.
When we do this, only the part involving the perturbed polarizability tensor has a non-zero average. Thus, to calculate the M.C.I.D. components, the appropriate equations are (2.5.26-29). However, these can be simplified considerably. From the tensor patterns in Chapter 8 we note the following point about the polarizability and the perturbed polarizability components. This is that, apart from the third component of the perturbed polarizability tensor, all the components involve only x and y. This allows us to simplify greatly the M.C.I.D. expressions. To show

this, we simplify $I_z^R(90^o)-I_z^L(90^o)$

$$\tilde{a}_{\alpha\beta}\varepsilon_{\beta\alpha\delta}\tilde{a}^*_{\gamma\delta} = \tilde{a}_{\alpha\beta}\varepsilon_{\beta\alpha\delta}\tilde{a}_{z\delta z} = 0 \qquad (3.5.1)$$

$$\tilde{a}_{\alpha\beta}\varepsilon_{\beta\gamma\delta}\tilde{a}^*_{\gamma\delta\alpha} = a_{z\beta}\varepsilon_{\beta\gamma\delta}\tilde{a}^*_{\gamma\delta z} = 0 \qquad (3.5.2)$$

$$\begin{aligned}\tilde{a}_{\alpha\beta}\varepsilon_{\beta\gamma\delta}\tilde{a}^*_{\alpha\delta\gamma} &= \tilde{a}_{\alpha\beta}\varepsilon_{\beta\gamma z}\tilde{a}^*_{\alpha\delta z}\\ &= \tilde{a}_{\alpha\gamma}a_{\alpha xz}-\tilde{a}_{\alpha x}\tilde{a}^*_{\alpha\gamma z}\\ &= \tilde{a}_{x\gamma}\tilde{a}^*_{xxz}+\tilde{a}_{y\gamma}\tilde{a}^*_{yxz}-\tilde{a}_{xx}\tilde{a}^*_{xyz}-\tilde{a}_{yx}\tilde{a}^*_{yyz}\end{aligned} \qquad (3.5.3)$$

Thus $I_z^R(90^o)-I_z^L(90^o)$

$$= KBz/15\times Im[\tilde{a}_{xy}\tilde{a}^*_{xxz} + \tilde{a}_{yy}\tilde{a}^*_{yxz} - \tilde{a}_{xx}\tilde{a}^*_{xyz} - \tilde{a}_{yx}\tilde{a}^*_{yyz}] \qquad (3.5.4)$$

Similarly we have

$$I_x^R(90^o)-I_x^L(90^o)$$

$$= 2KBz/15\times Im[\tilde{a}_{xy}\tilde{a}^*_{xxz} + \tilde{a}_{yy}\tilde{a}^*_{yxz} - \tilde{a}_{xx}\tilde{a}^*_{xyz} - \tilde{a}_{yx}\tilde{a}^*_{yyz}] \qquad (3.5.5)$$

Thus our calculations show that for non-degenerate modes of vibration, the polarized difference spectra should be exactly twice the depolarized difference spectra. (cf. the corresponding result for natural R.O.A., mentioned in Chapter 1. As in the natural case, the result holds when axial symmetry is present.) In the same way, we obtain the following for the sum spectra

$$I_x(90^o)+I_x(90^o) \qquad (3.5.6)$$

$$= (K/30)[4|\tilde{a}_{xx}|^2+4|\tilde{a}_{yy}|^2+3|\tilde{a}_{xy}|^2+3|\tilde{a}_{yx}|^2+Re(\tilde{a}_{xx}\tilde{a}^*_{yy}+\tilde{a}_{xy}\tilde{a}^*_{yx})]$$

$$I_z(90^o)+I_z(90^o) \qquad (3.5.7)$$

$$= (K/15)[|\tilde{a}_{xx}|^2+|\tilde{a}_{yy}|^2+2|\tilde{a}_{xy}|^2+2|\tilde{a}_{yx}|^2-Re(\tilde{a}_{xx}\tilde{a}^*_{yy}-\tilde{a}_{xy}\tilde{a}^*_{yx})]$$

For the magnetic optical activity generated by this mechanism, we obtain single peaks of positive or negative sign. To determine the appropriate sign, we need to consider not only the tensor patterns but also the frequency dependence of the difference spectra. We do this in the next section.

3.6 The Frequency Dependance of the Scattering Parameters in the Case of Resonance

3.6.1 Introduction

In the previous chapters, we have developed expressions for the polarizability and magnetically perturbed polarizability tensors. So far, however, we have only considered the frequency dependence of these expressions for the case of transparent scattering. We now extend the development so as to include the resonance case. Once we do that, we then go on to calculate the frequency dependence of the various scattering observables. This will be of importance later, when we compare theory with experimental observation.

3.6.2 Lineshape functions for resonance scattering

For transparent scattering, both the polarizability and the magnetic polarizability contain frequency terms involving the reciprocal of $(\omega_{jn}^2-\omega^2)$, where j is an excited state and n is the ground state. Now for the case of resonance scattering, the frequency of the exciting radiation is very close to the frequency ω_{jn}. According to the above term, the scattering tensors should tend to infinity as the frequency tends to the resonance frequency. That this does not happen is due to the fact that excited states have finite lifetimes.

When a molecule is in an excited state j, spontaneous emission occurs.[13] Because of this, the excited state only

has a finite lifetime. To incorporate this into the wavefunction for the state j, we include an exponential decay term $e^{-1/2\Gamma t}$, where $1/\Gamma$ is the lifetime of the state.[14] (Note that spontaneous emission is described by Einstein's A coefficient, for which quantum mechanical expressions exist. Thus in principle it is possible to calculate the value of the decay constant.[15])

Inserting this into the time dependent Schrodinger equation gives the following change to the energy of the excited state j

$$w_j \longrightarrow w_j - ih\Gamma/2 \qquad (3.6.1)$$

In all the cases of interest to us, the molecular system in question will be in the ground state, which has in theory an infinite lifetime. Thus we make the following modification $w_{jn} \longrightarrow w_{jn} - i\Gamma/2$ (3.6.2)

Inserting this into the frequency term mentioned earlier gives us

$$\begin{aligned} 1/(w_{jn}^2 - w^2) \longrightarrow\ & 1/[\ (w_{jn}^2 - w^2) - iw_{jn}\Gamma_j - \Gamma_j^2/4\ ] \\ =\ & \frac{(w_{jn}^2 - w^2) + iw\Gamma_j}{[\ (w_{jn}^2 - w^2)^2 + w^2\Gamma_j^2\ ]} \\ =\ & f_j + ig_j \end{aligned} \qquad (3.6.3)$$

where f_j and g_j are called the dispersion and absorption lineshape functions.[16] They are equal to the real and imaginary parts respectively of the above expression. (Note that they only apply close to resonance, because we have used the approximation $w = w_{jn}$ several times.) Below in Figs. 3.2(a) and 3.2(b) are graphs of f_j and g_j for frequencies around the resonance frequency w_{jn}.[17] As can be seen from the graphs, Γ_j is approximately the band width of g_j at half it's maximum height, and approximately the

separation between the peaks of f_j. Another important point to note is that f_j changes sign as we go through the resonance frequency. This will be of importance later.

It can be shown from general dynamical considerations that it is the imaginary part of (3.6.3) which is responsible for the absorption of radiation-hence g is called the absorption function.[18] Also, it is g which gives the characteristic shape to absorption curves. f is termed the dispersion lineshape function because it is responsible for the form of the dispersion law, which gives the variation of refractive index with frequency.[19]

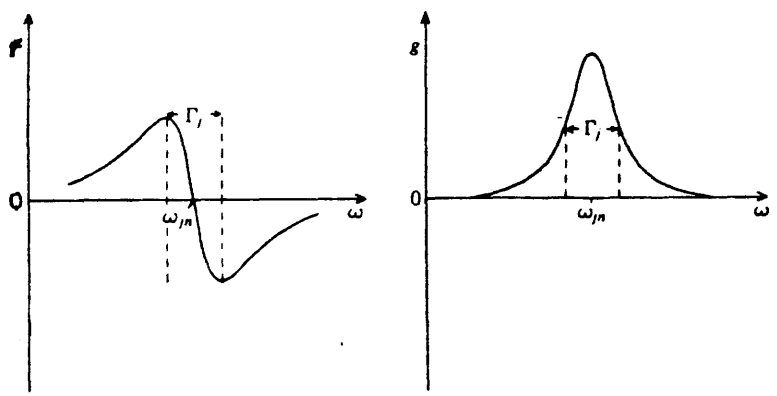

Fig. 3.2 The absorption and dispersion lineshape functions f and g.

3.6.3 The frequency dependance of the molecular scattering tensors

For resonance with the excited electronic state j_e, the expressions for the polarizability tensors have to be modified. Substituting lineshape functions in place of frequency factors we obtain the following results for the symmetric and antisymmetric polarizability tensors respectively:-

$$\tilde{a}^{s}_{\alpha\beta} = aV\begin{pmatrix}\Gamma Q & \Gamma_\mu & \Gamma_\mu \\ q & \beta & \alpha\end{pmatrix} \times [\, w_{o-o}(f+ig)_{o-o} + w_{o-1}(f+ig)_{o-1}\,] \qquad (3.6.4)$$

and

$$\tilde{a}^{a}_{\alpha\beta} = aV\begin{pmatrix}\Gamma Q & \Gamma_\mu & \Gamma_\mu \\ q & \beta & \alpha\end{pmatrix} \times [\, w(f+ig)_{o-o} - w(f+ig)_{o-1}\,] \qquad (3.6.5)$$

Making the same substitution in the the magnetically perturbed polarizability tensors at resonance we obtain

$$\tilde{a}^{s}_{\alpha\beta z} = \langle m\rangle aV\begin{pmatrix}\Gamma Q x A_2 & \Gamma_\mu & \Gamma_\mu \\ q & \beta & \alpha\end{pmatrix} 2w^2 x\,[\, w_{o-o}(f+ig)_{o-o} - (-1)^{j_v} w_{o-1}(f+ig)_{o-1}] \qquad (3.6.6)$$

for symmetric scattering, and

$$\tilde{a}^{a}_{\alpha\beta z} = \langle m\rangle aV\begin{pmatrix}\Gamma Q x A_2 & \Gamma_\mu & \Gamma_\mu \\ q & \beta & \alpha\end{pmatrix} 2w^2 x[w(f+ig)_{o-o} + w(f+ig)_{o-1}] \qquad (3.6.7)$$

for antisymmetric scattering.

Using these expressions, we can now investigate the frequency dependance of the scattering scattering tensors as the frequency of the incident radiation traverses a resonance frequency.

Inspection of the above expression shows that there are two extreme situations which can occur. The simplest case occurs when the 0-0 and 0-1 vibronic absorptions are not well resolved. The more complicated case occurs when these

two absorptions are well resolved, so that it is possible to be in exact resonance with either the 0-0, the 0-1, or to be in between the two. We deal with these separately below.

(a) No resolution of the 0-0 and 0-1 vibronic bands

For this case, the frequency dependance of the symmetric polarizability tensors are given by $(f+ig)_{je}$, where we have made the approximation that $(f+ig)_{0-0}$ and $(f+ig)_{0-1}$ are equal. The antisymmetric polarizability tensors vanish in this case, because the lineshape functions cancel out exactly.

(b) Complete resolution of the 0-0 and 0-1 vibronic bands

In this case, the frequency dependance of the symmetric polarizability tensors can be approximated by a single pair of lineshape functions $(f+ig)_{je}$. This is because the 0-0 and 0-1 lineshapes reinforce each other. Hence we would expect no dramatic change in the magnitude of the symmetric polarizability tensors as we go through resonance.

However, the situation with the antisymmetric polarizability tensors is entirely different. For this case, the appropriate frequency dependance is $[(f+ig)_{0-0}-(f+ig)_{0-1}]$. As we go through exact resonance with either the 0-0 or the 0-1 band, the situation described in (a) above obtains, i.e. there is no rapid change in the magnitude of the polarizability tensors. The most interesting effects occur as the incident frequency passes between the 0-0 and the 0-1 bands. From the above we would expect very rapid variation of magnitudes as we sweep from near to resonance with one of the pair, giving high magnitudes, through the mid-point where the magnitudes are low because they cancel out, and back to near resonance with

the other, giving high values again.

Similar comments apply to the perturbed polarizability tensors. The remarks above for symmetric polarizability tensors apply to the perturbed polarizability tensors for A modes. Also, the remarks above for antisymmetric polarizability tensors apply to the perturbed polarizability tensors for non-degenerate modes other than A modes.

Using these expressions, we now investigate the frequency dependance of the scattering observables.

3.6.4 The frequency dependance of the depolarization ratio and the M.C.I.D. at resonance

(a) Frequency dependance of the scattered intensity.

From the expressions obtained for the frequency dependance of the polarizability tensors, we see that the frequency dependance of the scattered intensity at resonance depends on the type of scattering involved. For isotropic and anisotropic scattering, the scattered intensity has a frequency factor

$$w^2[\ (f+ig)_{0-0} + (f+ig)_{0-1}\ ]^2 \qquad (3.6.8)$$

We deduce from this that the scattered intensity should peak when we are in exact resonance with either the 0-0 or the 0-1 bands, falling to a minimum when we are between the two bands. However, as already pointed out, this minimum is in general non-zero. In fact, depending on the separation of the bands, it could be quite large, due to the reinforcement of the two contributions. Thus we would not expect very large variations as we sweep through resonance.

As a consequence of the observations already made about the magnitude of the polarizability tensor for antisymmetric scattering, large variations are expected in this case as we sweep through resonance. For this case,the frequency dependance is given by

$$w^2[\ (f+ig)_{0-0} - (f+ig)_{0-1}\ ]^2 \qquad (3.6.9)$$

Thus we calculate that the scattered intensity should peak when in exact resonance with either the 0-0 or the 0-1 bands, falling to zero as we sweep between the bands. This dramatic change for the case of antisymmetric scattering is in fact observed experimentally.

(b) Frequency dependance of the depolarization ratio.

From the expressions which we have obtained for the polarizability tensor, it is clear that for any non-degenerate normal mode, the scattering is either symmetric or antisymmetric, but never a mixture of the two. Therefore from expression (2.5.18) for the depolarization ratio, we see that both the numerator and denominator have the same frequency dependance, which cancel each other out. Hence the depolarization ratio should remain constant as we sweep through resonance, even though there may be dramatic changes in the scattered intensities. However, this applies only when there is a single normal mode symmetry contributing to a particular band. In practice, several normal mode symmetries may be contributing to the same band, especially for large low-symmetry molecules. For example, both normal mode symmetries A_1 and A_2 may contribute to the same band. For this reason, we in general observe large variations in the depolarization ratio as we sweep through

the 0-0 and 0-1 resonances.

(c) Frequency dependance of the M.C.I.D. parameters for molecules with degenerate ground states.

For molecules with degenerate ground states, (I^R-I^L) is given by expressions (2.5.20-21). These involve the product of a polarizability component with the complex conjugate of another, i.e. exactly the same form as the scattered intensity. Hence they have exactly the same frequency dependance as the scattered intensity. Also, since both numerator and denominator have the same frequency dependance. the M.C.I.D. components have the same frequency dependance as the depolarization ratio. Theory therefore predicts that the M.C.I.D. components should remain constant as we go through resonance. In particular, there should be no change of sign as we sweep through the resonance frequency. (Although the magnitude of I^R-I^L should change.)

(d) Frequency dependance of the M.C.I.D. parameters for molecules with non-degenerate ground states.

For molecules with non-degenerate ground states, the M.C.I.D.s are generated by the second mechanism. Hence (I^R-I^L) involve sums of products of an unperturbed with a perturbed polarizability tensor. Because of this, the frequency dependance is different for the three different types of scattering. We therefore deal with these separately below. Before doing this, it is necessary to deal with some common features.

For all the systems which we are considering, the unperturbed polarizability tensor is real. However, the

perturbed polarizabiities are all imaginary, because of the term ⟨m⟩, which is imaginary. Hence from expressions (2.5.26-27) which stipulate the imaginary part, it is clear that to find the frequency factor for (I^R-I^L), it is necessary to take only the real part of the frequency terms in the aforementioned products.

(i) Isotropic scattering.

Since isotropic scattering occurs only for A_1 modes, we make use of the frequency factors obtained for totally symmetric scattering. Thus the intensities of the difference spectra have frequency dependance

$$w^2[\ (f+ig)_{o-o} + (f+ig)_{o-1}\ ]^2(f_{o-o}+f_{o-1}) \qquad (3.6.10)$$

From this we deduce that the magnitudes of the difference spectra peak when in exact resonance with either the 0-0 or the 0-1. Because of the f lineshape functions, the sign of the difference spectra should reverse as we go from one side of a resonance peak to another. However, provided we are on the same side of the absorption bands, the 0-0 and 0-1 resonances should give the same sign.

(ii) Pure anisotropic scattering.

Pure anisotropic scattering arises from the non-totally symmetric modes other than A_2 modes. Hence the difference spectra have frequency dependance

$$w^2[\ (f+ig)_{o-o} + (f+ig)_{o-1}\ ]^2(f_{o-o}-f_{o-1}) \qquad (3.6.11)$$

As in the previous case, this shows that the difference spectra should change sign as we go from one side of a resonance band to the other. However, in contrast to the case for A_1 modes, the signs for the 0-0 and 0-1 resonances

are opposite when we are on the same side of the resonance peak. This important result is a generalization of a result first found experimentally for ferrocytochrome c.[20]

(iii) Antisymmetric scattering.

Antisymmetric scattering originates in A_2 normal modes. Thus, the frequency dependance of the difference spectra is given by

$$w^2[\ (f+ig)_{o-o} - (f+ig)_{o-1}\ ]^2(f_{o-o}+f_{o-1}) \qquad (3.6.12)$$

From the form of this expression, it is clear that the behaviour of the difference spectra for the A_2 modes is the same as for the A_1 modes. We shall see that this again agrees with the experimental observations on cytochrome.

[Note: As was mentioned in Section 3.6.4, there are often several normal mode symmetries contributing to the same band. When this occurs, a combination of the three different types of behaviour will in general occur. Thus the situation is not so clear cut as described above. In this case, the frequency dependance of the sign of the M.C.I.D. is determined by the normal mode which makes the dominant contribution to the scattering.]

Chapter 3 : References

1) J.C.D. Brand, J.C. Speakman and J.K. Tyler, Molecular Structure : The Physical Approach, 2nd Edition, Edward Arnold, Glasgow, p.86

2) J.A. Koningstein, Introduction to the Theory of the Raman Effect, D. Reidel Publishing Company, Dordrecht, Holland, 1972. p.66-78

3) See ref. 2

4) [A],

5) L.D. Barron, Molec. Phys.,31,129(1976)

6) L.D. Barron, C. Meehan and J. Vrbancich, J. Raman Spectrosc. 12,251(1982)

7) [C],

8) L.D. Barron, C. Meehan and J. Vrbancich, J. Raman Spectrosc. 12,251(1982)

9) [A], p.196-202

10) [D], p.135

11) L.D. Barron, C. Meehan, C. Phys. Letts. 66,444(1979)

12) A. Abragam and B. Bleaney, Electron Paramagnetic Resonance of Transition Ions, Clarendon Press, Oxford, 1970.

13) A.S. Davydov, Quantum Mechanics, 2nd Edition, Pergamon Press, Oxford, p.405

14) [A], p.81

15) V. Weisskopf and E. Wigner, Z. Phys. 3,54 and 5,18(1930)

16) [A], p.81-82

17) [A], p.81-82

18) [A], p.83,84

19) P.W. Atkins, Molecular Quantum Mechanics, Vol.II,

Clarendon Press, Oxford, 1970. p.413-414

20) L.D. Barron, C. Meehan and J. Vrbancich, J. Raman Spectrosc. 12,251(1982)

CHAPTER 4

EXPERIMENTAL METHOD FOR OBSERVING RAMAN OPTICAL ACTIVITY

4.1 Introduction

In order to observe Raman optical activity, it is necessary to be able to modulate the polarization of an incident laser between right and left cicularity, and measure the spectra obtained for both the sum and the difference of these. The experimental arrangement necessary to do this is described in Section 4.2. In Section 4.3 a brief description of the procedure used for making some of the compounds tested is given.

4.2 Experimental apparatus and configuration

In this section, the experimental apparatus used throughout the project will be summarized. Almost all the experimental apparatus was in existence at the start of the project.

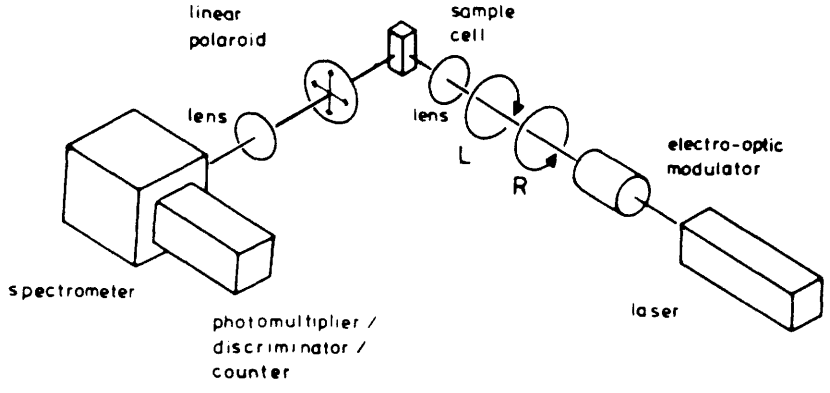

Fig. 4.1 Block diagram showing the experimental configuration for measuring M.R.O.A.

(i) The experimental apparatus is shown in block diagram form (see Fig.4.1). Below, a description of the various components is given.

(a) Laser + Dye Laser

The main laser used was an argon ion laser (Spectra Physics 171-03). The principal lines used for observing resonance Raman spectra were the green 514.5nm line and the blue 488.0nm line. The maximum power obtainable for either these lines was 4W. Various other lines were available, all at lower power. On all lines together, obtainable using a special mirror, the maximum output was 15W.

For certain experiments involving porphyrins, it was necessary to try and extend the excitation frequency range. In order to do this, the argon ion laser was used to optically pump a dye-laser (Spectra Physics 375). There were two main problems involved in using the dye-laser. The first of these was the difficulty of aligning the dye-laser. The second involved finding a dye which gave an adequate output power over the desired frequency range, and which had a sufficiently long lifetime in the beam for experimental observation. Of several dyes tried, the most useful was sodium fluorescein. In order to maximise the usable lifetime of the dye, as well as obtain maximum output from the dye, "additive A" from Spectra Physics was added to the dye-solution. From an input power of 5W all lines (the maximum the dye could withstand without rapid decomposition, a maximum of 1.2W was obtained from the dye-laser.

(b) Incident Beam Optics

In order to measure M.R.O.A. spectra, it is necessary to switch the incident laser radiation alternately and rapidly between right and left circular polarization . To do this, an electro-optic modulater (Electro-Optic Developments Model PC 105) was used, which cut the power of the beam reaching the sample by approximately half. To collimate the beam, an assortment of lenses were used.

(c) Sample Holder

In most cases, standard fluorescence cells are sufficient for holding the sample, even for resonance Raman spectra. However, in order to observe M.R.O.A., it is necesary to make measurements over a period of hours (up to 24 hours in some cases.) Because of this, special precautions had to be taken to prevent at worst local-overheating and burn-up of the sample, or merely decay of the scattered beam intensity. Several remedies to alleviate this problem were attempted. First of all, the samples were contained in a specially ordered spinning cell, which rotated rapidly. Although this minimised the risk of local overheating, the scattered intensity still decayed unacceptably with time, due to the unavoidable rise in temperature of the sample. The most successful method was the use of a peristaltic pump to pass the solution through a specially adapted fluorescence cell. This allowed the solution to be cooled by circulating it through an ice cooled reservoir.

(d) Collection Optics and Spectrometer

In all experiments, only light scattered at 90° was

collected. To obtain the polarized and depolarized spectra, a conventional polarizer was used. The signal thus obtained was analysed using a triple monochromator (Coderg Model T800). The normal slit width used was $15cm^{-1}$. A typical scan speed used for measuring M.R.O.A. spectra was $1cm^{-1}min^{-1}$. The scan speed was determined by the necessity of obtaining sufficient counts so that a statistically signifigant difference was observed. In practice, the scan speed was chosen so that M.CI.D. magnitudes of approximately 10^{-3} could be measured, entailing a total count of over 10^{7}(since the standard deviation of the count goes as the square root).

To produce the sum and difference spectra, a dual photon counting system was used (SSR 1110). This consisted of a pair of matched counters A and B, with the A counter devoted to the spectra arising from right circularly polarized excitation and the B counter devoted to the corresponding left measurement. The switching between the A and B counters was synchronised with the switching of the electro-optic modulator mentioned above.

(e) Recording Equipment

The sum and difference spectra were recorded on hardcopy using an Oxford Insruments X-Y recorder.

(f) Magnetic Field

To obtain a sufficiently large M.R.O.A. output for reliable measurement, it was necessary to have as large a magnetic field as possible, applied parallel to the incident

laser radiation. To achieve this, a permanent magnet with holes bored through the poles was used. This produced a field of 0.7T over a pole gap of 1cm.

(ii) Preparation of samples

(a) Degenerate ground state experiments.

The samples used during the project were either bought commercially and solutions made, or else were made using standard procedures.

For the cytochrome experiments, horse heart ferrocytochrome c was bought from Sigma (Type III). This was made up as a 1 x 10^{-4}M aqueous solution, with excess sodium dithionite used to preserve the sample from decomposition at high excitation intensities.

Various free porphyrins were tested in the hope of finding other examples of M.R.O.A. generated by excited electronic state degeneracy. These were prepared using standard methods.

(b) Raman E.P.R. experiments.

Iridium hexachloride was bought from Alfa and used without any further purification. The other complexes used were $[FeBr_4]^-$ and $[CuBr_4]^{2-}$. These were prepared as tetraethyl ammonium salts using standard methods.[1]

(iii) Problems associated with measuring M.R.O.A.

Some of the problems encountered in measuring M.R.O.A. have been given in (a) above, i.e. overheating of sample and varying scattered intensity. Another problem which arises is

that the magnitudes of the right and left circularly polarized beams become slightly different as they pass through the sample, due to magnetic circular dichroism effects. Thus one would expect a slight bias in the M.R.O.A. spectra. Although this has not so far appeared, this is expected to be a problem for Raman E.P.R. experiments, because the compounds which one would expect to exhibit the effect also usually have fairly large M.C.D.s. One way round this problem, if very accurate M.C.I.D. measurements were required, would be to use a tunable laser. With this, one could tune through the M.C.D. node.

Another problem occurs because of incomplete separation of the diagonal and off-diagonal contributions, which reduces greatly the intensities in the difference spectra. The only way around this problem in the future is the use of much larger magnetic fields, possibly obtainable from superconducting magnets.

One problem which occurs in natural R.O.A. experiments is the appearance of artifacts in the difference spectra, particularly for polarized scattering. (A recent paper by Barron and Vrbancich outlines some of the mechanisms which generate these artifacts.[2]) For reasons which are not yet fully understood, artifacts are minimised when one is dealing with resonance Raman scattering. Thus since we were concerned solely with resonance experiments, theproblem of artifacts did not occur. Thus it was possible to measure both polarized and depolarized difference spectra.

1) N.S. Gill and R.S. Nyholm, J.Chem. Soc. 3997(1959)

2) L.D. Barron and J. Vrbancich, J. Raman Spectrosc. 15,41(1984)

CHAPTER 5

RAMAN OPTICAL ACTIVITY IN FERROCYTOCHROME C

5.1 Introduction

Magnetic Raman optical activity was first observed in the resonance Raman spectrum of ferrocytochrome c.[1] Although M.R.O.A. has since been observed in other compounds, this remains the only compound which has it's optical activity generated via the second mechanism (see subsection 3.5.3).

In the paper reporting it's observation, only a single excitation frequency was used. Since then, further experimental studies have been performed. These involved the measurement of M.C.I.D.'s at a range of excitation frequencies, first of all using a second argon ion laser line, and then using an optically pumped sodium fluorescene dye laser. (These experimental results have been published by Barron, Meehan and Vrbancich.[2] It should be noted that the M.R.O.A. spectra obtained using the tunable dye-laser were obtained by Vrbancich after the experimental work for the present thesis had finished. During the project, insufficient dye laser power meant that no M.R.O.A. features were observable.) The spectra reported in this paper are shown in Figs. 5.3-7.

In this chapter,the theory developed for simply reducible groups will be used to account for the Raman spectra of ferrocytochrome c. Section 5.2 deals with the electronic structure of ferrocytochrome c. This is followed by a discussion of some important symmetry considerations,

after which the molecular tensors are calculated.

First of all, the polarizability tensor patterns for the various normal modes will be calculated, and these will be used to calculate depolarization ratios. Following this, the tensor pattern for the magnetically perturbed polarizability tensor will be calculated. Using this, the M.C.I.D. parameters will be calculated. The final section in the chapter will involve a comparison between the calculated and experimental results.

In the resonance Raman studies of ferrocytochrome c, the electronic absorption bands with which we are in resonance originate from the basic chromophore of the molecule, the porphyrin ring. The porphyrin ring is a planar conjugated ring system (see Fig. 5.1) whose symmetry depends on it's environment. To a first approximation, the symmetry of a metal porphyrin is D_{4h}. (Free porphyrins have an approximate symmetry of D_{2h}.)

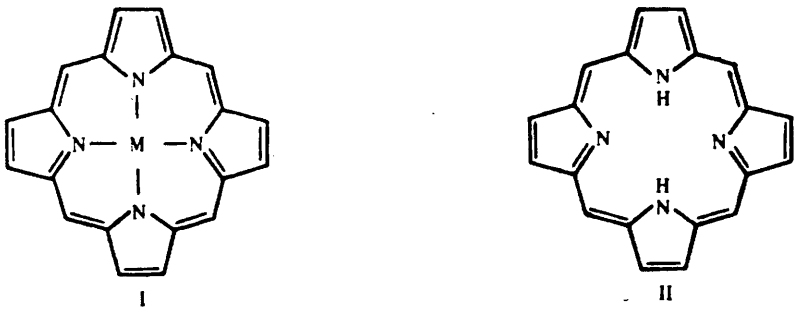

Metal porphyrin Free porphyrin

Fig. 5.1 Simplified diagram of the porphyrin ring.

Molecular orbital calculations have been performed for metal porphyrins, and these have been reviewed by Gouterman. From this reference, we obtain the following information.[3]

In metal porphyrins there are 26 π electrons occupying the 13 lowest lying molecular orbitals. The two highest occupied orbitals have symmetries a_{2u} and a_{1u} respectively, yielding a ground state of symmetry $A_{1g}(a_{1u}^2 a_{2u}^2)$. The first two excited states both have E_u symmetry, arising respectively from the $a_{1u}^2 a_{2u}^1 e_g^1$ and $a_{1u}^1 a_{2u}^2 e_g^1$ configurations. These two states then undergo configuration interaction,

which separates them. The resulting first two excited states are denoted E_{ua} and E_{ub}. (See Fig. 5.2 (a).)

The observed visible absorption of metal porphyrins shows three distinct bands. The most intense of these bands, at 400nm, is assigned to the transition $E_{ub}(a_{1u}a_{2u}e_g) \longleftarrow A_{1g}(a_{1u}a_{2u}e_g)$. This is called the Soret band, and is found in all metal porphyrin spectra. (See Fig. 5.2(b).) The other two bands are found at 540nm and 570nm, and are designated the Q_1 and Q_0 bands respectively. Both of these bands are attributed to the electronic transition $E_{ua}(a_{1u}^{1}a_{2u}^{2}e_g^{1}) \longleftarrow A_{1g}(a_{1u}^{2}a_{2u}^{2}e_g^{0})$. The Q_0 band corresponds to the 0-0 transition, i.e. the transition from the ground vibrational level of the ground electronic state to the ground vibrational level of the excited electronic state. The Q_1 envelope corresponds to the 0-1 transitions, i.e. the transitions to the singly excited vibrational levels of the excited electronic state.

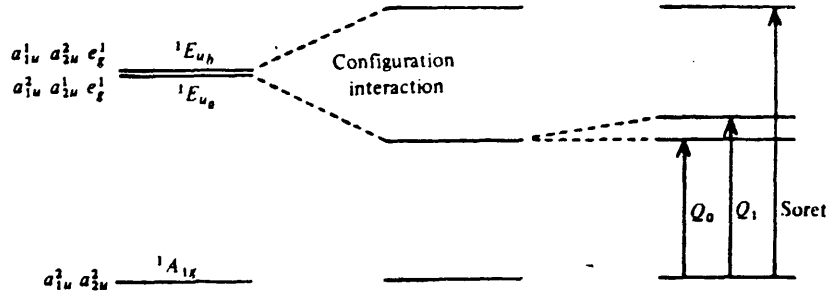

Fig. 5.2 The excited states of the porphyrin ring.

5.3 Symmetry Considerations for Ferrocytochrome c

To calculate the relevant molecular tensors for ferrocytochrome c, we need to use expressions (3.6.4-7). To apply these, we first of all need to consider the molecular point group to which they belong. As was noted in section 5.2, to a first approximation, the appropriate point group is D_{4h}. To evaluate the polarizability tensor pattern, we need to know the V coeeficients for this point group. However, D_{4h} is a direct product group, one of which is the group D_4. Hence we need only use the V coefficients for the group D_4.[4]

In the point group D_{4h}, the following applies[5]

Table 5.1 : showing the representations spanned by the dipole moment components.

Operator	Irreducible Representation
u_x)	E
u_y)	E
u_z	A_2
m_z	A_2

The above symmetry information, along with the V coefficients[6] for D_4 , allow us to calculate the unperturbed polarizability tensors.

Complex components in a magnetic field.

To calculate the perturbed polarizability tensors, it is necessary to calculate expectation values of the magnetic moment operator. For this, it is necessary to use complex

components. In our scattering system, we take the applied magnetic field to be along the z-axis. It is appropriate therefore to use the following complex components[7] for the operators given above :-

$$u_x = i2^{-1/2}(u^E - u^E) \qquad (5.3.1a)$$

$$u_Y = 2^{-1/2}(u^E + u^E) \qquad (5.3.1b)$$

$$u_z = u^{A_2} \qquad (5.3.1c)$$

$$m_z = m^{A_2} \qquad (5.3.2)$$

Using the above components, the appropriate form of the Wigner-Eckart theorem is expression (2.6.11). The appropriate V coefficient are the complex coefficients given in ref. 6.

Having considered the symmetry aspects of the problem, we now proceed to calculate the molecular tensors.

5.4 The Patterns for the Polarizability Tensors in Ferrocytochrome c

(a) Polarizability tensor patterns.

In order to calculate the tensor patterns for the normal modes, we apply the resonance expressions (3.6.4-5). Using these, the following tensor patterns are obtained for the non-degenerate normal modes of ferrocytochrome c.

$$(\tilde{a}_{\alpha\beta})_{A_1} = C_J(A_1)\begin{bmatrix}1&0&0\\0&1&0\\0&0&0\end{bmatrix} \quad (\tilde{a}_{\alpha\beta})_{A_2} = C_J(A_2)\begin{bmatrix}0&-1&0\\1&0&0\\0&0&0\end{bmatrix}$$

$$(\tilde{a}_{\alpha\beta})_{B_1} = C_J(B_1)\begin{bmatrix}1&0&0\\0&-1&0\\0&0&0\end{bmatrix} \quad (\tilde{a}_{\alpha\beta})_{B_2} = C_J(B_2)\begin{bmatrix}0&1&0\\1&0&0\\0&0&0\end{bmatrix} \qquad (5.4.1)$$

where

$$C_J(Q) = 2(w/h)a(j)[(f+ig)_{0-0}+(-1)^{J_V}(f+ig)_{0-0}] \qquad (5.4.2)$$

Before we use these tensor patterns to calculate the depolarization ratios for the non-degenerate normal modes, we make some observations about them. First of all, we see that only for the A_1 normal mode is there any isotropic contribution to the scattering. Secondly, as previously noted, only the A_2 modes support antisymmetric scattering. Also, it is only for A_2 modes that the absolute sign of the tensor pattern reverses as we go from exact resonance with the 0-0 band to exact resonance with the 0-1 band, via the term $(-1)^{J_V}$ in (5.4.2). The last point we note is that for B_1 and B_2, the scattering is completely anisotropic.

(b) Perturbed polarizability tensor patterns.

To calculate the tensor patterns, we use the resonance expressions (3.6.6-7). We obtain the following tensor patterns.

$$(a_{\alpha\beta z})_{A_1} = D_j(A_1)\begin{bmatrix} 0 & 1 & 0 \\ -1 & 0 & 0 \\ 0 & 0 & 0 \end{bmatrix} \quad (a_{\alpha\beta z})_{A_2} = D_j(A_2)\begin{bmatrix} 1 & 0 & 0 \\ 0 & 1 & 0 \\ 0 & 0 & 0 \end{bmatrix}$$

$$(a_{\alpha\beta z})_{B_1} = D_j(B_1)\begin{bmatrix} 0 & 1 & 0 \\ 1 & 0 & 0 \\ 0 & 0 & 0 \end{bmatrix} \quad (a_{\alpha\beta z})_{B_2} = D_j(B_2)\begin{bmatrix} -1 & 0 & 0 \\ 0 & 1 & 0 \\ 0 & 0 & 0 \end{bmatrix}$$

(5.4.3)

where

$$D_j(Q) = 8^{1/2}(w/h)^2\langle m\rangle a(j)[(f+ig)_{0-0}+(-1)^u(f+ig)_{0-0}] \quad (5.4.4)$$

Above, $(-1)^u$ is +1 for A_1 and A_2 modes, and -1 otherwise.

It is interesting to note that the perturbed tensor is antisymmetric whenever the unperturbed tensor is symmetric and vice-versa. This is due to the presence of $Q \times A_2$ in (3.6.6-7). We also note that, as we saw earlier, it is only for modes other than A_1 and A_2 that the absolute sign of the perturbed tensor pattern changes when we go from exact resonance with the 0-0 band to exact resonance with the 0-1 band.

We now go on to calculate the depolarization ratio and the M.C.I.D. components, using the above results.

5.5 Calculation of the Depolarization Ratio and M.C.I.D. Components for Ferrocytochrome c

(a) Calculation of the depolarization ratio.

To calculate the depolarization ratio, we use equation (2.5.18)), which covers both symmetric, antisymmetric and mixed scattering. The results obtained are given in the table below

Table 5.2 : the depolarization ratios for the non-degenerate modes of cytochrome c

NORMAL MODE	A_1	A_2	B_1	B_2
$\rho(x)$	0.125	00	0.75	0.75

These values predict that the A_1 bands should be polarized, the A_2 band should show inverse polarization, and the B_1 and B_2 modes should be unpolarized. This is in reasonable agreement with the experimental observations. It is not easy to obtain a direct experimental comparison with these calculated results. This is because several normal modes are thought to contribute to the intensity of almost all of the observable bands. For this reason also, the depolarization ratio varies with frequency instead of remaining constant, as was predicted earlier.

(b) Calculation of the M.C.I.D. components.

To calculate the M.C.I.D. components, the appropriate equations are (2.5.26-29)). However, we notice that the form

of the tensor patterns fulfil the assumptions made in Section 3.5. Hence we can use expressions (3.5.4-7) for the sum and difference spectra derived in that section.

In calculating the results which are presented below, it is necessary to evaluate the real part of the ratio D(Q)/C(Q). From (5.4.4) of the previous section, and the fact that ⟨m⟩ is pure imaginary, we see that this ratio has the following value:

$$D(Q)/C(Q) = (-1)^u(-i8^{1/2}wf/h)\langle m\rangle \qquad (5.5.2)$$

where $(-1)^u$ is -1 if we are dealing with B modes and are in resonance with the 0-1 transition, and is +1 otherwise.

Including the magnetic field strength Bz, this gives us the factor $8^{1/2}(-iwf/h)\langle m\rangle Bz$. This is the ratio of the magnitudes of the contributions of the perturbed and unperturbed polarizability tensors to the overall polarizability when we are in resonance. It will be seen in Chapter 8 that this factor occurs in all calculated M.C.I.D.'s originating from excited state degeneracy. It is a dimensionless quantity which contains the essential frequency dependence of the M.C.I.D. components (see Section 3.5). In what follows we denote it by a_B. Thus

$$a_B = 8^{1/2}(-iwf/h)\langle m\rangle Bz \qquad (5.5.2)$$

As an illustrative example, we present the calculation of Δ_z for the totally symmetric mode.

$$\begin{aligned} I_z^R - I_z^L &= (K/15)Bz[\tilde{a}_{xy}\tilde{a}_{xxz} + \tilde{a}_{yy}\tilde{a}_{yxz} - \tilde{a}_{xx}\tilde{a}_{xyz} - \tilde{a}_{yx}\tilde{a}_{yyz}] \\ &= (K/15)BzC(A_1)D(A_1)[\ 0 + (-1x1) - 0 - (1x1)\ ] \\ &= -(2/15)KBzC(A_1)D(A_1) \qquad (5.5.3) \\ I_z^R + I_z^L &= (K/15)\ x \\ &\quad [\,|\tilde{a}_{xx}| + |\tilde{a}_{yy}| + 2|\tilde{a}_{xy}| + 2|\tilde{a}_{yx}| - Re(\tilde{a}_{xx}\tilde{a}_{yy} - \tilde{a}_{xy}\tilde{a}_{yx})\,] \\ &= (K/15)\ C(A_1)^2[\ 1 + 1 + 0 + 0 - Re(1-0)\ ] \end{aligned}$$

$$= (K/15)|C(A_1)|^2 \qquad (5.5.4)$$

Thus

$$\Delta_z = -(2/15)B_z C(A_1)D(A_1)/(K/15)|C(A_1)|^2$$

$$= -2a_B \qquad (5.5.5)$$

All the calculated values for the four non-degenerate normal mode symmetries are given in Table 5.3 below.

Table 5.3 : M.C.I.D. values for exact resonance with the 0-0 band.

Symmetry	Δ_x	Δ_z
A_1	$-8a_B/9$	$-2a_B$
A_2	$-8a_B/5$	$-2a_B/3$
B_1	$-8a_B/7$	$-2a_B/3$
B_2	$-8a_B/7$	$-2a_B/5$

As we have already mentioned, the sign of the M.C.I.D. components for the B modes change when we go to exact resonance with the 0-1 mode.

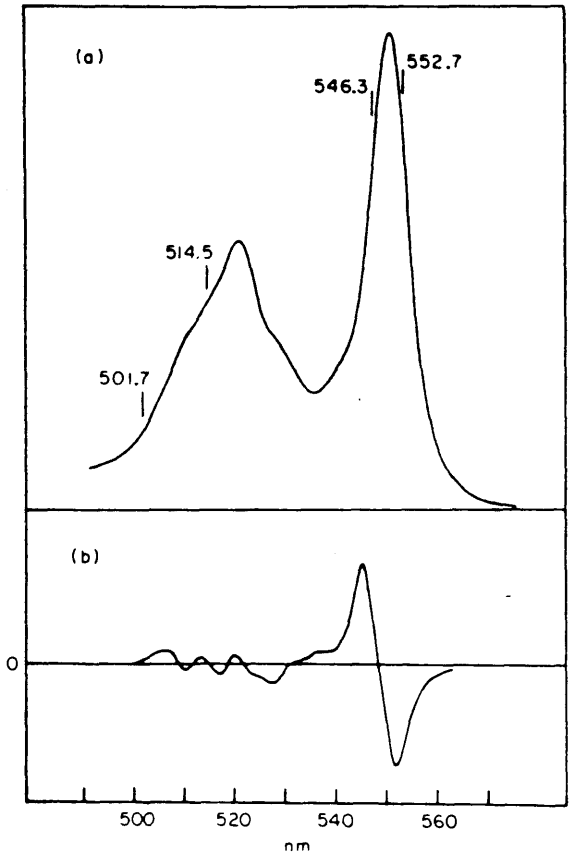

(a) The electronic absorption bands and (b) the associated magnetic circular dichroism of ferrocytochrome *c*. The intensity scale is arbitrary. The exciting wavelengths used in the resonance-Raman studies are marked above the absorption band.

Fig. 5.3 Electronic absorbtion and magnetic circular dichroism spectra of cytochrome c, including the positions of the incident laser frequencies used.

(This figure is extracted from the 3rd paper at the end of this thesis.)

5.6 Comparison between Theory and Experiment.

From the experimental results, we see that the intensities for the polarized difference spectra are exactly double those for the depolarized spectra. This agrees with the general result obtained in Section 3.5.3.

From Table 5.1, it seems that when we are in resonance with the 0-0 band, all the M.C.I.D.'s, both polarized and depolarized, are negative. However, we have so far not taken account of the fact that the lineshape function f is included in the factor a_B. As we saw earlier, this is positive if the radiation frequency is below the resonance frequency, and negative if it is above the resonance frequency. Thus in order to compare theory with experiment, it is necessary to know how the laser excitation frequencies are situated with respect to the electronic absorption bands. These are shown in Fig.5.3.

For an incident frequency of 546.3nm, the incident radiation is in resonance with the 0-0 electronic transition. Moreover, this frequency corresponds to a region of high absorption. We would therefore expect strong resonance enhancement of all the bands. Since the incident frequency is greater than the 0-0 resonance frequency, all bands should have the same sign (negative) in the difference spectra. This is in fact observed.

For incident frequency 552.7nm, almost all the comments made above for the 546.3nm line apply. In this case however, we would expect all the bands to have the same sign (positive) for the M.C.I.D., opposite to that for 546.3nm. This is because we are on the other side of the absorption

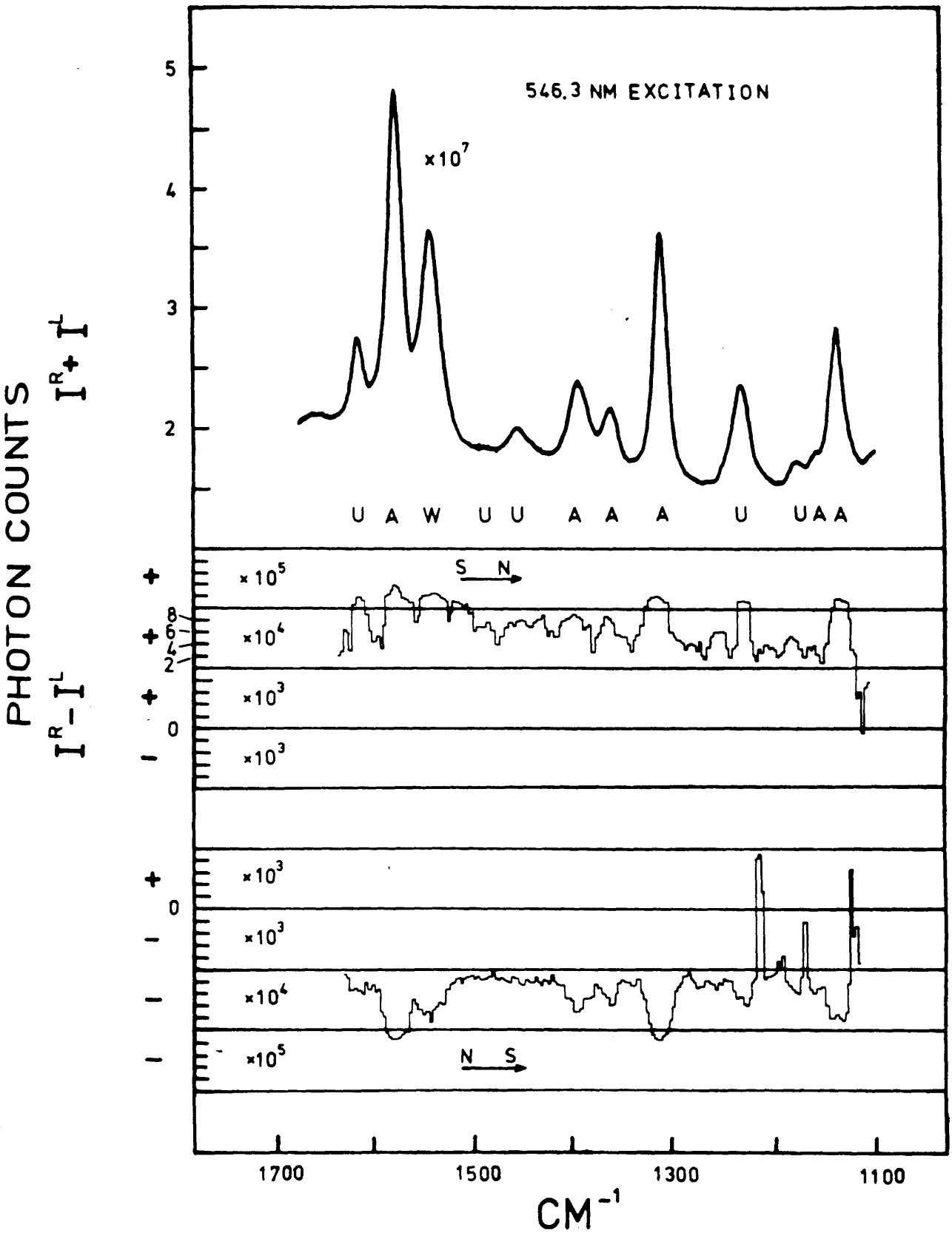

Fig. 5.4 Raman and M.R.O.A. spectra obtained using an incident frequency of 546.3nm.

peak. This agrees with the experimental observations.

Both the 501.7nm and the 514.5nm lines lie within the 0-1 absorption envelope. Thus, from Table 5.1 we should expect that not all the bands should give the same sign.

For the 501.7nm line, we are in a region of low absorption. It therefore might be expected that the only bands for which strong resonance enhancement would occur would be those bands for which the line is near exact resonance. (In the previous cases, the excitation lines lay in a region of very high absorption. Thus significant enhancement of all bands was observed for those cases.) As we see from the spectra obtained, only a few bands whose resonance frequencies are very close to the incident frequency show significant resonance enhancement. In the difference spectra obtained at this frequency, only three signifigant M.C.I.D. peaks are observed. The most intense of these corresponds to an A_2 normal vibrational mode. From the expressions obtained earlier, since the excitation frequency is above the exact vibronic resonance frequency, we would expect this peak to have the same sign as that observed using 546.3 nm excitation (since for A_2 modes there is no change in the M.C.I.D. sign, and the excitation frequency is above resonance in both cases.) This is observed experimentally. For the other two bands which are signifigantly enhanced, Fig.5.4 shows us the main contribution comes from B modes. From the general result obtained in Chapter 3, we would therefore expect these to opposite in sign to the A_2 band. This is also observed.

The situation is slightly more complicated for the 514.5 line. This frequency lies in a region of high absorption.

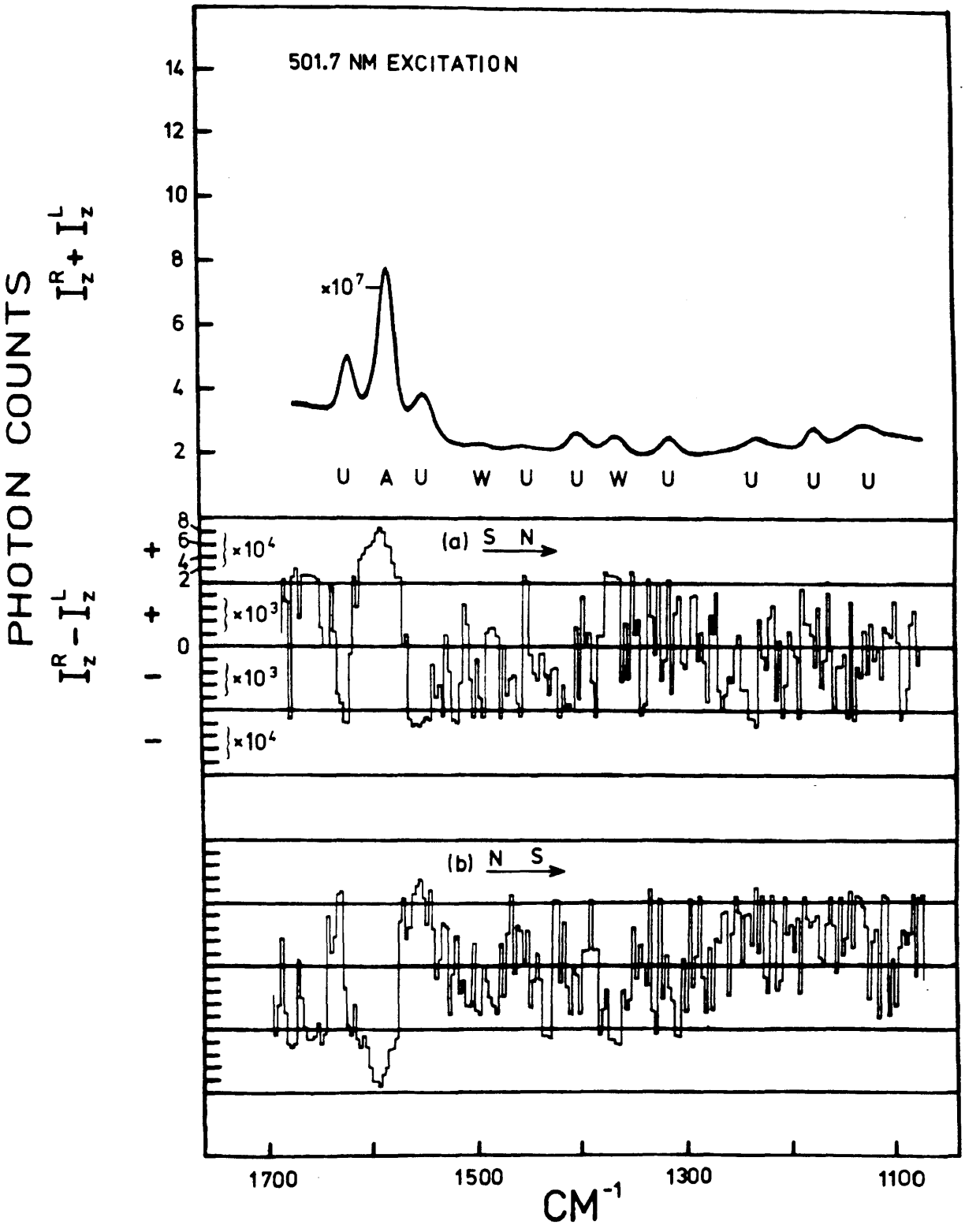

Fig. 5.6 Raman and M.R.O.A. spectra obtained using an incident frequency of 501.7nm.

Thus we might expect more bands to show resonance enhancement than for the 501.7nm line. This is borne out by the much larger number of bands which are resonance enhanced, which in turn gives many more M.C.I.D. peaks. Figure 5.3 shows exactly where the excitation frequency lies with respect to the Raman bands. From this we see that the excitation frequency is greater than the vibronic resonance frequency for all the bands except the two Raman bands which lie below 1200cm^{-1}. From the previous discussion we would therefore predict that for all the bands whose vibronic resonance frequency is below the excitation frequency, and for which the dominant scattering contribution arises from A modes, the signs of the M.C.I.D. peaks should be the same as those occuring for excitation frequency 552.7nm, i.e. for a positive magnetic field (N$\longrightarrow$S), the peaks should be positive. Similarly the peaks for which the dominant contribution comes from B mode scattering, and for which the vibronic resonance frequency is below the excitation frequency, the M.C.I.D. peaks should be negative. (Because of the reversal in sign for B modes in resonance with O-1.) Both these predictions agree with the experimentally observed signs.

For the two bands whose vibronic frequency is greater than the excitation frequency, the opposite is expected. Thus for a positive magnetic field, we would expect A modes to give a negative M.C.I.D. peak, and B modes to give a positive M.C.I.D. peak. This is in fact the case for the two observed bands.

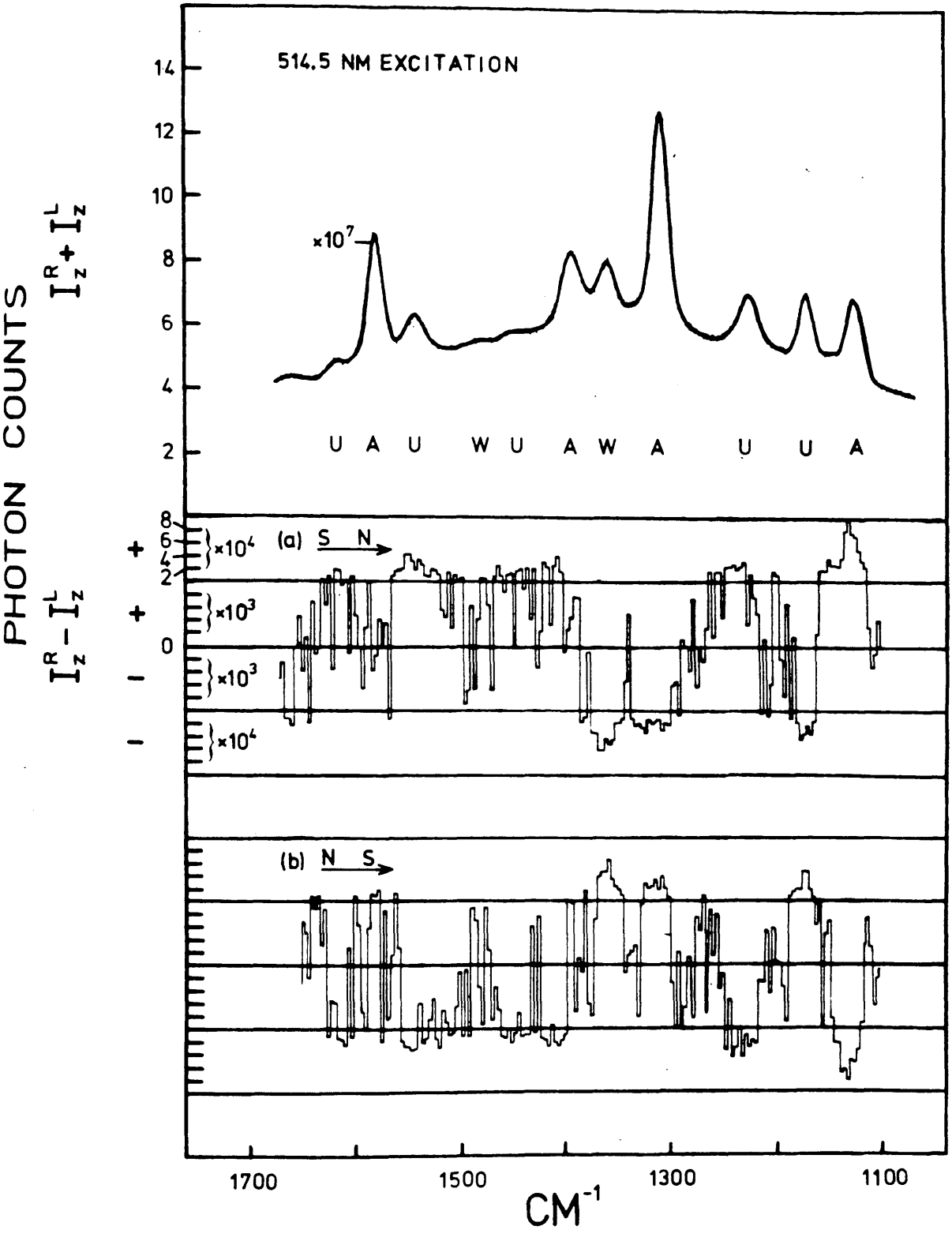

Fig. 5.7 Raman and M.R.O.A. spectra obtained using an incident frequency of 514.5nm.

5.7 Conclusion

In this chapter, we have seen that the theory presented in Chapter 3 accounts for all the main features of the M.R.O.A. spectra of ferrocytochrome c. This explanation is basically the same as that presented in ref. 2. The only difference lies in the more general calculational methods which are used in this treatment.

So far, ferrocytochrome is the only molecule for which M.R.O.A. originating in excited state electronic degeneracy has been observed. During the present project, various free porphyrins were tested, but none of them gave detectable M.R.O.A. signals. However, the explanation which has been given in this chapter is also applicable to any free porphyrins for which M.R.O.A. values are observed in the future.

Chapter 5 : References

1) L.D. Barron, Nature. 257,372(1975)

2) L.D. Barron, C. Meehan and J. Vrbancich, J. Raman Spectroscopy. 12,251(1982)

3) M. Gouterman, J. Molec. Spectrosc.6,138(19619

4) [C], p.26

5) P.W. Atkins, Molecular Quantum Mechanics, Vol.I,Clarendon Press, Oxford,1970, p.156-158

6) [C], p.120

7) [C], p.31

CHAPTER 6

RAMAN ELECRON PARAMAGNETIC RESONANCE

6.1 Introduction

In this chapter we look at the new phenomenon of Raman Electron Paramagnetic Resonance, or Raman E.P.R. for short. This was observed for the first time during the present project, in the Raman scattering of three transition metal complexes.[1] The experimental results for these cases are given in Section 6.2.

In the remainder of the chapter, the theory built up so far will be used to account for the resonance Raman spectra and the M.C.I.D.s of the iridium hexachloride ion. This will be done , as before, by calculating the polarizability tensor patterns for the various normal modes, and then using these to evaluate the depolarization ratio and the M.C.I.D. values. The calculation is split up into two parts. First of all, the totally symmetric normal mode will be considered. After this, the much more difficult case of the non-totally symmetric modes will be considered. After each calculation, a comparison will be made between theory and experiment.

6.2 Experimental Observation of Raman E.P.R.

6.2.1 Introduction

In Chapter 3, we saw that for a molecule with a degenerate ground state, a magnetic field orients the dipole moment of the molecule, so that the components of the degenerate state are split in energy, with one component being raised in energy by the magnetic field, and one component lowered. This splitting is usually studied experimentally in the branch of spectroscopy called Electron Paramagnetic Resonance, or E.P.R. for short. From such experiments, much information about the electronic structure of the molecule can be obtained.[2]

Now as we saw also saw in Chapter 3, the contributions to Raman scattering arising from the diagonal and off-diagonal scattering pathways are also split by an applied magnetic field. For magnetic fields of the order of 1 T, such splittings are too small to be detected in conventional Raman scattering experiments. This is because of the large overlap of the different contributions, all of which reinforce each other. However, when we look at $I^R - I^L$ for such molecules, we find that one of the three contributions becomes zero, and that the other two are of mutually opposite sign. Because of this cancellation, it is possible to observe a couplet in the M.R.O.A. spectra for such molecules. From the analysis given later in this chapter, it will become clear that in principle, similar information about the magnitude of the ground state magnetic moment to that usually obtained by E.P.R. experiments can be gained.

For this reason, this type of M.R.O.A. has been called Raman E.P.R.[3] In fact, it is possible to obtain more information about the ground state magnetic moment than in normal E.P.R. experiments. The latter allow only the magnitude of the ground state magnetic moment to be calculated. From Raman E.P.R., as we shall see later, the sign of the g-factor can also be measured. The first molecule for which Raman E.P.R. was observed was the $[IrCl_6]^{2-}$ molecule. Following this, the effect was observed in two other complexes, namely $[FeBr_4]^-$ and $[CuBr_4]^{2-}$. These results are presented in the next section.

One prerequisite for a molecule to give an M.R.O.A. peak is that there must be strong spin orbit coupling in the molecule.[4] This is necessary so that the intermediate electronic state of the molecule is in a JM coupled state. If this state is an $|LM_LSM_S\rangle$ state, then it is not possible for the initial and final spin states to be different. This is due to the fact that none of the operators involved in Raman scattering contain any terms involving spin. Only when the spin and orbital states are coupled can matrix elements connecting different initial and final spin states be non-zero. That such transitions are allowed is due to the fact that Raman E.P.R. is generated by a pure antisymmetric scattering tensor. The latter transforms in the same way as an axial vector and thus can give rise to $M = +1$ transitions.[5]

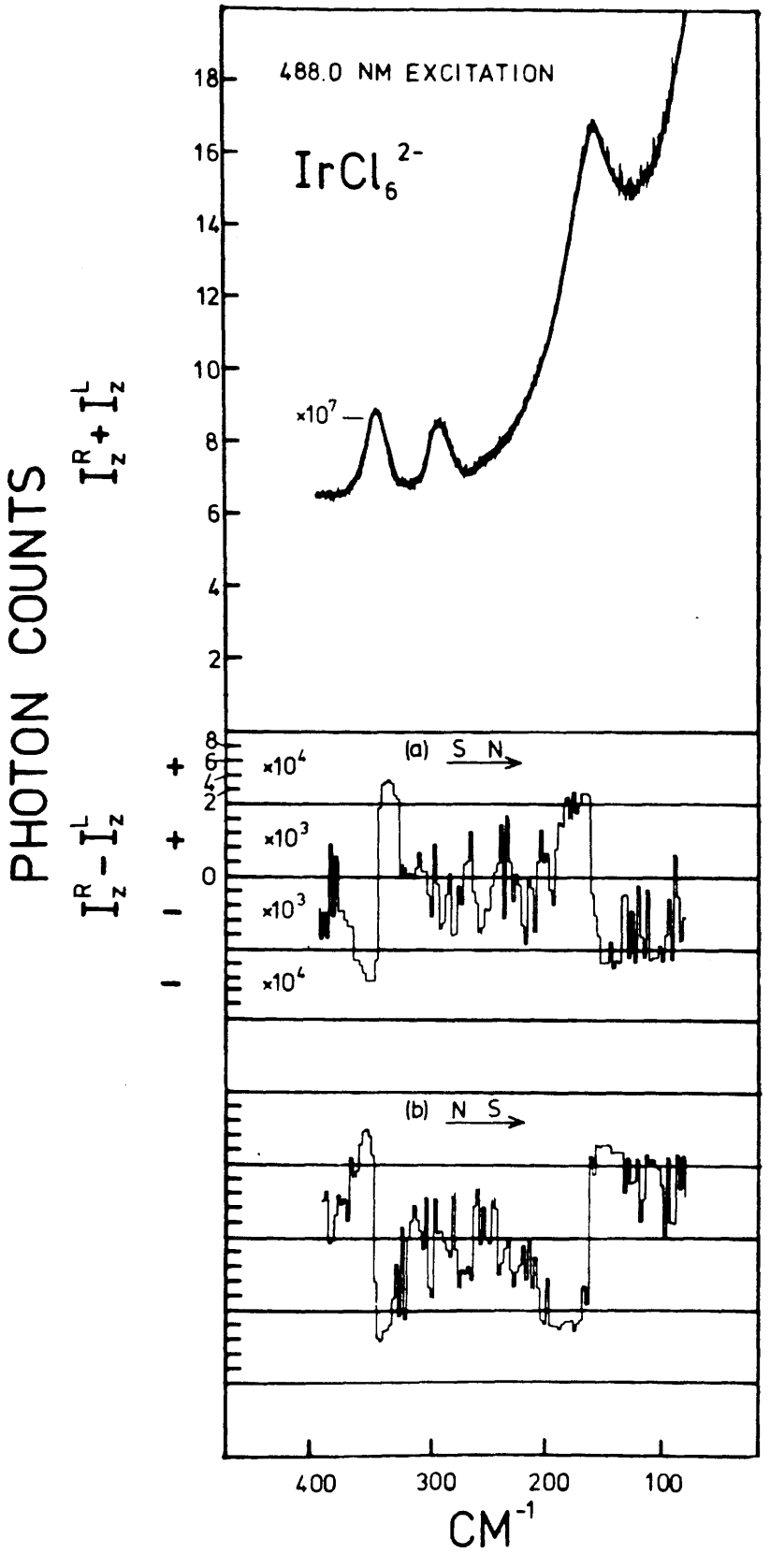

Fig. 6.1 Raman and M.R.O.A. spectra for iridium hexachloride.

6.2.2 Experimental results

i) The $[IrCl_6]^{2-}$ Ion.

The resonance Raman spectrum and the depolarized difference spectra for $[IrCl_6]^{2-}$ are shown in Fig. 6.1 (These spectra was obtained using the 488nm laser line.) Three bands are observed. These are assigned to the three Raman active fundamentals of the octahedral MX_6 structure. The details are given in Table 6.1

Table 6.1 : showing details of the M.R.O.A. spectra of iridium hexachloride.

Frequency cm^{-1}	Normal Mode Symmetry	Depolarized M.C.I.D.
341	A_1	+/-
290	E_g	-
161	T_{2g}	-/+

In the table above, +/- means that an M.C.I.D. couplet was obtained with the lower frequency wing of the couplet + (assuming a positive magnetic field.) As indicated above, there was insufficient scattering intensity to observe any M.R.O.A. for the E mode.(However, see Section 9.3.)

Spectra were also obtained for the 514.5 and the 496.5 laser lines. These are not displayed since they are identical in form. Now the electronic absorption band is centred at 500nm. Thus we see experimentally that the M.C.I.D.s do not change sign as we sweep through the resonance frequency.

No polarized difference spectra are presented, since none of these displayed any observable features.

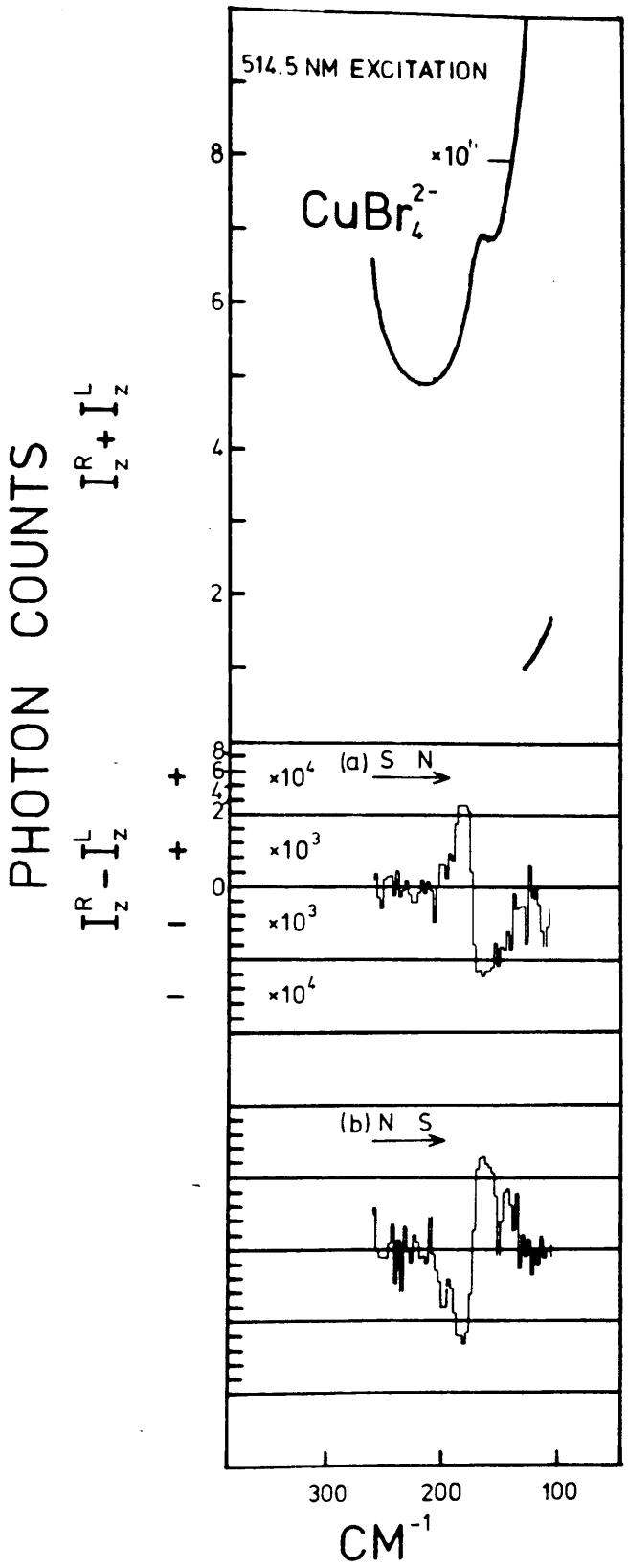

Fig. 6.2 Raman and M.R.O.A. spectra for copper(II) tetrabromide.

ii) The $[CuBr_4]^{2-}$ Ion

The resonance Raman and the depolarized difference spectra for $[CuBr_4]^{2-}$ are shown in Fig 6.2. The spectra were obtained using the 514.5nm laser line. The only observed band occurs at $174cm^{-1}$, and is weakly polarized (although there was not enough intensity to measure the depolarization ratio.) This showed a large -/+ M.C.I.D. couplet, leading to it's assignment as the symmetric stretch.

iii) The $[FeBr_4]^{1-}$ Ion.

Resonance Raman and depolarized difference spectra were obtained for the $[FeBr_4]^{1-}$ using the 488nm laser line. These are shown in Fig.6.3. The two bands observed occur at $201cm^{-1}$ and $290cm^{-1}$. These are assigned to the two Raman-active fundamentals A_1 and T_2 respectively. (The other two fundamentals appear not to be resonance enhanced at this frequency.)

A -/+ M.C.I.D. couplet is observed for the A_1 band, but nothing is observed for the T_2 band. The M.C.I.D. observed for the former has greater magnitude than that observed for the other M.C.I.D.'s mentioned above. This is attributed to the fact that $[FeBr_4]^{1-}$ has a larger g-factor, and hence a higher ground state magnetic moment, and thus there is less overlap between the two wings of the M.C.I.D. couplet.

Having presented the main experimental results, we now go on to calculate the form of the M.C.I.D. spectra. We perform detailed calculations for the iridium complex, and a general result is used for the A_1 modes of the other molecules.

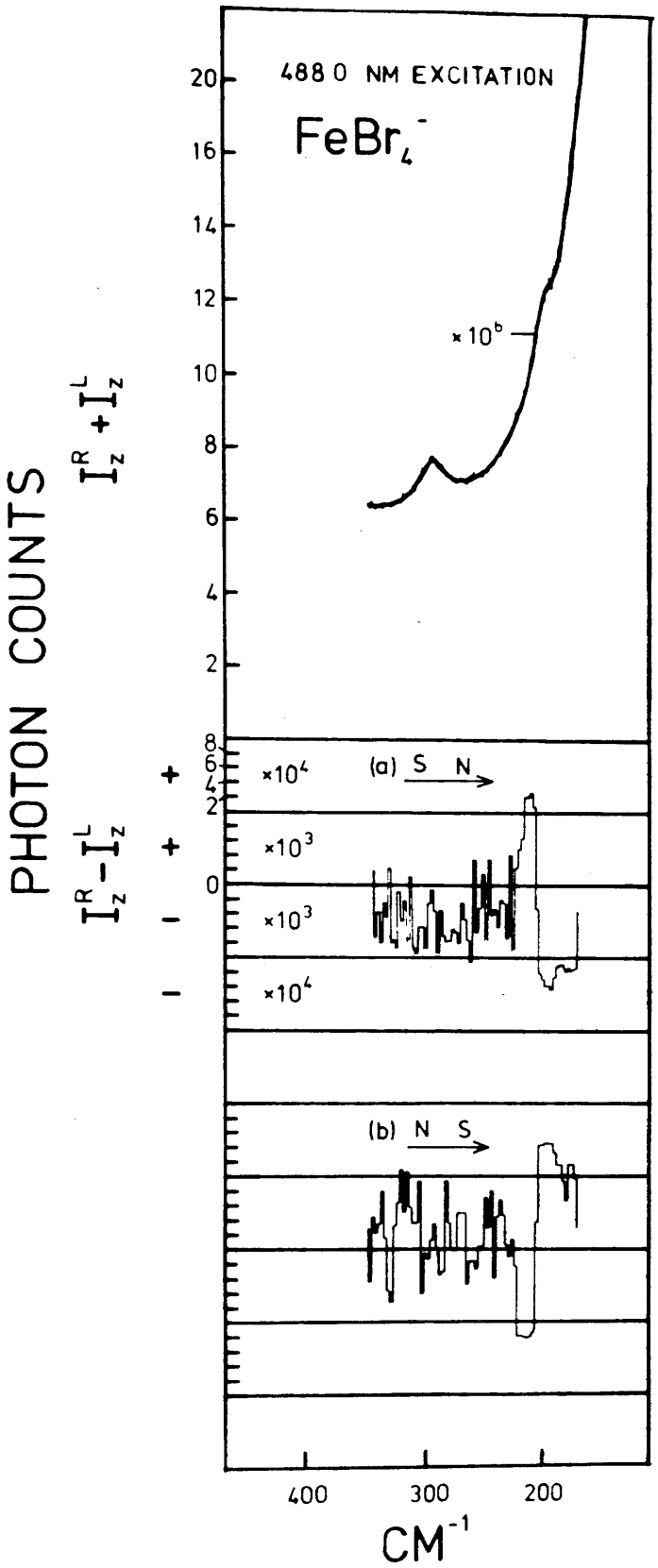

Fig. 6.3 Raman and M.R.O.A. spectra for iron(III) tetrabromide.

6.3 Electronic Sructure of $[IrCl_6]^{2-}$

In the iridium hexachloride ion, the electronic configuration of iridium is $(5d)^5$. Since it is a low spin system, the ground electronic configuration[6] in the absence of spin-orbit coupling is $(t_{2g})^5, {}^2T_{2g}$. However, as iridium is a third row transition metal, it exhibits strong spin-orbit coupling. This coupling of the spin and orbital states splits the ${}^2T_{2g}$ ground state into E_g'' and U_u' states, the former being lower in energy, as seen from M.C.D. results.[7] Thus the ground electronic state of the complex ion is a Kramers doublet. The determination of the symmetry of the excited states corresponding to the visible electronic absorption bands is less straightforward. From the intensity of the electronic absorption bands at 20200 and 22700cm^{-1} it follows that they must arise from transitions to charge transfer states. These charge transfer states are $\pi\pi$ molecular orbitals, having electronic configurations $(t_{1u}(\pi)\ t_{2g})T_{1u}$ and $(t_{2u}(\pi)\ t_{2g})T_{2u}$.[8] Taking account of spin-orbit coupling, we therefore obtain the excited state symmetries shown in Fig. 6.4. Also given in Fig. 6.4 are the expressions for the components of the excited states in terms of their spin and orbital contributions. These expressions are obtained using equation (2.6.14), with the constituents of the spin-orbit state being the E' spin state representation and the appropriate orbital state representation. These differ from the combinations given by Brown et al.[9]

There still remains the question of the relative energies of the excited states given in Fig 6.4.

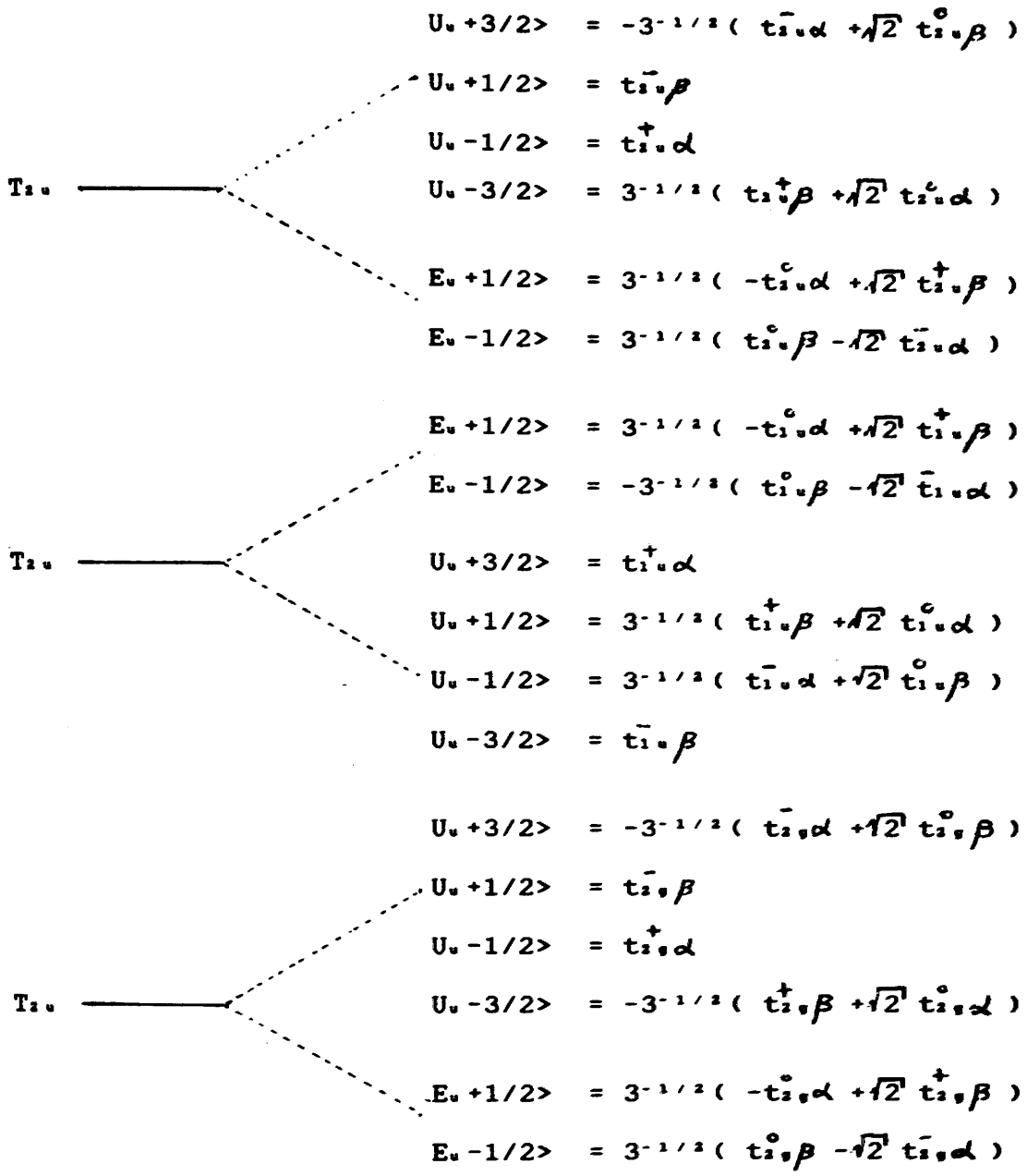

Fig. 6.4 The ground and excited electronic states of iridium hexachloride, plus the spin-orbit expressions for these states.

This problem has been studied by both Schatz[10] et al and Jorgensen[11] et al. The first group calculated the signs and magnitudes of the MCD bands arising from the various excited states, and by comparing these with the observed M.C.D. spectrum, they were able to assign the 20200 absorption band to the $E_u \longleftarrow E_g$ transition, and the 22700 band to the $U_u \longleftarrow E_g$ transition . This leads to the ordering of the states given in the first figure. These assignments were called into question by the experimental confirmation, reported in ref. 12, of the theoretical prediction that the $[IrCl_6]^{2-}$ ion has a negative g-value. In this same reference, it was suggested that these assignments should be reversed.[12] In fact, as pointed out by Schatz[13], the sign of the M.C.D. couplets is independent of the sign of the g-value, depending only on it's magnitude.

The second group (Jorgensen et al) based their assignments only on absorption spectra results, which do not give as much information as M.C.D. results. From these they deduced assignments which were opposite to those in ref. 10.

From a comparison of the experimental and the theoretical values of the depolarization ratios of the bands in the resonance Raman spectrum, it will be seen that only Schatz's assignments give consistent answers. These values will be calculated later in this chapter, and were first reported by Brown et al.[14]

6.4 Calculation of the Polarizability Tensor Components for the Totally Symmetric Mode of $[IrCl_6]^{2-}$

6.4.1 Introduction

In this section, we calculate the polarizability components for all the normal modes of $[IrCl_6]^{2-}$. This is done in two stages. First of all we consider the simplest case, that of the totally symmetric mode. In the following section we deal with non-totally symmetric modes.

6.4.2 Symmetry preliminaries

As before, we calculate the tensor patterns for the totally symmetric mode of vibration using irreducible tensor methods. As has already been discussed, $[IrCl_6]^{2-}$ has octahedral geometry and is an odd electron system. Therefore the appropriate symmetry group is the octahedral spinor group O^*. The correct combinations for the electric dipole moment , which transforms as T_1 in O^*, are[15]

$$u_x = i2^{-1/2}(u^T - u^T) \qquad (6.4.1a)$$

$$u_Y = 2^{-1/2}(u^T + u^T) \qquad (6.4.1b)$$

$$u_Z = -iu^T \qquad (6.4.1c)$$

The electronic states with which we are dealing are spinor states and so their components are already expressed as irreducible tensors. In order to obtain the expressions for the components of these spinor states in terms of of the orbital and spin components, which are given in Fig.6.1, we use equation (2.6.15).

To use this expression, we need to know the symmetry

properties of the spin states. In O* the spin states transform according to E_1. Using tables of V coefficients for the octahedral spinor group, it is straightforward to calculate the correct combinations.

Having obtained the correct combinations, one can proceed to calculate the tensor components without further use of irreducible tensor methods, since all the operators involved act only on the orbital contribution to the wave function. This is the approach taken by Brown et al. (see ref.14) However, considerable labour can be saved by using tensor methods, and we use this approach in what follows.

6.4.3 Calculation for the totally symmetric mode

The electronic polarizability tensor components for a totally symmetric mode are calculated using equation (2.4.6). This involves a sum over all excited states. Now for the case of molecules which have a totally symmetric ground electronic state, we do not need to invoke the resonance condition. However, for the present case, we assume that we are in exact resonance with an excited electronic state j_e. (Note that it is not necessary to assume resonance with a specific vibronic state $j_e j_v$.) This allows us to considerably simplify the above expression, by ignoring all the electronic contributions in the sum over all excited states apart from that involving j_e. This is a good approximation due to the presence of the energy denominator.

Thus expression (2.3.11) reduces to the following

$$\tilde{a}_{\alpha\beta} = wS(f+ig)_J X_{\alpha\beta} \qquad (6.4.2)$$

where $(f+ig)_J$ are the line shape functions corresponding to the resonance state j_e, S is a product of Franck-Condon overlap integrals, w is the resonance frquency and

$$X_{\alpha\beta} = \sum_t \langle m_e | u_\alpha | j_{et} \rangle \langle t_{er} | u_\beta | n_e \rangle \qquad (6.4.3)$$

As we have seen, for iridium the ground electronic state is E_g''. There are consequently four possible combinations of initial and final state components. We use the notation $(\alpha_{\alpha\beta})_{r,s}$, where r is the final component and s is the initial component, to denote which of the four different scattering pathways we are considering.

If we consider $E'' \otimes T_1 = E'' + U'$, the direct product of the irreducible representations for the ground electronic state and the electric dipole moment operator, we see that the two excited electronic states with which we can be in resonance are E" and U'. Although in our experimental set-up we are resonance with U_u', we also perform calculations for the case of resonance with E_u'.

As a specimen calculation, we evaluate $(X_{XY})_{1/2,1/2}$ below for the case of resonance with U_u.

$$(X_{XY})_{1/2,1/2} = \sum \langle E_g+1/2 | u_X | U_{ut} \rangle \langle U_{ut} | u_Y | E_g 1/2 \rangle \qquad (6.4.4)$$

$$= \langle E_g+1/2 | 2^{-1/2}(u_{+1}-u_{-1}) | U_{ut} \rangle \langle U_{ut} | 2^{-1/2}(u_{+1}+u_{-1}) | E_g 1/2 \rangle$$

$$= \langle E_g \| u^T \| U_u \rangle \langle U_u \| u^T \| E_g \rangle 1/2 i S \, (-1)^{u(E\,-1/2+U-t)} \times$$

$$\left[V\begin{pmatrix} E_2 & T_1 & U \\ \frac{1}{2} & +1 & t \end{pmatrix} - V\begin{pmatrix} E_2 & T_1 & U \\ -\frac{1}{2} & -1 & t \end{pmatrix}\right]\left[V\begin{pmatrix} U & T_1 & E_2 \\ t & +1 & \frac{1}{2} \end{pmatrix} + V\begin{pmatrix} U & T_1 & E_2 \\ t & -1 & \frac{1}{2} \end{pmatrix}\right]$$

$$= \langle E_g \| u^T \| U_u \rangle \langle U_u \| u^T \| E_g \rangle 1/2 i S \, (-1)^{u(E\,-1/2+U-t)} \times$$

$$(-1)^2\left[V\begin{pmatrix} E_2 & T_1 & U \\ -\frac{1}{2} & +1 & -\frac{1}{2} \end{pmatrix} - V\begin{pmatrix} E_2 & T_1 & U \\ -\frac{1}{2} & -1 & -\frac{1}{2} \end{pmatrix}\right]\left[V\begin{pmatrix} U & T_1 & E_2 \\ \frac{1}{2} & +1 & \frac{1}{2} \end{pmatrix} + V\begin{pmatrix} U & T_1 & E_2 \\ \frac{1}{2} & -1 & \frac{1}{2} \end{pmatrix}\right]$$

$$+ (-1)^0\left[V\begin{pmatrix} E_2 & T_1 & U \\ -\frac{1}{2} & +1 & \frac{3}{2} \end{pmatrix} - V\begin{pmatrix} E_2 & T_1 & U \\ -\frac{1}{2} & -1 & \frac{3}{2} \end{pmatrix}\right]\left[V\begin{pmatrix} U & T_1 & E_2 \\ -\frac{3}{2} & +1 & \frac{1}{2} \end{pmatrix} + V\begin{pmatrix} U & T_1 & E_2 \\ -\frac{3}{2} & -1 & \frac{1}{2} \end{pmatrix}\right]$$

$$= -i/12 \langle E_g \| u^T \| U_u \rangle \langle U_u \| u^T \| E_g \rangle = -i/12 \, |\langle E_g \| u^T \| U_u \rangle|^2$$

Tensor Patterns For The A_1 Mode

After calculations similar to those on the previous page, we arrive at the tensor patterns presented below. These are identical to those quoted by Barron.[16]

Resonance with U_u

$$(\tilde{a}_{\alpha\beta})_{-1/2,1/2} = \begin{bmatrix} 0 & 0 & -1 \\ 0 & 0 & -i \\ 1 & i & 0 \end{bmatrix} \qquad (\tilde{a}_{\alpha\beta})_{1/2,-1/2} = \begin{bmatrix} 0 & 0 & 1 \\ 0 & 0 & -i \\ -1 & i & 0 \end{bmatrix}$$

$$(\tilde{a}_{\alpha\beta})_{1/2,1/2} = \begin{bmatrix} 2 & -i & 0 \\ i & 2 & 0 \\ 0 & 0 & 2 \end{bmatrix} \qquad (\tilde{a}_{\alpha\beta})_{-1/2,-1/2} = \begin{bmatrix} 2 & i & 0 \\ -i & 2 & 0 \\ 0 & 0 & 2 \end{bmatrix}$$

Resonance with E_u

$$(\tilde{a}_{\alpha\beta})_{-1/2,1/2} = \begin{bmatrix} 0 & 0 & 1 \\ 0 & 0 & i \\ -1 & -i & 0 \end{bmatrix} \qquad (\tilde{a}_{\alpha\beta})_{1/2,-1/2} = \begin{bmatrix} 0 & 0 & -1 \\ 0 & 0 & i \\ 1 & -i & 0 \end{bmatrix}$$

$$(\tilde{a}_{\alpha\beta})_{1/2,1/2} = \begin{bmatrix} 1 & i & 0 \\ -i & 1 & 0 \\ 0 & 0 & 1 \end{bmatrix} \qquad (\tilde{a}_{\alpha\beta})_{-1/2,-1/2} = \begin{bmatrix} 1 & -i & 0 \\ i & 1 & 0 \\ 0 & 0 & 1 \end{bmatrix}$$

(6.4.5)

It is clear from inspection that the above tensor patterns have the forms predicted in Section 3.5. As we saw the, only the antisymmetric scattering contribution is non-zero for the off-diagonal scattering pathways. Also, unlike molecules with a non-degenerate ground state, the tensor patterns are different for resonance with different excited states.

We now use these patterns to calculate the various scattering parameters.

6.4.4 Calculation of the depolarization ratio and M.C.I.D. values for the totally symmetric modes of $[IrCl_6]^{2-}$.

The tensor patterns for the totally symmetric mode were calculated in the prevous section. We can now use these to calculate the depolarization ratio and the M.C.I.D. parameters for the two separate cases of zero and non-zero magnetic fields, using equations (2.5.18)) and (2.5.20-23).

(i) Scattering in the absence of an applied magnetic field.

In the case of a zero applied magnetic field, the four different combinations of the initial and final components of the degenerate electronic state all produce scattered radiation of the same frequency. (These separate contributions to the scattering are shown in Fig. 6.5.) The correct procedure is to add together the scattering tensors which involve the same initial state.[17] Having done this, we then calculate the scattering intensities for each of these independently. The final step in the calculation is to add together the scattering intensities obtained above.

The results of these calculations for the cases of resonance with U_u' and E_u'' respectively are given in Table 6.2, along with the experimental values for the same quantities. It will be noted that the experimental and calculated values of the depolarization ratio for each of the resonance states show good agreement. This strongly supports Schatz's assignments for the electronic absorption spectra. As expected, the polarized and depolarized M.C.I.D.'s are both zero, due to the cancellation of the $\leftarrow +1/2$ and $\leftarrow -1/2$ scattering contributions.

(ii) Scattering in a strong applied magnetic field.

For the situation in which we have an applied magnetic field parallel to the incident radiation, we assume the limiting case of the field being of sufficient strength to totally resolve the ground state Kramers doublet E_g''. Assuming that this condition holds, the single totally symmetric Raman band splits into a triplet. As we have already seen, off-diagonal scattering contributions have their frequencies shifted to the right and left of the diagonal scattering contribution, whose frequency is unchanged by the applied magnetic field. For each band in this triplet, the depolarization ratio and the polarized and depolarized M.C.I.D.'s are evaluated using equations (2.5.10) and (2.5.20-23). The reason for using these rather than the isotropically averaged expressions (2.5.18) and (2.5.26-29) is that given in Section 3.5, namely that the magnetic field causes the spin states of the molecules to be completely oriented about the magnetic field, and therefore no orientational averaging is required.

The calculated values of these parameters for resonance with both of the excited electronic states are given in Table 6.2. It will be noted that the two outer bands of the triplet, corresponding to off-diagonal Raman scattering, show complete inverse polarization i.e. all the scattering intensity is polarized in the plane perpendicular to that of the incident radiation. For this reason the polarized M.C.I.D.'s vanish. The polarized component is also zero for the case of diagonal scattering. This is caused by the cancelling out of the $+1/2\langle -1/2$ and $-1/2\langle +1/2$ contributions to the polarized scattering component. Thus the theory

predicts that no polarized M.C.I.D. should be observed, agreeing with the experimental observations given in Table 6.2. (There will be a small residual M.C.I.D. expected because of the population differences between the initial +1/2 and -1/2 states.)

For the depolarized spectra, only two out of the three bands of the triplet show an M.C.I.D. peak. As in the polarized case, the contributions of the two diagonal scattering pathways to the depolarized M.C.I.D.'s are equal and opposite, and so the depolarized M.C.I.D. for the central band of the triplet vanishes.

The two observed M.C.I.D. peaks arise from the two off-diagonal scattering pathways, $+1/2 \leftarrow -1/2$ and $-1/2 \leftarrow +1/2$. The calculated values of the depolarized M.C.I.D.'s for these two scattering pathways are +1 and -1 respectively. Physically, this means that for these two scattering processes, all the scattering intensity arises from the scattering of either a right or a left cicularly polarized photon only.

For both of these bands, the calculated line shape of I^R-I^L is (f^2+g^2).(See Section 3.6.) Therefore theory predicts that I^R-I^L should not change sign as the frequency of the incident radiation passes through the resonance value.

To compare the above calculated resulted with experiment, it is necessary to consider how the ground state Kramers doublet of $[IrCl_6]^{2-}$ is affected by the applied magnetic field. This will be considered in the next section.

6.4.5 Comparison between theory and experiment for the totally symmetric mode

As we have seen, theory predicts non-zero values of Δ_z for the two off-diagonal scattering processes $-1/2 \longleftarrow +1/2$ and $+1/2 \longleftarrow -1/2$, each of these having the opposite sign. From the spectra presented in Fig. 6.2, it can be seen that for the totally symmetric vibrational mode we do indeed have two equal and opposite peaks in the difference spectra.

Now in theory, since we are assuming a strong enough magnetic field to totally resolve the single peak into a triplet, it should be possible to obtain an accurate numerical value of Δ_z for comparison with theory. In practice however, the magnetic field strength was insufficient to separate the three peaks of the triplet. Thus only the signs of the peaks could be measured with confidence. To compare these signs with the calculated values, we need to know the frequency shifts for the two off-diagonal scattering pathways, relative to the diagonal pathway. This is determined by the sign of the electronic g-factor for $[IrCl_6]^{2-}$, which we will now discuss.

Observation of a negative g-factor for $[IrCl_6]^{2-}$

For an isolated atom with spin 1/2, the g-factor is always positive. Physically, this corresponds to the situation shown in Fig. 6.5(a). In this situation, under a +ve applied magnetic field, the -1/2 spin state is lowered, and the +1/2 spin state is raised in energy. (The reverse is true for a negative g-factor, as in Fig. 6.5(b).)

For a transition metal complex ion however, the g-factor can be negative. (This is because, for a complex ion, the spin referred to is the effective spin, and has both spin and orbital contributions). The normal way to measure the g-factor of a complex is to study it's E.P.R. spectrum. From this, the magnitude of the g-factor for $[IrCl_6]^{2-}$ is found to be 1.82. This gives no information about the the sign of the g-factor however.

To measure the sign of a g-factor, an experiment involving circularly polarized radiation is necessary. Such experiments were performed by Hutchison and Weinstock[18], involving the absorption of circularly polarized microwave radiation by crystals of complex ions. In these experiments, the first observation of a -ve g-factor was made, for a 4th row transition metal ion. This was quite in accord with theory, which had predicted this g-factor.

In the complex ion $[IrCl_6]^{2-}$, with a low spin d^5 configuration for Ir, theory predicts a -ve g-factor.[19] As will emerge later, our observations provide strong evidence that the g-factor is negative. Hence in the following analysis of the experimental set-up, it will be assumed that the complex has a -ve g-factor.

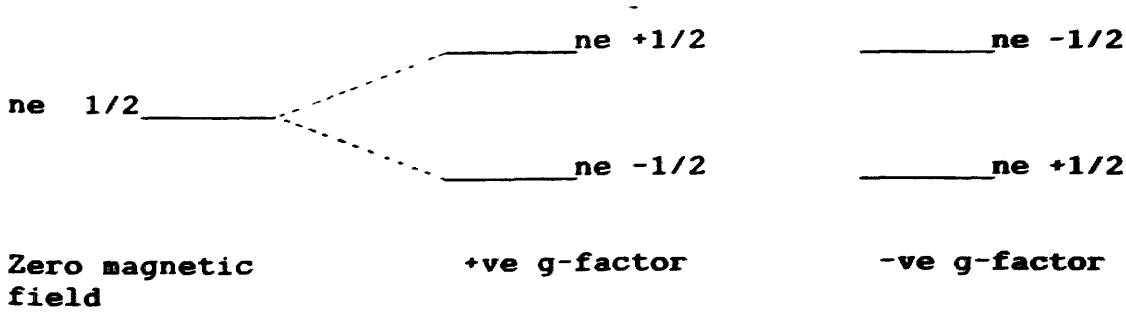

Fig. 6.5 The splitting of the degenerate electronic ground state for both positive and negative g-factors

Analysis of the experimental arrangement

In our experimental arrangement, described in Section 4.2, the incident light beam is parallel to the applied magnetic field. It is therefore convenient to quantize the spin of the $[IrCl_6]^{2-}$ along this direction, which we shall designate the z-direction. We shall also take the direction of propagation of the incident light beam to be in the +ve z-direction. (See Fig. 6.6) Finally, we specify that the applied magnetic field is positive.

Under the above conditions, the ground state Kramers doublet is split so that the $|E_g''+1/2\rangle$ component is of lower energy than the $|E_g''-1/2\rangle$.

We next consider the frequecies of the scattering triplet. The two diagonal Raman transitions $|E_g''+-1/2\rangle|0_v\rangle \longleftarrow |E_g''+-1/2\rangle|1_v\rangle$ produce scattering of frequency $v-v_{A1}$. (Here v is the frequency of the incident radiation and v_{A1} is the frequency of the totally symmetric mode transtion.) Also, we see from Fig. 6.6 that the Raman transition $|E_g''-1/2\rangle|1_v\rangle \longleftarrow |E_g''+1/2\rangle|0_v\rangle$ has frequency $v-v_0+d$, with the reverse electronic pathway having a frequency $v-v_0-d$. Here d is the splitting of the ground state produced by the magnetic field. Thus the frequency of the $-1/2 \longleftarrow +1/2$ scattering pathway lies between the Rayleigh band and the A_1 Raman band. Hence this scattering pathway will have a smaller Raman shift than the the A_1 Raman band.

From our analysis, we therefore deduce that the M.C.I.D. for the the right hand side of the observed couplet, in a +ve magnetic field, should be that of the $-1/2 \longleftarrow +1/2$ scattering pathway. The calculated value for this is -1.

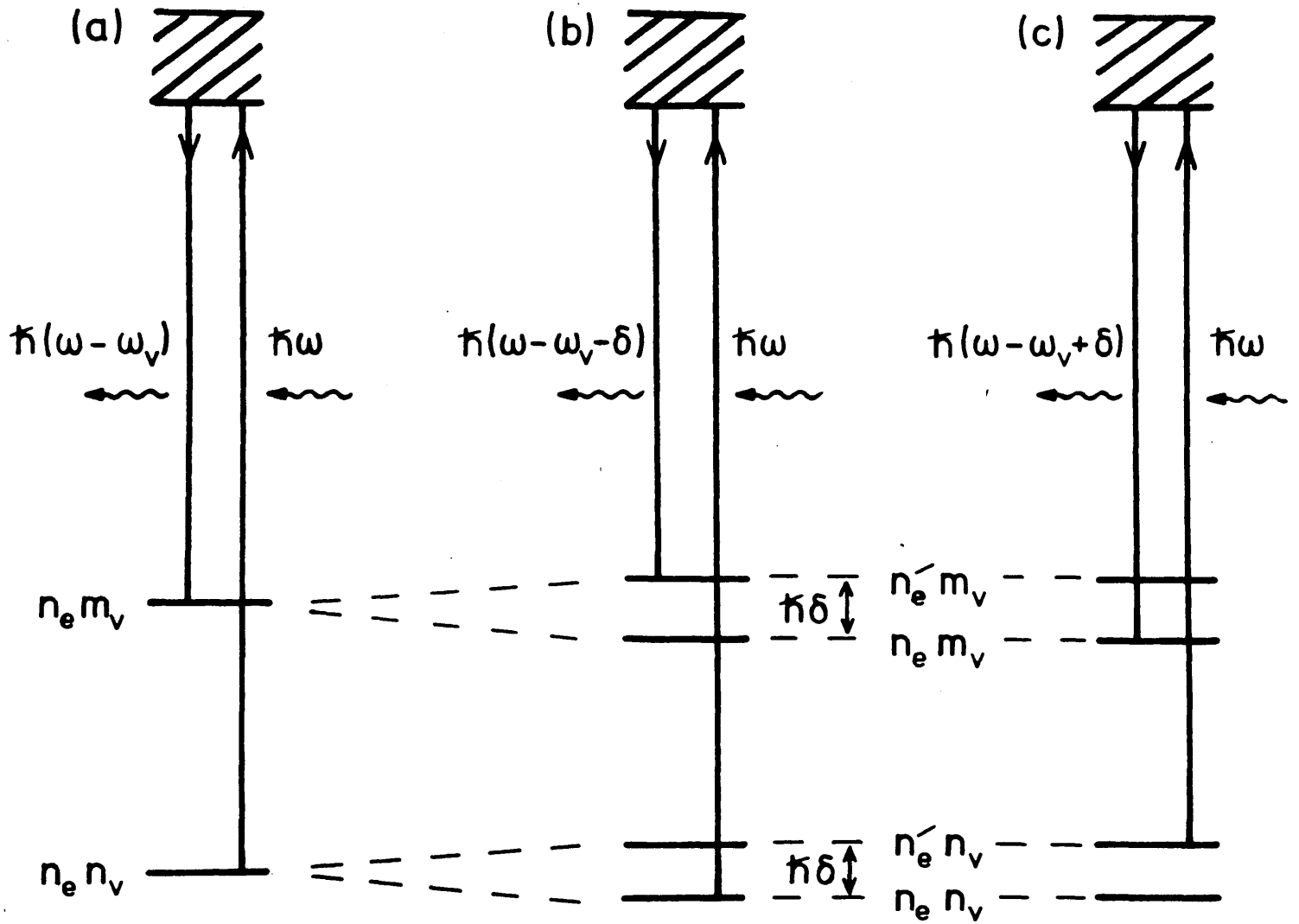
(a)
(b)
(c)
ħ(ω - ω_v)
ħω
ħ(ω-ω_v-δ)
ħω
ħ(ω-ω_v+δ)
ħω
n_e m_v
ħδ
n_e' m_v
n_e m_v
n_e n_v
ħδ
n_e' n_v
n_e n_v

This negative value is in agreement with the experimentally observed sign, therefore supporting the assumption regarding the sign of the g-factor.

As has already been noted, the applied magnetic field was insufficient to completely resolve the three components of the triplet. Because of this, the observed values for the M.C.I.D components have a modulus less than unity.

In final comparison with experiment, the M.C.I.D. spectra were measured for several excitation frequencies on either side of the resonance frequency. As expected from the frequency dependance of M.C.I.D.'s generated by the first mechanism, there was no change in the sign of the A_1 couplet.

Thus the detailed calculation outlined above gives fairly good agreement between calculation and experiment for the totally symmetric mode in the iridium spectra. In the last part of this section, we look at a simple, general method of calculating the form of the Raman E.P.R. couplet for totally symmetric modes.

6.4.6 A simplified model for calculating the Raman E.P.R. of A_1 modes.

In this section, a simplified model will be used for the calculation of totally symmetric mode Raman E.P.R. couplets. This method is taken from Section 8.5.3 of Barron's book.[20]

Fig. 6.7 shows the various scattering pathways available when a molecule has a doubly degenerate ground state. From the discussion in the previous section, it is clear that in the diagram we have assumed that the g-factor for the molecular system we are considering is positive.

Now a circularly polarized photon has an angular momentum quantum number of 1, with components +1 for right and left circular polarization respectively. We discuss separately the scattering pathways for each of these two polarizations.

When the incident photon is right circularly polarized, it effects a transition from the +1/2 component of the

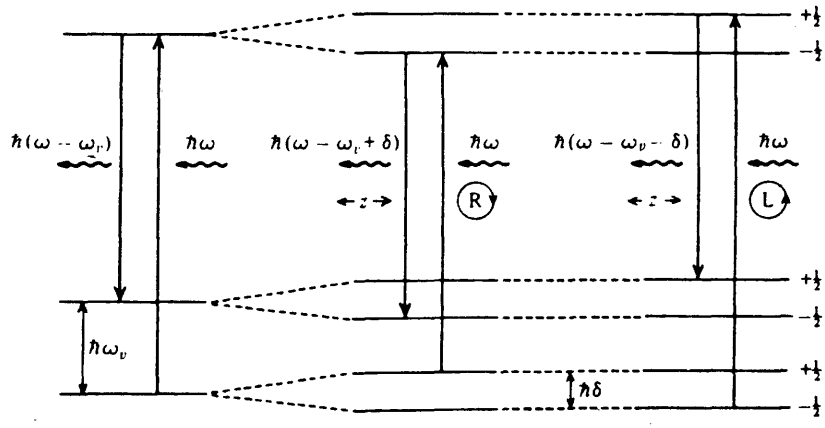

Fig. 6.7 Diagram showing the pathways mediated by right and left circularly polarized light.

degenerate ground state to some virtual excited electronic state with M_J = -1/2. We then have a transition back down to the final excited vibronic state, with the ground state electronic component being -1/2. From the diagram, we see that for a system with a positive g-factor, this Raman transition will have a smaller frequency shift than the diagonal scattering pathways. Hence the positive part of the M.C.I.D. couplet should lie nearest to the Rayleigh scattering side.

Similarly, the negatively polarized photon induces a transition to a virtual excited state with M_J=+1/2. We then arrive, after the emission of the scattered photon, back at an excited vibronic state with ground electronic state component +1/2. From the the diagram, we see that this process has a frequency shift greater than the diagonal scattering pathways. Hence the negative part of the M.C.I.D. couplet should lie furthest away from the Rayleigh scattering wing.

This analysis leads to exactly the opposite of what we observe for the A_1 normal mode of $[IrCl_6]^{2-}$. This has already been interpreted as evidence for the g-factor for $[IrCl_6]^{2-}$ being negative.

For the other two complexes, $[FeBr_4]^-$ and $[CuBr_4]^{2-}$, this analysis predicts the correct form for the M.C.I.D. couplets corresponding to the A_1 normal mode.

Having dealt with the totally symmetric mode of $[IrCl_6]^{2-}$, we now go on to consider the non-totally symmetric modes.

6.5 Calculations for the Non-Totally Symmetric Normal Modes of $[IrCl_6]^{2-}$

6.5.1 Introduction

This Section follows the same pattern as Section 6.3. First the tensor patterns are calculated. Next the M.C.I.D. and depolarization ratios are calculated. Finally, the calculations are compared with experiment.

6.5.2 Symmetry preliminaries

As we have seen in Chapter 3, there are two non-totally symmetric modes of vibration in the resonance Raman spectrum of $[IrCl_6]^{2-}$, namely the T_{2g} and E_g modes. In the calculation of the tensor patterns for these normal modes, we use operators having the same irreducible representation as the normal mode. Thus it is necessary to express the cartesian components of these representations in terms of the irreducible tensor components appropriate for use in the group O^*.

For the E mode, the (θ,ε) components remain unchanged.

In the case of the T_2 mode, the cartesian components (T_{2x},T_{2y},T_{2z}) must be expressed in terms of the complex components $(T_2{-1},T_2O,T_2{+1})$ as follows[21]

$$T_{2x} = i2^{-1/2}(T_2{+1} - T_2{-1}) \qquad (6.5.1a)$$

$$T_{2y} = 2^{-1/2}(T_2{+1} - T_2{-1}) \qquad (6.5.1b)$$

$$T_{2z} = -iT_2O \qquad (6.5.1c)$$

6.5.3 Simplification of the Z tensor using the resonance condition

For non-totally symmetric modes of vibration, expressions (2.3.10) for the polarizability in terms of the Z tensors must be used. Now expression (2.3.12) for the Z tensors involves two sums over all excited electronic states and two sums over all excited vibrational states of the molecule. As it stands, it is impossible to calculate.

However, in our experimental observations, the exciting radiation was in resonance with one of excited states of the molecule. We therefore assume that we are in exact resonance with the excited electronic state j_e. The summation over all j_e disappears, due to the frequency denominator. The two summations over the excited vibrational states can be performed separately from the remaining electronic summation, so that we obtain the following expression.

$$Z_{\alpha\beta} = \sum_{j_e \neq k_e} \left[\frac{\langle k_e|H_\alpha|n_e\rangle(\langle m_e|u_\alpha|j_e\rangle\langle j_e|u_\beta|k_e\rangle}{\hbar\omega_{n_e k_e}} + \frac{\langle k_e|H_\alpha|m_e\rangle(\langle k_e|u_\alpha|j_e\rangle\langle j_e|u_\beta|n_e\rangle}{\hbar\omega_{m_e k_e}} + \frac{\langle k_e|H_\alpha|j_e\rangle(\langle m_e|u_\alpha|j_e\rangle\langle k_e|u_\beta|n_e\rangle}{\hbar\omega_{j_e k_e}} + \frac{\langle k_e|H_\alpha|j_e\rangle(\langle m_e|u_\alpha|k_e\rangle\langle j_e|u_\beta|n_e\rangle}{\hbar\omega_{j_e k_e}} \right] \quad (6.5.2)$$

This expression can be approximated further, due to the presence of the frequency denominators $\omega_{j_e k_e}$ and $\omega_{n_e k_e}$. The main contribution to the polarizability comes from the excited electronic states which are close in energy to the ground state and the resonance state. In fact, the frequency

denominator $w_{j_e k_e}$ for the excited states shown in Fig. 6.1 is roughly a tenth of $w_{n_e k_e}$. It is therefore a reasonable approximation to ignore the contribution of all the terms with energy denominator $w_{n_e k_e}$. We make the final approximation that the vibrational terms are equal, i.e.

$$\langle m_v | j_v \rangle \langle j_v | Q | n_v \rangle = \langle m_v | Q | j_v \rangle \langle j_v | n_v \rangle \qquad (6.5.3)$$

This can be seen to be approximately true using from the same considerations which allowed us to simplify equation (3.2.10).

With the above extensive approximations, the following expression is obtained for the $Z_{\alpha\beta}$ contribution to the complex polarizability tensor, $(Z_{\alpha\beta})_{r,s}$ connecting the initial component of the ground electronic state $|E_g s\rangle$ with the final component $|E_g r\rangle$.

$$(Z_{\alpha\beta})_{r,s} = k[\ (E^{(1)}_{\alpha\beta})_{r,s} + (E^{(2)}_{\alpha\beta})_{r,s}\ ] \qquad (6.5.4)$$

where

$$k = w(f+ig)_j / \hbar^2 \ w \ x \ \langle m_v | Q | j_v \rangle \langle j_v | n_v \rangle \qquad (6.5.5)$$

$$(E^{(1)}_{\alpha\beta})_{r,s} = \langle k_e | H_Q | j_e \rangle \langle E_g r | u_\alpha | k_e \rangle \langle j_e | u_\beta | E_g s \rangle \qquad (6.5.6)$$

$$(E^{(2)})_{r,s} = \langle k_e | H_Q | j_e \rangle^* \langle E_g r | u_\alpha | j_e \rangle \langle k_e | u_\beta | E_g s \rangle \qquad (6.5.7)$$

In the above expressions, a summation over the components of a degenerate state is assumed.

In Section 3.3, various general expressions were obtained using symmetry arguments. These showed that for diagonal scattering, the polarizability has the form (3.4.37) or (3.4.47). This shows, as was pointed out earlier, that both real and imaginary parts of the polarizabilty tensor can be symmetric and antisymmetric for non-totally symmetric modes, unlike the situation for A_1 modes.

For off-diagonal scattering, the appropriate expressions are (3.4.35) and (3.4.45). Similar comments apply to these.

We can use these expressions to save calculation, or we can use them to provide a check on such calculation.

6.5.4 Tensor patterns for the E normal vibrational mode

We first of all calculate the tensor patterns for the E vibrational mode. There are two possible excited states with which we could experimentally be in resonance. These are the E_u' and the U_u' states. We consider each of these separately.

(a) Resonance with U_u'.

If we are in resonance with U_u', there are three possible excited states k_e with which we can mix.

(i) $k_e = E_u'$

(ii) $k_e = U_u'$ (non Jahn-Teller case)

(iii) $k_e = U_u'$ (Jahn-Teller case)

For each of these cases detailed calculations were performed. As a specimen calculation, the xz component of the polarizability tensor involving the initial electronic component $E_g''1/2\rangle$ and the final component $E_g''-1/2\rangle$ for (i) above will be evaluated.

$$(E_{xz})_{-1/2,1/2} = \sum_{r,s,t} \langle E_g''-1/2|u_x|E_u't\rangle\langle U_ur|u_z|E_g''1/2\rangle\langle E_ut|H_E^s|U_ur\rangle \qquad (6.5.8)$$

By inspection we can eliminate most of the terms in the summation over the components. From the first matrix element we see that r must equal -3/2 or 1/2 and s = -1/2. The second is only non-zero if t= 1/2, and the third vanishes unless r= -3/2. Thus

$$(E_{xz})_{-1/2,1/2} = \langle E_g''-1/2|u_x|E_u1/2\rangle\langle U_g'-3/2|u_z|E_g''1/2\rangle\langle E_u1/2|H_E^s|U_u-3/2\rangle$$

$$= (-1/2)x(6^{-1/2}i)x(-6^{-1/2}i)\langle E''_g\|u\|E'_u\rangle\langle U'_g\|u\|E''_g\rangle\langle E'_u\|H_E\|U'_u\rangle$$

$$= -1/12x\langle E''_g\|u\|E'_u\rangle\langle U'_u\|u\|E''_g\rangle\langle E'_u\|H_E\|U'_u\rangle$$

$$= -1/12xM_1 \qquad (6.5.9)$$

Similarly,

$$(E_{xz})_{-1/2,1/2} = (-1+3^{1/2})/24x\langle E''_g\|u\|U'_u\rangle\langle E'_u\|u\|E''_g\rangle x\langle E'_u\|H_E\|E''_g\rangle^*$$

$$= (-1+3^{1/2})/24xM_2 \qquad (6.5.10)$$

To complete the calculation of $(Z_{\alpha\beta})_{-1/2,1/2}$, it is necessary to know the relationship between M_1 and M_2. This can be calculated in the following way. First of all, use the hermiticity of all the operators to establish equalities such as

$$\langle E''_{g-1/2}|u_z|E'_{u-1/2}\rangle = \langle E'_{u-1/2}|u_z|E''_{g-1/2}\rangle \qquad (6.5.11)$$

Using the Wigner-Eckart theorem, we can write this as

$$-6^{-1/2}i\langle E''_g\|u\|E'_u\rangle = +6^{-1/2}i\langle E'_u\|u\|E''_g\rangle^* \qquad (6.5.12a)$$

i.e.
$$\langle E''_g\|u\|E'_u\rangle = -\langle E'_u\|u\|E''_g\rangle^* \qquad (6.5.12b)$$

If we now consider the reduced matrix element above in detail, we see that it is pure imaginary. Hence we have

$$\langle E''_g\|u\|E'_u\rangle = \langle E'_u\|u\|E''_g\rangle \qquad (6.5.13)$$

Similar arguments for the other two reduced matrix elements give us

$$\langle E''_g\|u\|U'_u\rangle = -\langle U'_u\|u\|E''_g\rangle \qquad (6.5.14)$$

where both are pure imaginary.

Finally, we can deduce that $\langle E'_u\|H_E\|U'_u\rangle$ is real.

We therefore end up with the result that

$$M_1 = -M_2 \qquad (6.5.15)$$

where both products are real.

This allows us finally to write

$$(E_{xz})_{-1/2,1/2} = (1+3^{1/2})M_1 \qquad (6.5.16)$$

Proceeding in this way, the tensor patterns for off-diagonal and diagonal scattering for each of the

situations (i),(ii), and (iii) above were calculated. For all three situations, the calculated tensor patterns were identical. They are given below.

E Mode Tensor Patterns

As mentioned already, the tensor patterns are identical, no matter what combination of states k_e and j_e we choose. Thus, however crude our approximations were at the start, the tensor patterns obtained are a fairly good approximation, because any other contributions would give the same pattern.

$$(\tilde{a}_{\alpha\beta})_{-1/2,1/2} = \begin{bmatrix} 0 & 0 & -(1+3^{1/2}) \\ 0 & 0 & -(1-3^{1/2})i \\ (1+3^{1/2}) & (1-3^{1/2})i & 0 \end{bmatrix}$$

$$(\tilde{a}_{\alpha\beta})_{1/2,-1/2} = \begin{bmatrix} 0 & 0 & (1+3^{1/2}) \\ 0 & 0 & -(1-3^{1/2})i \\ -(1+3^{1/2}) & (1-3^{1/2})i & 0 \end{bmatrix}$$

$$(\tilde{a}_{\alpha\beta})_{-1/2,-1/2} = \begin{bmatrix} (1-3^{1/2}) & -i & 0 \\ +i & (1+3^{1/2}) & 0 \\ 0 & 0 & -2 \end{bmatrix}$$

$$(\tilde{a}_{\alpha\beta})_{1/2,1/2} = \begin{bmatrix} (1-3^{1/2}) & i & 0 \\ -i & (1+3^{1/2}) & 0 \\ 0 & 0 & -2 \end{bmatrix} \qquad (6.5.17)$$

Several points emerge from inspection of the above patterns. First of all, there is a marked similarity to the

tensor patterns for the A_1 normal mode. As for the A_1 mode, only imaginary antisymmetric scattering occurs. A second point to note is that the patterns for the diagonal transitions do indeed satisfy (3.4.35) and (3.4.37)

(b) Resonance with E_u'.

For this resonance, there is only one symmetry for which mixing is possible, namely $k_e = U_u'$. It has already been shown generally that this should give the same result as for $j_e = U_u'$, $k_e = E_u'$. Thus the tensor patterns for this resonance are identical to those given above.

6.5.5 Tensor patterns for the T_{2g} normal vibrational mode

As before, we deal separately with the two possible states with which we can be in resonance.

(a) Resonance with U_u.

For resonance with $j_e = U_u'$, there are three possible excited symmetries with which we can mix. These are

(i) $k_e = E_u'$

(ii) $k_e = U_u'$ (non Jahn-Teller case)

(iii) $k_e = U_u'$ (Jahn-Teller case)

(b) Resonance with E_u'

For this resonance, only one mixing symmetry is possible:-

(i) $k_e = U_u'$

Detailed calculations, very similar to the specimen calculation shown in the last subsection, were performed for all the combinations in (a) and (b). Every one of these combinations gave exactly the same tensor patterns. Again, this means that although gross approximations were made at the outset, the tensor patterns obtained are fairly good

approximations. This because they show that every possible excited state symmetry would make the same contribution to the tensor pattern.

We now give the tensor patterns for the T_{2g} mode.

T_{2g} Mode Tensor Patterns

$$(\tilde{a}_{\alpha\beta})_{-1/2,1/2} = \begin{bmatrix} 0 & 1-i & i \\ -1+i & 0 & +1 \\ -i & -1 & 0 \end{bmatrix} \quad (6.5.18a)$$

$$(\tilde{a}_{\alpha\beta})_{1/2,-1/2} = \begin{bmatrix} 0 & -1-i & i \\ 1+i & 0 & -1 \\ -i & 1 & 0 \end{bmatrix} \quad (6.5.18b)$$

$$(\tilde{a}_{\alpha\beta})_{-1/2,-1/2} = \begin{bmatrix} 0 & -1 & -1-i \\ -1 & 0 & -1+i \\ -1+i & -1-i & 0 \end{bmatrix} \quad (6.5.18c)$$

$$(\tilde{a}_{\alpha\beta})_{1/2,1/2} = \begin{bmatrix} 0 & 1 & 1-i \\ 1 & 0 & 1+i \\ 1+i & 1-i & 0 \end{bmatrix} \quad (6.5.18)$$

Several points about the T_{2g} mode tensor pattern can be seen immediatly. The first point to note is that the off-diagonal scattering pathways support only antisymmetric scattering, as was the case for the other two modes. The second point to note is that for the diagonal scattering pathways, the real scattering contribution is symmetric, and the imaginary contribution is antisymmetric.

In the next section, we use the tensor patterns to calculate the various scattering observables.

6.5.6 Calculation of the depolarization ratio and M.C.I.D. parameters for E and T_{2g} modes

In order to calculate the depolarization ratios for the two modes , we need to use (2.5.18). This is because, for the off diagonal scattering pathways, both the real and imaginary parts of the polarizability have symmetric and antisymmetric contributions. To calculate the M.C.I.D.'s, we use (2.5.20-23), since we are dealing with magnetic optical activity produced by the first mechanism. As before, we present the calculations for E and T_{2g} separately.

(a) Calculation for the E normal mode

(i) Zero Magnetic Field

To calculate the depolarization ratio and the M.C.I.D.'s for the case of a zero magnetic field, we adopt the same procedure as for the A_1 mode, i.e. we calculate separately the contributions to the depolarization ratio for scattering originating from the +1/2 and -1/2 initial ground state components, and then add these. As a specimen calculation, we now give details of the computations.

For initial state +1/2, we have

$$\alpha^2 = 1/9\tilde{a}_{\alpha\alpha}\tilde{a}_{\beta\beta}^{*} = 1/9|k|^2(1-3^{1/2}+1+3^{1/2}-2)^2 = 0 \quad (6.5.19)$$

$$\beta(\alpha)^2 = 1/2(3\tilde{a}^{s}_{\alpha\beta}\tilde{a}^{s*}_{\alpha\beta} - \tilde{a}_{\alpha\alpha}\tilde{a}_{\beta\beta})$$

$$= 1/2|k|^2[3((1-3^{1/2})^2 + (1+3^{1/2})^2 + (-2)^2) - 0]$$

$$= 18|k|^2 \quad (6.5.20)$$

$$\beta(\alpha')^2 = 3/2(a^{a}_{\alpha\beta}a^{a*}_{\alpha\beta}) = 3/2|k|^2[2(1+3^{1/2})^2 + 2(1-3^{1/2})^2 + 2]$$

$$= 27|k|^2 \quad (6.5.21)$$

Initial state -1/2 calculations are identical. Thus

$$\rho(x) = \frac{3\beta(\alpha)^2 + 5\beta(\alpha')^2}{45\alpha^2 + 4\beta(\alpha)^2}$$

$$= \frac{(3x18 + 3x18) + (5x27 + 5x27)}{(45x0 + 45x0) + (4x18 + 4x18)} = 2.625 \qquad (6.5.22)$$

Again , since we have a zero magnetic field, we calculate the M.C.I.D.'s separately for the two initial states and then add. This is because all pathways have the same frequency in the absence of the magnetic field.

$$\Delta_x(90^0) = 2Im(\tilde{a}_{xy}\tilde{a}_{xx})/Re(|\tilde{a}_{xx}|^2 + |\tilde{a}_{xy}|^2)$$

$$= 2|k|^2 Im[\, i.(1-3^{1/2})^* + -i.(1-3^{1/2})^*]/Re(....)$$

$$= 0 \qquad (6.5.23)$$

Similarly,

$$\Delta_z(90^0) = 0 \qquad (6.5.24)$$

(ii) Non-zero Magnetic Field

In this case, we assume that the external magnetic field is strong enough to totally resolve the single E mode band into 3 separate bands, corresponding to the sets -1/2 ⟵ 1/2, 1/2 ⟵ 1/2 and -1/2 ⟵ -1/2, and 1/2 ⟵ -1/2. We calculate the scattering parameters for each of these separately. However, since there has been no measurement of the depolarization ratio for the three separate peaks, we do not calculate these. The M.C.I.D.'s are given in Table 6.1

(b) Calculation for the T_{2g} normal mode

The procedure for calculating the scattering parameters for T_{2g} is identical to that for E. The results of these calculations are given in Table 6.2.

Table 6.2(a) Calculated and experimental values for the depolarization ratio for resonance with the excited state U of $[IrCl_6]$

Symmetry	A_1	E_g	T_{2g}
$\rho(x)$. Calc.	0.25	2.625	2.23
$\rho(x)$. Expt.	0.31	0.73	1.91

Table 6.2(b) Calculated and experimental values for the depolarization ratio for resonance with the excited state E of $[IrCl_6]$

Symmetry	A_1	E_g	T_{2g}
$\rho(x)$. Calc.	1.0	2.625	2.23
$\rho(x)$. Expt.	1.0		

Table 6.2(c) Calculated depolarized M.C.I.D. for $[IrCl_6]$

Symmetry	Depolarized M.C.I.D.	
	$W + W_0$	$W - W_0$
A_1	+1.0	−1.0
E_g	−0.5	+0.5
T_{2g}	−1.0	+1.0

6.5.7 Comparison of calculated results with experiment for the E and T_{2g} vibrational modes

(a) E mode of Vibration

The first point to notice about the calculated depolarization ratio is that it is independent of the frequency of the incident radiation, unlike the A_1 mode. As we saw in the detailed calculation presented earlier, there is no isotropic contribution to the scattering. Only anisotropic and antisymmetric contributions are non-zero, leading to a depolarization ratio of 2.6. Thus the E band is predicted to exhibit inverse polarization. This is confirmed experimentally. However, the exact value for the depolarization ratio has not been measured exactly.

Our calcuations predict that $\Delta_x(90^\circ)$ should be zero for all three scattering contributions. Experimentally, no polarized M.C.I.D. was observed for the E mode.

The calculated $\Delta_z(90^\circ$ for the three Raman peaks are +1/2 for the -1/2 $\longleftarrow$ 1/2 scattering pathway, -1/2 for the 1/2 $\longleftarrow$ -1/2 scattering pathway and 0 for the diagonal pathways. (See Table 6.2) From our experimental analysis in Section 6.3.4, we saw that the right hand side of the M.C.I.D. couplet corresponds to the -1/2 $\longleftarrow$ 1/2 pathway. Thus we calculate that the E mode should give a couplet opposite in sign to that for the A_1 mode. Now for $[IrCl_6]^{2-}$, there was insufficient intensity to measure the M.C.I.D. for the E mode. However, as will be explained later, the above calculations are valid for any system with a similar electronic structure. Measurements of the M.C.I.D. for the E

mode, using a tuneable dye-laser, have been made for the iridium hexabromide[22] complex. (These experiments were performed by Barron, Vrbancich and Watts after the end of the experimental work for the present thesis.) It is gratifying that the calculated sign for the M.C.I.D. couplet agrees with this experimentally determined sign.

(b) T_{2g} mode of vibration

As with the E mode, but unlike the A_1 mode, the depolarization ratio is independent of the frequency of the incident light. The calculated value of the depolarization ratio is 2.46. Thus calculation predicts that the T_{2g} band should exhibit inverse polarization. Observations confirm this prediction, although not the exact calculated value. As in the case of the A_1 and E bands, the calculated value for $\Delta_x(90^\circ)$ is zero. Again, this agrees with experimental observation.

The calculated values for $\Delta_z(90^\circ)$ for the three scattering pathways are -1 for the $-1/2 \longleftarrow 1/2$ pathway, +1 for the $1/2 \longleftarrow -1/2$ pathway and zero for the diagonal pathways. Thus calculation predicts that the M.C.I.D. couplet for the T_{2g} mode should be the same as for the E mode, and opposite to that for the A_1 mode. This is confirmed experimentally, although again, the resolution of the the bands was insufficient for a good measurement of the numerical value of Δ_z.

As a final check between calculation and experiment, M.C.I.D. measurements were made for several different frequencies. The sign of the M.C.I.D. was constant for all these values, as predicted by theory.

Chapter 6 : References

1) L.D. Barron and C. Meehan, Chem. Phys. Lett. 66,444(1979)

2) A. Abragam and B. Bleaney, Electron Paramagnetic Resonance of Transition Ions, Clarendon Press, Oxford, 1970

3) [A], p.385

4) H. Hamaguchi and T. Shimanouchi, Chem. Phys. Letts.38,370(1976)

5) [A], p.383

6) See ref. 2

7) G.N. Henning, A.J. McCaffrey, P.N. Schatz and P.J. Stephens,J. Chem. Phys. 48,5656(1968)

8) See ref. 7

9) P. Stein, J.M. Brown and T.G. Spiro, Chem. Phys. 25,237(1977)

10) G.N. Henning, A.J. McCaffrey, P.N. Schatz and P.J. Stephens,J. Chem. Phys. 48,5656(1968)

11) See ref. 7

12) L.D. Barron, C. Meehan and J. Vrbancich, Mol. Phys. 41,945(1980)

13) P.N. Schatz, Mol. Phys. 47,673(1982)

14) See ref. 9

15) [D], p.135

16) [A], p.372

17) E.M. Lifshitz and L.P. Pitaevski, Statistical Physics , part 1, Pergamon Press, Oxford.

18) C.A. Hutchison and B. Weinstock, J. Chem. Phys. 32,56(1960)

19) See ref. 2

20) [A], p.385-386

21) [D], p.164

22) L.D. Barron, J. Vrbancich and R.S. Watts, Chem. Phys. Letts. 89,71(1982)

CHAPTER 7

LIGHT SCATTERING BY ATOMIC SODIUM

7.1 Introduction

In this chapter, we present a treatment of Rayleigh scattering for atoms which is similar to that given for Rayleigh scattering of molecules. In particular, we calculate the general form of the tensor patterns for diagonal and off-diagonal scattering when we have a doubly degenerate ground state.

7.2 Rayleigh Scattering by Atoms

7.2.1 Symmetry preliminaries

For atoms, the appropriate symmetry group is the full rotation group R_3. We thus classify the atomic states using a JM coupling scheme. When expressed in this way, the atomic states are in the form of irreducible tensors with respect to the full rotation group. It therefore only remains to express all the operators we are using in irreducible tensor form. The correct combinations for the electric dipole moment operator, which transforms as a state with J=1, are[1]

$$u_x = -2^{-1/2}(u_1 - u_{-1}) \qquad (7.2.1a)$$

$$u_y = i2^{-1/2}(u_1 + u_{-1}) \qquad (7.2.1b)$$

$$u_z = u_0 \qquad (7.2.1c)$$

The combinations for the magnetic dipole moment operator, which also transforms as J=1, have identical form. Using

these, we can express the second rank cartesian tensor operator $A_{\alpha\beta}$ in terms of its complex components A_{ij} in an identical way to Section 3.3. , except that the right hand sides must all be multiplied by -1.

7.2.2 Derivation of general expression

Since we are dealing with atomic Rayleigh scattering, the polarizability is given by

$$(a_{\alpha\beta})_{M_1,M_2} = \frac{w_{jn}\mathrm{Re}[(X_{\alpha\beta})_{M_1,M_2}] - i w \mathrm{Im}[(X_{\alpha\beta})_{M_1,M_2}]}{(w_{jn}-w_2)} \quad (7.2.2)$$

where

$$(X_{\alpha\beta})_{M_1,M_2} = \langle neM_1|u_a|jec\rangle\langle jec|u_b|neM_2\rangle \quad (7.2.3)$$

In general the ground electronic state will be degenerate. The above expression has been written therefore, to include the possibility of the initial and final component being different. Since we are using a JM coupling scheme, we can rewrite the above as

$$(X_{ij})_{M_1,M_2} = \sum_{M'} \langle (SL)JM_1|u_i|(S'L')J'M'\rangle\langle (S'L')J'M'|u_j|(SL)JM_2\rangle \quad (7.2.4)$$

We can develop this as follows

$$(X_{ij})_{M,M}$$

$$= (-1)^{J-M}(-1)^{J'-M'}\langle (SL)J\|u\|(S'L')J'\rangle\langle (S'L')J'\|u\|(SL)J\rangle \times \begin{pmatrix} J & 1 & J' \\ -M_1 & i & M' \end{pmatrix}\begin{pmatrix} J' & 1 & J \\ -M' & j & M_2 \end{pmatrix}$$

$$= (-1)^{J-M_1}(-1)^{J'-M'}(-1)^{2J+2J'+2} \begin{pmatrix} J & 1 & J' \\ M_1 & i & M' \end{pmatrix}\begin{pmatrix} J' & 1 & J \\ -M' & j & M_2 \end{pmatrix} \times |\langle (SL)J\|u\|(S'L')J'\rangle|^2$$

$$= (-1)^{2J+2J'}\ (-1)^{J-M_1}(-1)^{J'-M'}\begin{pmatrix} J & 1 & J' \\ M_1 & -i & -M' \end{pmatrix}\begin{pmatrix} J' & 1 & J \\ M' & -j & -M_2 \end{pmatrix} \times |\langle (SL)J\|u\|(S'L')J'\rangle|^2$$

$$= (-1)^{2J+2J'} \quad [(-1)^{J-M_1}(-1)^{J'-M'}\begin{pmatrix} J & 1 & J' \\ M_1 & -i & M' \end{pmatrix}\begin{pmatrix} J' & 1 & J \\ -M' & -j & -M_2 \end{pmatrix}$$

$$\text{x} \quad \langle (SL)J \| u \| (S'L')J' \rangle^2]$$

$$= (-1)^{2J+2J'} \quad (-1)^{-2M_1-2M'}(X_{-i,-j})_{-M,-M} \qquad (7.2.5)$$

Now from the bottom row of the first 3-j symbol, we see that $M' = M_1 - i$. Thus $-2M_1-2M' = -4M_1-2i$. This is clearly even, since i is an integer and M_1 is either an integer or a half integer. Again using the first 3-j symbol, we know that J+J'+1 must be an integer. Thus 2J+2J' is also even.

We can thus write

$$(X_{i,j})_{M_1,M_2} = (X_{-i,-j})_{-M_1,-M_2} \qquad (7.2.6)$$

From this we deduce the result that

$$(\tilde{a}_{i,j})_{M_1,M_2} = (\tilde{a}_{-i,-j})_{-M_1,-M_2} \qquad (7.2.7)$$

7.2.3 Deductions from general result

(a) Doubly degenerate ground state.

Expression (7.2.6) for Rayleigh scattering is identical to result (3.4.11) which was deduced earlier for Raman scattering by totally symmetric modes. Also, the form of the combinations for the cartesian polarizability components in terms of the complex components are identical, except that they have opposite sign. Hence the form of the tensor patterns which were deduced for the case of a molecule with a doubly degenerate ground state, namely (3.4.18-19) and (3.4.22-23), apply also to the case of atomic Rayleigh scattering, where the ground state is doubly degenerate. Thus we can immediately deduce that atoms with a degenerate ground state should generate a Rayleigh M.C.I.D. couplet. To determine the signs of this couplet, we need to resort to

detailed calculations. We perform these in the next section for the case of atomic sodium.

(b) Non-degenerate Ground State

Further results can be deduced where the ground state is of the form $|JO\rangle$. In this case we can write

$$(\tilde{a}_{1,J})_{O,O} = (\tilde{a}_{-1,-J})_{O,O} \qquad (7.2.8)$$

Using this, we can for example deduce that

$$\begin{aligned}(\tilde{a}_{XY})_{O,O} &= -1/2i[\,\tilde{a}_{1,1}+\tilde{a}_{1,-1}-\tilde{a}_{-1,1}-\tilde{a}_{-1,-1}]_{O,O} \\ &= -1/2i[\,\tilde{a}_{-1,-1}+\tilde{a}_{-1,1}-\tilde{a}_{1,-1}-\tilde{a}_{1,1}]_{O,O} \\ &= -(\tilde{a}_{XY})_{O,O} \qquad (7.2.9)\end{aligned}$$

Thus

$$(\tilde{a}_{XY})_{O,O} = 0 \qquad (7.2.10)$$

Similarly, we can show that

$$(\tilde{a}_{YX})_{O,O} = (\tilde{a}_{XZ})_{O,O} = (\tilde{a}_{ZX})_{O,O} = 0 \qquad (7.2.11)$$

To eliminate the remaining non-diagonal terms, we remember that for an even electron system, we can always write the wave functions in real form. Thus the polarizability is real. However, using a similar argument to that used to deduce Table 3.1 in Section 3.4, we know that the YZ and ZY components are imaginary. Hence these must be zero.(cf. results obtained by Barron use time-symmetry arguments.[2]) Thus for an even electron system, the scattering tensor is real, with all off-diagonal polarizability components zero. Hence, as expected, atoms with non-degenerate ground states do not exhibit magnetic Rayleigh optical activity. (Apart from very small Faraday B type effects.)

7.3 Resonance Rayleigh Scattering by Atomic Sodium.

7.3.1 Electronic structure of atomic sodium.

Atomic sodium has electronic configuration $2s^1$. Thus the ground state has the form $|(0,1/2)1/2,M\rangle$ (using the notation of the previous section), where M = +1/2. The first two excited states, the $^2P_{1/2}$ and the $^2P_{3/2}$ are degenerate, if we neglect spin-orbit coupling, . As we see in Fig 7.1, including spin-orbit coupling removes this degeneracy. Thus it is possible to perform resonance Rayleigh experiments where the incident frequency has been tuned so that we are in resonance with one of the above states but not the other. Later in this section, calculations are performed for this case, and also for the case of near resonance with both states.

7.3.2 Symmetry considerations

Most of the relevant symmetry matters have been discussed in Section 7.2.1. We merely add that we use expression (2.6.5) to simplify the reduced matrix elements.

7.3.3 Calculation of the polarizability components.

As we have seen, the appropriate expressions for Rayleigh scattering are (7.2.2). These involve an infinite sum over all the excited states of the atom, making the calculation impractical. In order to calculate the polarizability tensor patterns, we assume that the frequency of the incident radiation is very close to the frequencies for the $^2P_{1/2} \longleftarrow {}^2S_{1/2}$ and $^2P_{3/2} \longleftarrow {}^2S_{1/2}$ transitions. Thus we may exclude all the excited states in the infinite sum except the $^2P_{3/2}$ and the $^2P_{1/2}$.

To calculate the matrix elements that remain, we use irreducible tensor methods. As an example, we calculate a specific matrix element.

$$\langle (0,1/2)1/2,-1/2|u_x|(1,1/2)1/2,1/2\rangle$$

$$= -2^{-1/2}[\ \langle (0,1/2)1/2,-1/2|u_1|(1,1/2)1/2,1/2\rangle + \langle (0,1/2)1/2,-1/2|u_{-1}|(1,1/2)1/2,1/2\rangle\ ]$$

(using (2.6.4))

$$= -2^{-1/2}(-1)^{1/2-(-1/2)} \langle (0,1/2)1/2\|u\|(1,1/2)1/2\rangle \times \left[\begin{pmatrix} 1/2 & 1 & 1/2 \\ 1/2 & 1 & 1/2 \end{pmatrix} - \begin{pmatrix} 1/2 & 1 & 1/2 \\ 1/2 & -1 & 1/2 \end{pmatrix}\right]$$

$$= -2^{-1/2}[0+(+3^{-1/2})]\langle (0,1/2)1/2\|u\|(1,1/2)1/2\rangle$$

$$= -6^{-1/2}\langle (0,1/2)1/2\|u\|(1,1/2)1/2\rangle$$

$$= -6^{-1/2}(-1)^2\,[(2.1/2+1)^2]^{1/2} \begin{bmatrix} 0 & 1/2 & 1/2 \\ 1/2 & 1 & 1 \end{bmatrix} \langle 0\|u\|1\rangle$$

(we have used (2.6.6) to reduce the reduced matrix element.)

$$= -1/3\langle 0\|u\|1\rangle \qquad (7.3.1)$$

Proceeding as above, we calculate all the matrix elements of interest. We then calculate the polarizability components using these. We assume that we are near resonance with

$^2P_{1/2}$ and $^2P_{3/2}$, so that only these states need be included in the summation over all excited electronic states. Below we calculate the XX polarizability component for the 1/2 ⟵ 1/2 pathway.

$$(\tilde{a}_{xx})_{1/2,1/2} \qquad (7.3.2)$$

$$= (2w/h)(f+ig)\sum_c |\langle (01/2)1/2,1/2|u_x|(1,1/2)1/2,c\rangle|^2$$

$$+(2w/h)(f+ig)\sum_c |\langle (01/2)1/2,1/2|u_x|(1,1/2)3/2,c\rangle|^2$$

$$= (2w/h)(f+ig)[\ (0+1/9)\,|\langle 0\|u\|1\rangle|^2]$$

$$+(2w/h)(f+ig)[\ (1/18+1/6)\,|\langle 0\|u\|1\rangle|^2]$$

$$= (2/9h)\,|\langle 0\|u\|1\rangle|^2[\ w\ (f+ig)_{1/2} + 2w\ (f+ig)_{3/2}\ ]$$

From calculations such as these we obtain tensor patterns for the various situations of interest to us, namely near resonance with both the +1/2 and +3/2 states, and exact resonance with either the +1/2 or the +3/2 state. We deal with these two situations separately below.

Near resonance with $^2P_{3/2}$ and $^2P_{1/2}$

We obtain the following tensor patterns for the case of the incident frequency being near resonance with the $^2P_{1/2}$ and $^2P_{3/2}$ excited electronic states.

$$(\tilde{a}_{\alpha\beta})_{1/2,\,1/2} = \begin{bmatrix} a+2b & (b-a)i & 0 \\ (a-b)i & a+2b & 0 \\ 0 & 0 & a+2b \end{bmatrix}$$

$$(\tilde{a}_{\alpha\beta})_{-1/2,-1/2} = \begin{bmatrix} a+2b & (a-b)i & 0 \\ (b-a)i & a+2b & 0 \\ 0 & 0 & a+2b \end{bmatrix}$$

$$(\tilde{a}_{\alpha\beta})_{-1/2,\,1/2} = \begin{bmatrix} 0 & 0 & a-b \\ 0 & 0 & (a-b)i \\ b-a & (b-a)i & 0 \end{bmatrix}$$

$$(\tilde{a}_{\alpha\beta})_{1/2,-1/2} = \begin{bmatrix} 0 & 0 & b-a \\ 0 & 0 & (a-b)i \\ a-b & (b-a)i & 0 \end{bmatrix} \qquad (7.3.3)$$

In the above tensor patterns,

$$a = (f_{1/2}+g_{1/2}) \text{ and } b = (f_{3/2}+g_{3/2}) \qquad (7.3.4)$$

Note that these only hold if are we are very near resonance, and if $w_{1/2}$ and $w_{3/2}$ are very nearly exactly equal.

We see that the tensor patterns produced have the form predicted in Section 7.1. We also see that it is the presence of spin-orbit coupling which allows the generation of antisymmetric scattering components. For in the absence of spin-orbit coupling, the factor a-b would vanish. (For then the +1/2 and +3/2 states would have the same energy, and so a would equal b.) Since this factor appears in all the antisymmetric scattering components, the antisymmetric scattering contribution would become zero. Antisymmetric scattering also vanishes when we are far from resonance, for then a and b are approximately equal and so cancel each other out. (cf. the vanishing of antisymmetric scattering away from resonance for molecules, which we discussed in Chapter 3.).

It is of interest to study what happens to the scattering as we sweep from near resonance with the +1/2 state to near resonance with the +3/2 state. The closer we get to exact resonance with the +1/2 state, the larger the antisymmetric contribution to the scattering becomes (because a becomes much larger than b.) As we then pass in between exact resonance with the two states, we reach a point where a and

b exactly cancel each other, so that the antisymmetric scattering vanishes. As we sweep through this point, the antisymmetric contribution rises again as we come into exact resonance with the +3/2 state. Finally, as we sweep further from exact resonance with the +3/2 state, the antisymmetric scattering contribution decreases to zero.

Thus it is only for the case of exact resonance with either the +1/2 or +3/2 states that there is a signifigant antisymmetric contribution to the scattering. We now look at these two cases in more detail.

Exact resonance with the +1/2 and +3/2 states.

For the case of exact resonance with the +1/2 excited state, b is negligable compared to a, and similarly when we are in resonance with +3/2. It is therefore straightforward to obtain the following tensor patterns.

Resonance with $^2P_{3/2}$

$$(\tilde{a}_{\alpha\beta})_{-1/2,1/2} = \begin{bmatrix} 0 & 0 & -1 \\ 0 & 0 & -i \\ 1 & i & 0 \end{bmatrix}$$

$$(\tilde{a}_{\alpha\beta})_{1/2,-1/2} = \begin{bmatrix} 0 & 0 & 1 \\ 0 & 0 & -i \\ -1 & i & 0 \end{bmatrix}$$

$$(\tilde{a}_{\alpha\beta})_{1/2,1/2} = \begin{bmatrix} 2 & -i & 0 \\ i & 2 & 0 \\ 0 & 0 & 2 \end{bmatrix}$$

Resonance with $^2P_{1/2}$

$$(\tilde{a}_{\alpha\beta})_{-1/2,1/2} = \begin{bmatrix} 0 & 0 & 1 \\ 0 & 0 & i \\ -1 & -i & 0 \end{bmatrix}$$

$$(\tilde{a}_{\alpha\beta})_{1/2,-1/2} = \begin{bmatrix} 0 & 0 & -1 \\ 0 & 0 & i \\ 1 & -i & 0 \end{bmatrix}$$

$$(\tilde{a}_{\alpha\beta})_{1/2,1/2} = \begin{bmatrix} 1 & i & 0 \\ -i & 1 & 0 \\ 0 & 0 & 1 \end{bmatrix}$$

$$(\tilde{a}_{\alpha\beta})_{-1/2,-1/2} = \begin{bmatrix} 2 & i & 0 \\ -i & 2 & 0 \\ 0 & 0 & 2 \end{bmatrix} \qquad (\tilde{\alpha}_{\alpha\beta})_{-1/2,-1/2} = \begin{bmatrix} 1 & -i & 0 \\ i & 1 & 0 \\ 0 & 0 & 1 \end{bmatrix}$$

(7.3.5)

We note that these tensor patterns are identical to those obtained for resonance with the E_u' and U_u' excited states of $[IrCl_6]^{2-}$. This is because the tensor patterns derive their form from purely symmetry considerations, and these are very similar for the two systems. (These patterns are also identical to those given in Barron's book.[3]) As a consequence of this, the depolarization ratio and M.C.I.D. calculations performed for the totally symmetric mode of $[IrCl_6]^{2-}$, (see Table 6.2) also hold for atomic sodium. Thus we should obtain a positive-negative couplet centred about the incident frequency. The lower frequency wing of the couplet is predicted to be negative.

To finish off this section, we note that to date, no experimental measurements of M.C.I.D. for atomic sodium have been made. However, comparatively recently, resonance Rayleigh scattering experiments involving atomic sodium have been reported by Hamaguchi, Buckingham and Kakimoto.[4] (The experiments were performed using a dye-laser.) Depolarization ratios of approximately unity were observed, as predicted by theory.

Chapter 7 : References.

1) [D], p.52

2) [A], p.199-200

3) [A], p.369

4) H. Hamaguchi, A.D. Buckingham and M. Kakimoto, Opt. Lett. 5114(1980)

CHAPTER 8

A SURVEY OF THE SCATTERING TENSORS FOR VARIOUS POINT GROUPS

8.1 Introduction

In Sections 3.2 and 3.3, we saw that it is not necessary to have detailed knowledge about the electronic structure of a molecule to calculate both the unperturbed and perturbed polarizability tensor patterns. (This is assuming we know it has a non-degenerate ground state.) To calculate these it is only necessary to know the molecular point group the molecule belongs to, and to have the appropriate set of V coefficients.

In this chapter, we go through the molecular point groups which we have not so far considered , and calculate the tensor patterns. To do this, we consider separately all the different molecular point groups, other than the octahedral group, which have a distinct set of V coefficient. No experimental results are being presented to compare these calculations with. Thus we go into little detail other than to give the tensor patterns and the calculated values for the depolarization ratio and the polarizability components.

8.2 Calculation of the Scattering Parameters for Molecular Point Groups

As was pointed out in Griffith's monograph[1], there are not nearly so many different sets of V coefficient tables necessary as there are molecular point groups. This is because all molecular point groups are either isomorphic with one of the pure rotation groups, or else is the direct product of a pure rotation group with a group which has as it's elements the identity and the inversion operations. In calculating the tensor patterns, we need to consider some groups other than the pure rotation groups. This is because the operators with which we are dealing sometimes span different irreducible in two different groups, even though the two groups are isomorphic.

(As mentioned in Chapter 3, all the tensors are real.)

The tensor patterns given below for the polarizability tensor are the same as those given by Koningstein[2], although as mentioned earlier, he did not use any specific formula. However, the results given below for the perturbed polarizability tensor patterns are new.

For the various point groups, only the calculated M.C.I.D. values for exact resonance with the 0-0 band have been given. From Chapter 3, we know that for the normal modes A_1 and A_2, the sign of the M.C.I.D.'s are unchanged, and for all other modes, the signs of the M.C.I.D.'s reverse when we go from the 0-0 resonance to the 0-1 resonance.

(a) Point Groups C_{2v} and D_2

Operator	Representation In	
	C_{2v}	D_2
ux	B_1	B_3
uy	B_2	B_2
uz	A_1	B_1
mx	A_2	B_1

Polarizability Tensor Patterns

$B_1:B_3$ $B_2:B_2$ $A_1:B_1$ $A_2:B_1$

$$\begin{bmatrix} A & 0 & 0 \\ 0 & B & 0 \\ 0 & 0 & C \end{bmatrix} \quad \begin{bmatrix} 0 & 1 & 0 \\ 1 & 0 & 0 \\ 0 & 0 & 0 \end{bmatrix} \quad \begin{bmatrix} 0 & 0 & 1 \\ 0 & 0 & 0 \\ 1 & 0 & 0 \end{bmatrix} \quad \begin{bmatrix} 0 & 0 & 0 \\ 0 & 0 & 1 \\ 0 & 1 & 0 \end{bmatrix}$$

Symmetry	$B_1:B_3$	$B_2:B_2$	$A_1:B_1$	$A_2:B_1$
(x)	[0,3/4]	3/4	3/4	3/4

Because there are no degenerate representation in either of these groups, the perturbed polarizabilities are zero. Hence if a molecule belongs to either of these point groups, it will not give an M.R.O.A. spectra. This could be the reason why the free porphyrins which were tested during the present project did not give any observable M.R.O.A. peaks. (Since such porphyrins are only expected to have an overall symmetry of D_{2d}.)

(b) Point Group C_{3v}

Operator	Representation In C_{3v}
ux	E
uy	E
uz	A_1
mz	A_2

Polarizability Tensor Patterns

A_1

$$\begin{bmatrix} 1 & 0 & 0 \\ 0 & 1 & 0 \\ 0 & 0 & c \end{bmatrix}$$

A_2

$$\begin{bmatrix} 0 & -1 & 0 \\ 1 & 0 & 0 \\ 0 & 0 & 0 \end{bmatrix}$$

E

$$\begin{bmatrix} -1 & 1 & 0 \\ 1 & 1 & 0 \\ 0 & 0 & 0 \end{bmatrix}$$

Symmetry	A_1	A_2	E
(x)	[0,3/4]	00	3/4

Perturbed Polarizability Tensor Patterns

A_1

$$\begin{bmatrix} 0 & 1 & 0 \\ -1 & 0 & 0 \\ 0 & 0 & 0 \end{bmatrix}$$

A_2

$$\begin{bmatrix} 1 & 0 & 0 \\ 0 & 1 & 0 \\ 0 & 0 & 0 \end{bmatrix}$$

E

$$\begin{bmatrix} -1 & -1 & 0 \\ -1 & 1 & 0 \\ 0 & 0 & 0 \end{bmatrix}$$

M.C.I.D. Values

Symmetry	Dx	Dz
A_1	$-8a_B/9$	$-2a_B$
A_2	$-8a_B/5$	$-2a_B/3$
E	$-8a_B/7$	$-1a_B/$

(c) Point Group D_3

Operator	Representation In D_3
ux	E
uy	E
uz	A_2
mz	A_2

Polarizability Tensor Patterns

A_1

$$\begin{bmatrix} 1 & 0 & 0 \\ 0 & 1 & 0 \\ 0 & 0 & c \end{bmatrix}$$

A_2

$$\begin{bmatrix} 0 & -1 & 0 \\ 1 & 0 & 0 \\ 0 & 0 & 0 \end{bmatrix}$$

E

$$\begin{bmatrix} -1 & 1 & 2 \\ 1 & 1 & -2 \\ -2/2 & 2/2 & 0 \end{bmatrix}$$

Symmetry	A_1	A_2	E
(x)	[0,3/4]	00	3/4

Perturbed Polarizability Tensor Patterns

A_1

$$\begin{bmatrix} 0 & 1 & 0 \\ -1 & 0 & 0 \\ 0 & 0 & 0 \end{bmatrix}$$

A_2

$$\begin{bmatrix} 1 & 0 & 0 \\ 0 & 1 & 0 \\ 0 & 0 & 0 \end{bmatrix}$$

E

$$\begin{bmatrix} -1 & -1 & 0 \\ -1 & 1 & 0 \\ 0 & 0 & 0 \end{bmatrix}$$

M.C.I.D. Values

Symmetry	Dx	Dz
A_1	$-8a_B/9$	$-2a_B$
A_2	$-8a_B/5$	$-2a_B/3$
E	$-8a_B/7$	$-1a_B$

(d) Point Groups C_{4v} and D_4

Operator	Representation In	
	C_{4v}	D_4
ux	E	E
uy	E	E
uz	A_1	A_2
mz	A_2	A_2

Polarizability Tensor Patterns

A_1 $\begin{bmatrix} 1 & 0 & 0 \\ 0 & 1 & 0 \\ 0 & 0 & c \end{bmatrix}$ A_2 $\begin{bmatrix} 0 & -1 & 0 \\ 1 & 0 & 0 \\ 0 & 0 & 0 \end{bmatrix}$ B_1 $\begin{bmatrix} 1 & 0 & 0 \\ 0 & -1 & 0 \\ 0 & 0 & 0 \end{bmatrix}$ B_2 $\begin{bmatrix} 0 & 1 & 0 \\ 1 & 0 & 0 \\ 0 & 0 & 0 \end{bmatrix}$ E $\begin{bmatrix} 0 & 0 & 1 \\ 0 & 0 & -1 \\ -1/2 & 1/2 & 0 \end{bmatrix}$

Symmetry	A_1	A_2	B_1	B_2	E
(x)	[0,3/4]	3/4	3/4	3/4	

Perturbed Polarizability Tensor Patterns

A_1 $\begin{bmatrix} 0 & 1 & 0 \\ -1 & 0 & 0 \\ 0 & 0 & 0 \end{bmatrix}$ A_2 $\begin{bmatrix} 1 & 0 & 0 \\ 0 & 1 & 0 \\ 0 & 0 & 0 \end{bmatrix}$ B_1 $\begin{bmatrix} 0 & 1 & 0 \\ 1 & 0 & 0 \\ 0 & 0 & 0 \end{bmatrix}$ B_2 $\begin{bmatrix} -1 & 0 & 0 \\ 0 & 1 & 0 \\ 0 & 0 & 0 \end{bmatrix}$ E $\begin{bmatrix} 0 & 0 & 0 \\ 0 & 0 & 0 \\ 0 & 0 & 0 \end{bmatrix}$

M.C.I.D. Values

Symmetry	Dx	Dz
A_1	$-8a_B/9$	$-2a_B$
A_2	$-8a_B/5$	$-2a_B/5$
B_1	$-8a_B/7$	$-2a_B/3$
B_2	$-8a_B/7$	$-2a_B/3$

(e) Point Group Csv

Operator	Representation In Csv
ux	E
uy	E
uz	A1
mz	A2

Polarizability Tensor Patterns

A1

$$\begin{bmatrix} 1 & 0 & 0 \\ 0 & 1 & 0 \\ 0 & 0 & c \end{bmatrix}$$

A2

$$\begin{bmatrix} 0 & -1 & 0 \\ 1 & 0 & 0 \\ 0 & 0 & 0 \end{bmatrix}$$

E1

$$\begin{bmatrix} 0 & 0 & 1 \\ 0 & 0 & -1 \\ -1/2 & 1/2 & 0 \end{bmatrix}$$

E2

$$\begin{bmatrix} 1 & 1 & 0 \\ 1 & -1 & 0 \\ 0 & 0 & 0 \end{bmatrix}$$

Symmetry	A1	A2	E1	E2
(x)	[0,3/4]	00		

Perturbed Polarizability Tensor Patterns

A1

$$\begin{bmatrix} 0 & 1 & 0 \\ -1 & 0 & 0 \\ 0 & 0 & 0 \end{bmatrix}$$

A2

$$\begin{bmatrix} 1 & 0 & 0 \\ 0 & 1 & 0 \\ 0 & 0 & 0 \end{bmatrix}$$

E1

$$\begin{bmatrix} 0 & 0 & 0 \\ 0 & 0 & 0 \\ 0 & 0 & 0 \end{bmatrix}$$

E2

$$\begin{bmatrix} -1 & 1 & 0 \\ 1 & 1 & 0 \\ 0 & 0 & 0 \end{bmatrix}$$

M.C.I.D. Values

Symmetry	Dx	Dz
A1	$-8a_B/9$	$-2a_B$
A2	$-8a_B/5$	$-2a_B/3$
E2	$-8a_B/7$	$-1a_B$

Chapter 8 : References

1) [C], p.26

2) J.A. Koningstein, Introduction to the Theory of the Raman Effect, D. Reidel Publishing Company, Dordrecht, Holland

CHAPTER 9

GENERAL CONCLUSIONS

9.1 Introduction

In this final chapter, we present the general conclusions of the thesis. First of all, in Section 9.2 below, we round up all the new properties and features of M.R.O.A. which have been obtained as a result of the development presented in the previous pages. In Section 9.3 we briefly summarise the new developments in the field of M.R.O.A. since the end of the experimental work of this project. Finally in Section 9.4, we use these properties of M.R.O.A. to predict possibilities for further work in this field.

9.2 Review of Polarizability Tensor and M.R.O.A. Properties

9.2.1 Introduction

In this section we gather together all of the new properties of the polarizability tensor and M.R.O.A. which have been deduced in the first eight chapters of the thesis. We deal with these separately in the two following subsections.

9.2.2 The polarizability tensor

(a) Simply reducible point groups

The main new results obtained relating to the unperturbed polarizability tensor apply only to molecules with a totally symmetric ground state. They were derived by using vibronic coupling as a perturbation to vibronic molecular states, rather than as a perturbation to states written as a product of electronic and vibrational parts. Applying irreducible tensor methods to the polarizability expressions produced by this approach, expressions (3.6.4) and (3.6.5) were obtained for symmetric and antisymmetric scattering respectively. These show that the form of the polarizability tensor is independent of the intermediate excited electronic state k_e, and is dependent on the excited state j_e only to the extent that the whole expression may be zero for certain j_e. They also show clearly a condition necessary for antisymmetric scattering to occur, namely that one of the direct products of the electric dipole moment

representations must contain the antisymmetric representation A_2. As we see also see in Section 3.2, another necessary condition is that the excited state j_e must be degenerate. (3.6.5) also displays clearly the reason why antisymmetric scattering is only observed at resonance. This is due to the fact that the 0-0 and 0-1 contributions, which have opposite sign, are approximately equal and therefore cancel out away from resonance.

Lastly, expressions (3.6.4) and (3.6.5) provide a simple and direct way of calculating the polarizability tensor patterns for all the simply reducible point groups. Alternative routes to these patterns rely on the application of irreducible tensor methods to each individual point group.

Using a similar approach to that used for the unperturbed polarizability tensor, analagous formulae, ((3.6.6) and (3.6.7)) were obtained for the magnetically perturbed polarizability tensor. These allow the ready calculation of the perturbed polarizability tensor patterns for the simply reducible point groups other than O, and these new results are given in Chapter 8.

Other more general points can be deduced from them. First of all, we see that if we are not at resonance, then apart from a small residual contribution not included in the formulae, the perturbed polarizability tensor becomes zero for anisotropic scattering i.e. non A modes. As before, this is due to the cancellation of the 0-0 and 0-1 contributions, which are opposite and approximately equal away from resonance. Along with the similar conclusion for antisymmetric scattering outlined above, we thus obtained

the new result that away from resonance, only A_1 modes give rise to a non-zero perturbed polarizability tensor. This partly explains why M.R.O.A. has not been seen at resonance.

Another general result follows from a comparison of the formulae for the unperturbed polarizability tensor. This is that if the unperturbed polarizability is symmetric, the perturbed polarizability is antisymmetric and vice-versa.

(b) Non-simply reducible point groups

It did not prove possible to deduce a formula for the polarizability tensor when the ground stae was not totally symmetric. However, it was possible to deduce the general forms of the polarizability tensor patterns for the octahedral spinor group, the most complicated possible case. The main results are (3.4.18-19) and (3.4.22-23) for totally symmetric scattering, (3.4.34-35) and (3.4.38-39) for E modes and (3.4.46-47) and (3.4.49-50) for T_{2g} modes. The results obtained for totally symmetric scattering are similar to those obtained by Barron and Norby-Svenson using time-reversal arguments, but those obtained for non-totally symmetric modes are new. These results are useful when detailed calculations are being performed, as well as allowing deuctions about Raman E.P.R. to be made.

9.2.3 Magnetic Raman optical activity

(a) Molecules with non-degenerate ground state

The first point we note is that the ratio of the

difference spectra signal to the sum spectra is approximately equal to the ratio of the perturbed to the unperturbed polarizability tensor. For transparent scattering, assuming the former to be non-zero, this is of the same order of magnitude as the ratio of the Zeeman splitting of an electronic absorption band to the energy of the absorption. Even using a strong magnetic field, this is of the order of 10^{-4}. Hence even for A_1 modes, the only mode for which the main perturbed polarizability contribution is non-zero at transparent frequencies, the magnitude of the difference spectra makes it's observation difficult. This explains why no transparent M.R.O.A. has yet been observed.

The results obtained for the polarizability tensor allowed several new and important general deductions to be made about M.R.O.A. for simply reducible point groups. First of all, from the form of the tensor patterns given in Chapter 8, we deduce that the magnitude of the polarized difference spectra should always be double that of the depolarized difference spectra. This is a generalization of the result obtained for cytochrome c. Secondly, equations (3.6.4-7) show that for A modes (i.e. for isotropic and antisymmetric scattering) the sign of the M.R.O.A. peaks remains unaltered as we change from resonance with the 0-0 vibronic transition to the 0-1 vibronic transition. However, for all other modes (i.e. for anisotropic scattering) the sign of the M.R.O.A. peaks does change. Again this is a generalization of the result previously reported for cytochrome c.

Lastly, the calculated tensor patterns allow the M.C.I.D.s for all the non-degenerate normal modes of all the

simply reducible groups other than 0 to be easily calculated. From these we see that for resonance with the 0-0 vibronic transition, all molecules give negative M.R.O.A. peaks.

(b) Molecules with degenerate ground states

For molecules with degenerate ground states, the main development made during the present project was the observation of Raman E.P.R. in three odd-electron transition metal complexes. This new manifestation of M.R.O.A. allows both the sign, and with a strong enough magnetic field, the magnitude of the electronic g-factor for complexes in solution to be measured.

The main theoretical development concerning Raman E.P.R., apart from the detailed calculation of the M.C.I.D.s for the Iridium complex given in Chapter 6, follows from equations (3.4.18) and (3.4.19). These show that providing the a molecule has a degenerate ground state, its totally symmetric vibrational modes should give an M.R.O.A. couplet.

9.3 Recent Developments in M.R.O.A.

Since the end of this project, various new results have been obtained in M.R.O.A. A short summary of these will be given in this section.

(a) The first new observation of Raman E.P.R. after it's discovery was made by Barron, Vrbancich and Watts[1] in 1982. The molecule they studied was the complex ion $[IrBr_6]^{2-}$, and M.R.O.A. spectra were obtained at both 514.5 and 577.5 nm using a tunable dye laser. The band magnitudes in both the resonance Raman and the M.R.O.A. spectra change dramatically when the incident frequency is tuned into resonance with different excited electronic states. The signs of the M.C.I.D. couplets obtained are consistent with those obtained for $[IrCl_6]^{2-}$. One difference between the two is that an M.R.O.A. couplet was observed for the E vibrational mode of $[IrBr_6]^{2-}$. The sign of this couplet agrees with that calculated in Chapter 6. (This calculation was performed before the experimentally observed value was obtained.)

(b) An interesting extension of the M.R.O.A. technique was made by Barron and Vrbancich[2] in 1983, when they made the first observations of magnetic optical activity in the pure electronic Raman scattering of $[OsBr_6]^{2-}$, $[IrCl_6]^{2-}$ and $U(C_8H_8)_2$. From these observations, information both about the sign of the electronic g-factor, and the ordering of magnetic sub-states was deduced.

(c) The third new development in M.R.O.A. has been the observation of anti-Stokes M.C.I.D.s in the resonance Raman scattering of $[IrCl_6]^{2-}$ in 1982 by Barron and Vrbancich.

9.4 Conclusions

9.4.1 Introduction

In this section , we use the developments presented in the previous chapters of the thesis, and summarised in Section 9.2, to assess possibilities for further work on Magnetic Raman Optical Activity . In particular, we are concerned firstly with which molecules might give an observable M.R.O.A. spectra, and secondly with possible areas where the technique could be usefully applied.

We split this into two parts ,dealing first with M.R.O.A. generated by ground state degeneracy , and then with that generated by excited state degeneracy .

9.4.2 Molecules with degenerate ground states

The most common circumstance in which a molecule has a degenerate ground state is when it has an odd number of electrons. Thus it is for odd-electron systems that Raman E.P.R. is expected to be most important. As we have seen, all the normal modes of such molecules are expected to generate a couplet in the depolarised difference spectra. However, there are other conditions which must be satisfied before an M.R.O.A. spectra can be observed. For off-diagonal scattering contributions to be present, it is necessary that both the ground and excited electronic states exhibit strong spin-orbit coupling. It is also necessary that a laser excitation frequency is available for performing resonance Raman measurements. Finally, it is necessary that the

vibrational modes of the molecule should show strong resonance enhancement.

Given that all these requirements are satisfied, there is a great deal of information which can be obtained from the measurement of the Raman E.P.R. spectra. From the sign of the M.C.I.D. couplet for the A_1, the sign of the ground state electronic g-factor can be obtained. (The only alternative means of doing this is to perform circularly polarised M.C.I.D. experiments.) Also, we can use Raman E.P.R. to study the effective symmetry of chromophores in large biological molecules.

9.4.3 Molecules with non-degenerate ground states

From Chapter 8, we see that in theory, an M.R.O.A. spectra should be obtained for any molecule whose point group contains a degenerate representation. However, as we have seen, there are various conditions which must be satisfied before one would expect a measurable M.R.O.A. to be observed. The main requirement, as discussed in Chapter 2, is that we should be in resonance with a degenerate excited electronic state of the molecule. However, although this is sufficient for the generation of observable M.C.I.D. components for totally symmetric modes, it is not sufficient for non-totally symmetric modes. This is because of the cancellation of the 0-0 and 0-1 scattering contributions for non-totally symmetric modes. Thus it is necessary to be in exact resonance with either the 0-0 or the 0-1 vibronic bands before M.C.I.D.'s for non-totally symmetric modes can be observed.

Given that sufficient intensity can be obtained to make accurate measurements possible, there is potentially much information to be obtained from the M.R.O.A. spectra. First of all, the appearance of any measurable M.C.I.D.'s show that the molecule contains greater than a two-fold axis of symmetry. Thus one can study the effective symmetry of a molecule as we change its environment. From the behaviour of the sign of the M.C.I.D., it is also possible, for the case of a Raman band which has contibutions from several normal modes, to determine whether isotropic or anisotropic scattering is the dominant contribution. If the former is dominant, then the sign of the M.C.I.D. couplet should reverse as we go from resonance with the 0-0 to the 0-1 vibronic band. If the latter is dominant, then we would expect no change in the sign of the M.C.I.D. components.

Chapter 9 : References

1) L.D. Barron, J. Vrbancich and R.S. Watts, Chem. Phys. Letts. 89,71(1982)

2) L.D. Barron and J. Vrbancich, J. Raman Spectrosc. 14,118(1983)

3) L.D. Barron and J. Vrbancich, Chem. Phys. Letts. 92,466(1982)